(2)

Research and Development Technical Report
SLCET-TR-84-0458-F

# STUDY OF SINTERED MAGNETS OF THE Nd-Fe-B TYPE

Karl J. Strnat, Electrical Engineering Department
Herbert F. Mildrum, Research Institute

University of Dayton
Dayton, Ohio 45469

February 1989

Final Report for Period September 1984 - September 1987



DISTRIBUTION STATEMENT

Approved for public release;
distribution is unlimited.

Prepared for
ELECTRONICS TECHNOLOGY AND DEVICES LABORATORY

US ARMY
LABORATORY COMMAND
FORT MONMOUTH, NEW JERSEY 07703-5000

# NOTICES

## Disclaimers

The citation of trade names and names of manufacturers in this report is not to be construed as official Government indorsement or approval of commercial products or services referenced herein.

UNCLASSIFIED
SECURITY CLASSIFICATION OF THIS PAGE

# REPORT DOCUMENTATION PAGE

Form Approved OMB No. 0704-0188

| | |
|---|---|
| 1a. REPORT SECURITY CLASSIFICATION: Unclassified | 1b. RESTRICTIVE MARKINGS |
| 2a. SECURITY CLASSIFICATION AUTHORITY | 3. DISTRIBUTION/AVAILABILITY OF REPORT: Approved for public release; distribution is unlimited. |
| 2b. DECLASSIFICATION/DOWNGRADING SCHEDULE | |
| 4. PERFORMING ORGANIZATION REPORT NUMBER(S) | 5. MONITORING ORGANIZATION REPORT NUMBER(S): SLCET-TR-84-0458-F |
| 6a. NAME OF PERFORMING ORGANIZATION: University of Dayton; 6b. OFFICE SYMBOL (If applicable) | 7a. NAME OF MONITORING ORGANIZATION: US Army Laboratory Command (LABCOM) Electronics Technology and Devices Laboratory |
| 6c. ADDRESS (City, State, and ZIP Code): Dayton, Ohio 45469 | 7b. ADDRESS (City, State, and ZIP Code): ATTN: SLCET-ED Fort Monmouth, NJ 07703-5000 |
| 8a. NAME OF FUNDING/SPONSORING ORGANIZATION; 8b. OFFICE SYMBOL (If applicable) | 9. PROCUREMENT INSTRUMENT IDENTIFICATION NUMBER: DAAK20-84-K-0458 |
| 8c. ADDRESS (City, State, and ZIP Code) | 10. SOURCE OF FUNDING NUMBERS |

| PROGRAM ELEMENT NO. | PROJECT NO. | TASK NO. | WORK UNIT ACCESSION NO. |
|---|---|---|---|
| 1L1 | 611102 | H47 02 | DA311266 |

11. TITLE (Include Security Classification): STUDY OF SINTERED MAGNETS OF THE Nd-Fe-B TYPE (U)

12. PERSONAL AUTHOR(S): Karl J. Strnat and Herbert F. Mildrum

| 13a. TYPE OF REPORT | 13b. TIME COVERED | 14. DATE OF REPORT (Year, Month, Day) | 15. PAGE COUNT |
|---|---|---|---|
| Final Report | FROM Sep 84 TO Sep 87 | 1989 February | 91 |

16. SUPPLEMENTARY NOTATION

| 17. COSATI CODES | | | 18. SUBJECT TERMS (Continue on reverse if necessary and identify by block number) |
|---|---|---|---|
| FIELD | GROUP | SUB-GROUP | |
| 20 | 03 | | permanent magnets; magnetic stability; coercivity; temperature compensation; traveling wave tubes. |
| | | | |

19. ABSTRACT (Continue on reverse if necessary and identify by block number)

This is the final report of a 3½-year effort to assess the utility and limitations of Nd-Fe-B based sintered magnets for microwave devices such as traveling wave tubes. In these devices, the magnetic properties at elevated temperatures are of importance, as is the flux stability during thermal cycling and long-term exposure. The experimental work described here involved several tasks: 1) the characterization of magnets from industrial R&D laboratories and from early pilot production; 2) development of our own techniques and the capabilities for preparing Nd-Fe-B alloys and sintered magnets from them; 3) modification of the alloy compositions and heat treatments in order to improve the elevated temperature magnetic properties, making the magnets more suitable for applications in the 100 to 200 deg C range at low operating permeance values; and 4) the attempt to better understand the magnetization reversal behavior and the relationship between coercivity and microstructure. The report describes our efforts in this sequence, which also corresponds approximately with the chronological progress of the work. Most results have by now been published in the form of conference papers or (contd)

| 20. DISTRIBUTION/AVAILABILITY OF ABSTRACT | 21. ABSTRACT SECURITY CLASSIFICATION | |
|---|---|---|
| ☐ UNCLASSIFIED/UNLIMITED ☒ SAME AS RPT. ☐ DTIC USERS | Unclassified | |
| 22a NAME OF RESPONSIBLE INDIVIDUAL: Herbert A. Leupold | 22b. TELEPHONE (Include Area Code): (201) 544-4300 | 22c. OFFICE SYMBOL: SLCET-ED |

DD Form 1473, JUN 86 — Previous editions are obsolete. — SECURITY CLASSIFICATION OF THIS PAGE: UNCLASSIFIED

19. ABSTRACT (cont'd)

journal articles, and reprints or manuscripts of these are appended. For further details, see report Introduction.

TABLE OF CONTENTS

LIST OF FIGURES

LIST OF TABLES

# 1. INTRODUCTION

This is the final report of a 3-1/2-year effort to assess the utility and limitations of Nd-Fe-B based sintered magnets for microwave devices such as traveling wave tubes. In these devices, the magnetic properties at elevated temperatures are of importance, as is the flux stability during thermal cycling and long-term exposure. The experimental work described here involved several tasks:
(1) The characterization of magnets from industrial R&D laboratories and from early pilot production.
(2) Development of our own techniques and capabilities for preparing Nd-Fe-B alloys and sintered magnets from them.
(3) Modifying the alloy compositions and heat treatments in order to improve the elevated temperature magnetic properties and making the magnets more suitable for applications in the 100° to 200°C range at low operating permeance values.
(4) Trying to better understand the magnetization reversal behavior and the relationship between coercivity and microstructure.
The report describes our efforts in this sequence, which also corresponds approximately to the chronological progress of the work. Most results have by now been published in the form of conference papers or journal articles, and reprints or manuscripts of these are appended. The report relies on these appendices for documentation of the individual subtasks and a discussion of their results.

Early commercial magnets were found seriously wanting, in several respects, for elevated temperature applications. Various alloy modifications were explored by us, and modified samples from other sources were also evaluated. The alloying additions included cobalt as a partial substituent for iron to raise the Curie temperature, dysprosium and erbium substitutions for some of the neodymium to reduce the temperature dependence of the remanence; and Dy, Al, Nb, Ti, and Zr as minor additives that increase the intrinsic coercive force. Certain alloys containing cobalt and dysprosium stand out as having much reduced irreversible losses at 125° and 150°C. Co plus Dy were, therefore, adopted as the basic modifiers needed for useful behavior above $\sim$100°C, with the other elements added individually, so that many of the magnets prepared and tested were six-component alloys. Different combinations of these additives were found to bring certain advantages; others (Al, Ti, Zr) are essentially useless for TWT magnets. All improvements so achieved were relatively minor.

Kerr-effect observations of magnetic domain patterns and wall motion, the analysis of minor loops, and ac thermomagnetic analysis shed light on the mechanisms of magnetization change and the physical origins of the coercivity and its temperature variation.

In practical terms, grinding, sintering, and heat-treating procedures were developed in order to make good magnets from (Nd,Dy)(Fe,Co)B alloys and several modifications with additional elements. Engineering design data were generated for the most useful of the magnets studied, considering the hard magnetic properties at room temperature and in the temperature range from -50°C to +150° or 200°C, as appropriate. In particular, this data includes temperature coefficients, the reversible and irreversible flux losses on heating, and information on the aging behavior during long-term exposure in air at elevated temperature.

## 2. OBJECTIVES AND GENERAL RESEARCH PLAN

The general objective of the work described in this report was to explore the utility of Nd-Fe-B-based permanent magnet materials for traveling wave tubes, filters, and other devices used in generating and processing electromagnetic energy in the millimeter wave and microwave ranges of the frequency spectrum. Based on a general knowledge of the requirements which these devices impose on the permanent magnets used in their focus/beam guiding structures, and some specific guidance provided by the sponsoring laboratory, we had to characterize and evaluate the early ternary alloy magnets and, then, try and modify the material in ways that might improve its properties to make it more suitable for microwave tube use.

Our work was not directly concerned with the devices or the design of their magnetic circuits. It was strictly a materials engineering effort, mostly experimental, aimed at improving certain permanent-magnet characteristics that are important for tube focusing structures, etc. Of primary concern are the hard magnetic properties and their stability at elevated temperatures. In the case of Nd-Fe-B, it was known that problems due to heating were already severe between 70° and 100°C, and the objective was to make the magnets useful in the 100° to 200°C range. Specific properties of interest are the intrinsic demagnetization curves in the entire range of potential operating temperatures, the temperature variation and reversible temperature coefficients (TC) of remanence $\alpha$ and intrinsic coercive force $\beta$ the irreversible flux losses incurred during short-term heating at various operating permeances $L_i$ and the long-term stability of the operating flux. We concentrated on magnets made like the older SmCo magnets by conventional powder metallurgy (by what is now often called the OPS method--orient/press/sinter); at the time the contract work began this was the only known way of producing the fully dense, grain-oriented, high energy magnets needed for tubes.

The work to be done was generally defined in terms of the following three tasks.

Task A: Obtain magnet samples from commercial R&D laboratories or from pilot production lines and characterize them in terms of these properties.

Task B: Develop our own capability for preparing such alloys and sintered magnets; learn to make magnets and optimize the magnet preparation methods using ternary Nd-Fe-B as the vehicle.

Task C: Modify the alloy composition in various ways that have the potential of improving the elevated temperature properties; modify the sintering/heat treating process as required. This implies extensive property characterization of promising magnets that result from Task C.

This contract effort was based on a proposal written soon after the feasibility of making useful sintered permanent magnets from a Nd-Fe-B alloy was announced by Sagawa et al. from the Sumitomo Special Metals Co. of Japan, at the Nov. 1983 Pittsburgh Conference on Magnetism and Magnetic Materials. The experimental work described here actually started about one year after that announcement, at which time the first evaluation samples of such magnets had become available from Sumitomo and some of the shortcomings of Nd-Fe-B were beginning to be understood. Because of the great promise which the new magnet material was perceived to offer for many applications, efforts to reproduce the Sumitomo results, to modify the Nd-Fe-B magnets by changing alloy compositions and preparation procedures, and to improve their properties in various ways had begun in many laboratories world-wide. As a consequence, our investigation was conducted in an atmosphere of intense scientific competition and global interaction, with many people working along similar lines, and new results and ideas being reported in rapid sequence.

This meant, for our work, that we had to continually modify the originally planned approach in its details. We were able to take advantage of results obtained elsewhere and avoid unnecessary duplication. Another reason for adapting the goals as the work progressed was that the growing body of basic knowledge about the 2-14-1 alloys and their fundamental properties made it clearer what magnet properties one might, and which results one could not, expect to achieve by alloying additions of cobalt and heavy rare-earth elements.

## 3. ORGANIZATION OF THIS REPORT AND PRESENTATION OF RESULTS

In the following chapter, the work done under the contract is described in a concise manner in the approximate chronological order of execution. The chapter is organized around the three tasks defined in the proposal; however, additional subchapter headings are used to identify parts of the investigation that were not clearly foreseen at the beginning, but which became relatively major and distinctive additional tasks.

Most of our results have been published in a series of eight journal articles, each summarizing a completed segment of the overall research project. The references given in these were intended to put the reported results in perspective relative to preceding papers, and they reflect the progress of work in the specific problem area made in our laboratory and elsewhere. Copies of these papers are appended to the report and they are made an integral part of it. Reference is made to them for a reasonably detailed description of the experimental methods and a presentation of results in tabular

and graphic form. To the extent that sections of the effort were not published, or where the description in the journal papers is not adequate for the understanding or reproduction of our results, additional details are given herein.

Finally, Chaper 5 is a summary and concise interpretation of the results obtained under this contract effort.

# 4. DISCUSSION OF WORK AND RESULTS OBTAINED

## 4.1. Task A: Characterization of Available Nd-Fe-B Magnets

### 4.1.1. High and Low-Temperature Properties of Early Neomax

We initially acquired two versions of early commercial-product prototypes from the Sumitomo Special Metals Co. (SSMC). Later, we received samples of early U.S.-made products from Crucible Magnetics Company (CMC) and the Hitachi Magnetics Corporation (HMC). All these were sintered magnets and fell into two categories: ternary Nd-Fe-B compositions with a nominal energy product of about 35 MGOe and a modest intrinsic coercivity at room temperature (RT) of about 12-13 kOe, and a Dy-containing version of about 30 MGOe and 18-20 kOe.

On SSMC's Neomax magnets, we first measured demagnetization curves at different temperatures over the range -200° to +200° and determined the temperature variation of the salient properties, $B_r$, $H_c$, $H_k$, $(BH)_{max}$. The reversible and irreversible losses on thermal cycling between +25 and temperatures up to +275°C were also measured. Hard-axis magnetization curves and low-AC-field thermomagnetic analysis plots ("TMA spectra") were used to study the peculiarities of the temperature dependence of anisotropy, coercivity, and the relation between these. The results of this work are presented in Appendix A. They demonstrate the severe shortcomings of ternary Nd-Fe-B at elevated temperatures: On heating, the remanence drops off (toward zero near the relatively low Curie temperature of 312°C) at the modest rate of $\alpha \approx 0.1$ percent per °C around RT. This is only about three times the temperature coefficient of Sm-Co magnets. However, the coercivity has a temperature coefficient of $\beta \approx 0.86$ percent/C, dropping to half of its RT value at 100°C. And the irreversible flux loss at a typical tube-magnet operating point, B/H=0.6, was found to be about 25 percent at 100°C, and nearly 60 percent at 150°C. Such behavior makes these simple ternary alloy magnets useless for most microwave tube applications.

We also investigated the behavior at cryogenic temperatures down to liquid nitrogen (LN) temperature, -196°C, to see what effect the onset of the spin reorientation in the 2-14-1 main phase (at about -150°C) has on the anisotropy and the second-quadrant properties of sintered magnets. Below about -75°C the main anisotropy constant

was found to decline on cooling and the demagnetization curve began to show distortions, with $H_k$ dropping off sharply. Near LN temperature the magnetization also drops about 20 percent below the remanence in the permeance region, where tube magnets typically operate. Through all this, the intrinsic coercivity continues to rise on cooling. It must be concluded that the magnets do not become useless at low temperatures, as was feared when the spin reorientation was first reported. Their performance at low permeance values is certainly degraded to a significant degree, and this must be taken into account in the design of magnetic circuits that have to function in a cryogenic environment.

4.1.2. Basic Studies of the Magnetization Reversal Mechanisms.

Minor loops and recoil-loop fields were also plotted at RT and at several elevated temperatures. They were found to look quite different for the high-coercivity magnets (Neomax 30), where the recoil lines were almost horizontal, and for the lower-coercivity version (grade 35), which has strongly curved recoil lines. The grade 35 magnets remagnetize after field demagnetization in two distinct steps, and they develop their full properties only at a forward field >20 kOe, which is 1.5 times the coercivity value and much more than the magnetizing field which the virgin (thermally demagnetized) magnet requires. For the sake of better understanding the mechanisms responsible for this and for the large irreversible losses on heating, Kerr-effect domain imaging was employed to observe the dynamics of magnetization change in applied fields and at elevated temperatures. The publication, Appendix B, discusses these experiments in detail.

4.1.3. Elevated Temperature Properties and Stability Tests on Commercial Prototype "Nd-Fe-B" Type Magnets.

Later in the contract period, additional magnet samples became available from commercial sources. These included US-produced sintered magnets that were nominally equivalent to the two grades from Sumitomo studied earlier, and also a new composition developed by the Hitachi Metals, Ltd. (HML) Research Laboratory in Japan specifically with better elevated temperature stability in mind. The latter is a sintered magnet that contains cobalt to increase the Curie temperature, plus some dysprosium (substituted for part of the neodymium) to restore the coercivity lost because of Co substitution. These and the two Neomax grades--eight brand-types in all, from four producers, and with three significantly different chemical compositions--were then characterized from the user's viewpoint. They were extensively tested with regard to their property stability at elevated temperatures (to 150°C) and during long-term air/heat exposure (to >5000 hours). These tests are described in the next subsection; the results were also summarized in a publication, Appendix 3.

TABLE 1

ELEVATED TEMPERATURE BEHAVIOR OF SINTERED "Nd-Fe-B TYPE" MAGNETS
(Summary prepared by H.F. Mildrum)

This task focused on a comparative evaluation of the effects of elevated temperature air exposure at 75°, 100°, 125° and 150°C on the open-circuit remanent flux (OCRF) of sintered neodymium type permanent magnets. This investigation included a comparison of:

- the initial irreversible losses on heating
- the initial and final demagnetization curves
- irrecoverable losses observed after long-term aging for over 5000 hours
- the long-term stability of open-circuit remanent flux as a function of time, temperature, level of exposure and operating point permeance from $-B_d/H_d$ = 3.2 to 0.5.

Test magnets representative of three different composition types were obtained from four commercial magnet producers:

| Source | Nd-Fe-B | Nd,Dy-Fe-B | Nd,Dy-Fe,Co-B |
|---|---|---|---|
| Sumitomo Special Metals, Japan | Neomax-35 | Neomax-30 | --- |
| Hitachi Magnetics Ltd., Japan | --- | --- | Hicorex-96S |
| Crucible Magnetics, USA | Crumax-35<br>Crumax-30B | Crumax-30A | --- |
| Hitachi Magnetics Corp., USA | ---<br>Hicorex-94B | Hicorex-94A | --- |

As indicated, the classification of these magnet types fall into two categories, that is, the ternary Nd-Fe-B sintered magnets exhibiting a nominal energy product of $\sim$ 35 MGOe and low intrinsic coercivity, and those with dysprosium and cobalt additions typically resulting in $\sim$ 30 MGOe with approximately double the coercivity. A total of eight different brand types were provided by these producers for evaluation. A comparison of the range of characteristic intrinsic and normal demagnetization curves of each type is illustrated in Figure 1.

All magnet samples received were axially orientated cylindrical rods 6.35 mm in diameter, and were prepared from larger production blocks by the producers. These pieces were then sliced with a slow-speed diamond wheel saw to lengths corresponding to open-circuit unit permeances required in the long-term stability evaluation. Unfortunately, at the time this task was initiated, magnet samples were in short supply. As a consequence, only one test sample of each type and permeance at each exposure temperature was incorporated in the evaluation.

All test magnets were pulse magnetized with a 100 kOe peak field prior to measurement using a dc hysteresigraph for samples with length to diameter ratios $\geq 0.42$, and an oscillating sample magnetometer for samples with a ratio $<0.42$. Initial demagnetization curves were recorded and salient magnetic properties determined for all test magnets for comparison at the conclusion of the evaluation. The initial data indicated consistent salient properties within each brand type.

Irreversible and long-term aging losses of flux were measured with the instrumentation system and fixture shown in Figure 2. This system consists of a close fitting pull-coil, a precision electronic rectifier, and integrating digital voltmeter (±0.005% accuracy and resolution to ±0.1 μV-sec.) for sensing the induced signal in the coil that is proportional to the open-circuit remanent flux. A digital temperature indicator (0.1°C) is used to monitor the sample temperature each time a measurement is made. In practice a measurement sequence is initiated starting with fully magnetized test magnets to obtain a reference value of open-circuit remanent flux at room temperature. Subsequent measurements are performed at preset elapsed time intervals of thermal exposure in air, after the magnets have cooled to room temperature for several hours. A computer program takes each successive data entry for a particular sample, logs the information, and proceeds to correct the data for the instantaneous background noise or drift (typically less than ±0.2 μV-sec.) and ambient temperature, using the appropriate magnet alloy's reversible temperature coefficient. The corrected data point is then normalized to unity using the value after 1 hour of exposure as the reference for aging stability data. Irreversible losses were determined as a comparison of the loss incurred in the first hour of exposure for each magnet type and permeance. The test magnets were not remagnetized between exposure intervals.

Typical results for best and worst case irreversible losses as a function of permeance and temperature for the three alloy compositions are given in Table 2, and further illustrated in Figures 3-5.

The results of long-term aging losses of open-circuit remanent flux are shown as composite plots for each alloy composition in Figures 6-7. At the conclusion of the long-term stability evaluation, the intrinsic demagnetization curves were remeasured in the "as aged" condition first, then remagnetized and plotted again to observe any irrecoverable losses that may have occured as a consequence of the duration of thermal exposure levels and permeance. These observations are shown in the composite Figures 9-11. The irrecoverable losses of remanent induction and intrinsic coercivity observed for each type are listed in Tables 3-5.

In summary, it may be said that the properties found in this evaluation can be considered as typical of current commercial production magnets made from these or similar compositions. These results indicate that there are very restrictive operational limits imposed by a combination of elevated temperatures $\geq$ 125°C and unit permeance values $\leq$ 1 that must be taken into consideration.

Irreversible loss data indicate that a severe decrease in flux will be encountered when exposing neodymium and neodymium-dysprosium magnets operating at low permeance to temperatures above 100°C, even though this is well within the nominal operating range reported by the manufacturers. However, flux losses observed on magnets containing dysprosium and cobalt were minimal by comparison and similar to those reported for $SmCo_5$ for the temperature range tested, i.e., <150°C.

Long-term aging losses observed also show the same relationship as a function of these two variables with time. Further examination of the data also indicates that magnets of the same composition having higher intrinsic coercivity and better loop squareness suffer less degradation than those with comparatively lower values.

The overall effects of thermal exposure on the characteristic demagnetization curves clearly illustrate the operational limits imposed on each material type. Magnets made from ternary alloy show substantial losses in induction and changes in magnetization curve shape with increasing levels of temperature. Magnets modified with dysprosium show some improvement, but are still unfavorable for applications that require operating near the maximum energy product. The addition of cobalt substantially improves the long-term performance. From these results, one should not construe that magnets with cobalt additions can be operated at substantially higher temperatures. The thermal dependency of coercivity and, therefore, operating point must also be taken into consideration in any given application.

There is one final observation not generally noted with RE-Co permanent magnets operating at these temperatures: the so-called irreversible loss of induction was not fully recoverable when the samples were remagnetized and measured again under the same conditions. This also applies to the intrinsic coercivity. The irrecoverable part of the loss depends upon the combination of exposure variables: it increases with increasing temperature and is inversely related to the permeance.

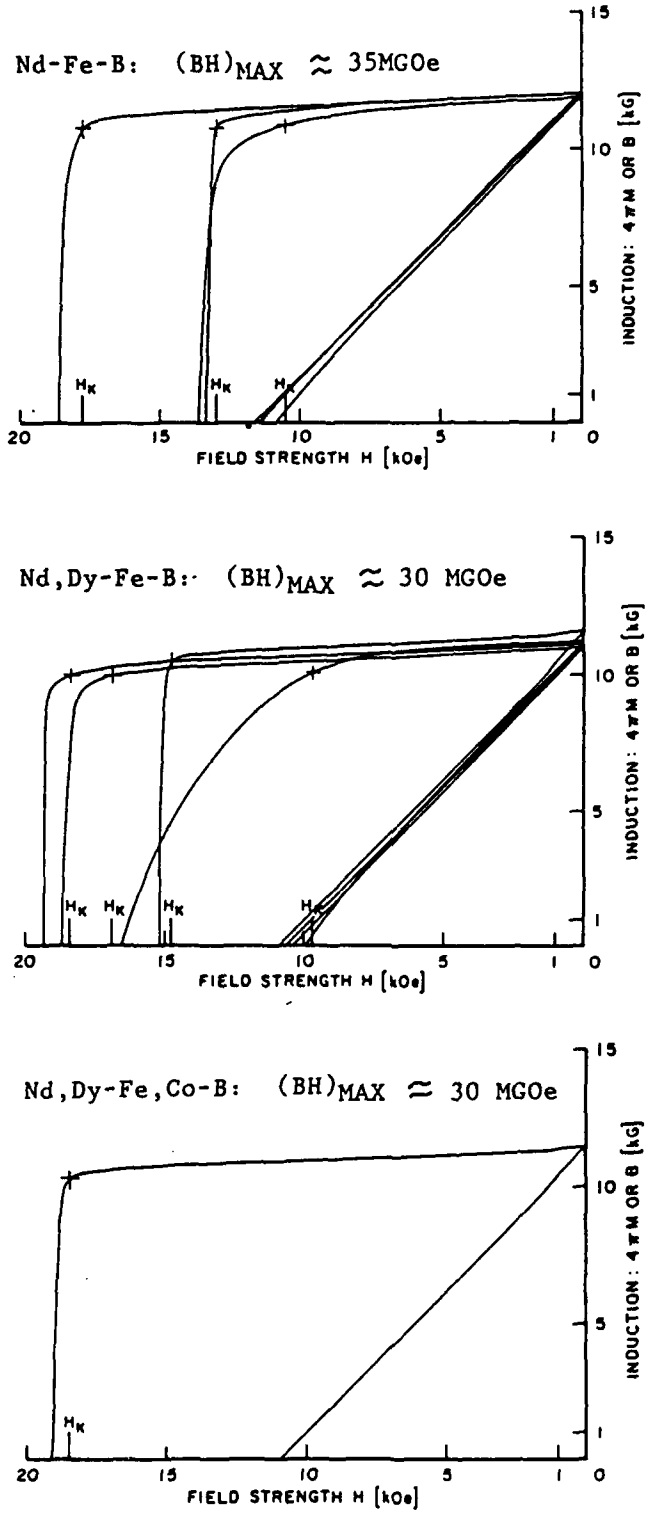


Figure 1 Typical intrinsic and normal demagnetization curves of eight commercial sintered "Nd-Fe-B type" permanent magnets used in this evaluation.

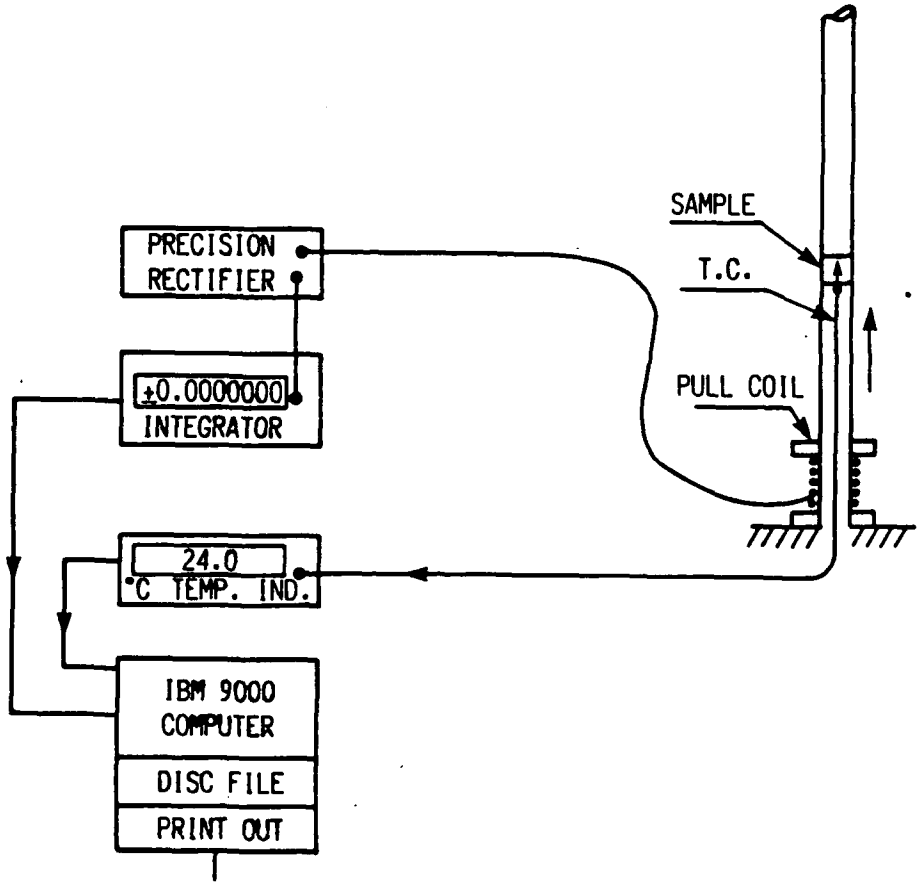


UNIVERSITY OF DAYTON MAGNETICS LAB. DATE: _____

PULL COIL MEASUREMENTS - OPEN CIRCUIT REMANENT FLUX

MAGNET SOURCE: XYZ MATERIAL TYPE: Nd-B-Fe
REFERENCE TEMPERATURE: 25 C
TEMPERATURE COEFFICIENT: -0.10
AGING TEMPERATURE: RT HOURS AGE: 0

| SAMPLE NO. | CORRECTED VALUE (Vs) | MEASURED TEMPERATURE (C) | ACTUAL VALUE (Vs) | PERCENT LOSS (%) |
|---|---|---|---|---|
| 1 | .60546E-02 | 27.4 | .606913E-02 | --- |
| 5 | .25645E-02 | 27.4 | .257065E-02 | --- |
| 9 | .11832E-03 | 27.4 | .118604E-03 | --- |
| 13 | .66227E-02 | 27.5 | .663926E-02 | --- |

Figure 2 Ambient temperature open-circuit remanent flux pull-coil measurement system and data log.

TABLE 2: RANGE OF INITIAL IRREVERSIBLE LOSS (1 HOUR) OF OPEN CIRCUIT REMANENT FLUX, AS A FUNCTION OF PERMEANCE AND ELEVATED TEMPERATURE

Nd-Fe-B: $(BH)_{MAX} \approx 35$ MGOe

| | EXPOSURE TEMPERATURE IN AIR | | | |
|---|---|---|---|---|
| $-B_d/H_d$ | 75°C | 100°C | 125°C | 150°C |
| 3.2 | 0.4 - 0.5 | 1.0 - 2.0 | 3.0 - 8.0 | 12 - 27 |
| 1.0 | 1.6 - 2.1 | 9.0 - 18 | 22 - 38 | 41 - 57 |
| 0.5 | 9.5 - 14 | 22 - 33 | 37 - 60 | 56 - 76 |

Nd,Dy-Fe-B: $(BH)_{MAX} \approx 30$ MGOe

| | EXPOSURE TEMPERATURE IN AIR | | | |
|---|---|---|---|---|
| $-B_d/H_d$ | 75°C | 100°C | 125°C | 150°C |
| 3.2 | 0.1 - 0.6 | 0.4 - 0.7 | 1.0 - 2.2 | 1.5 - 10 |
| 1.0 | 0.3 - 0.7 | 1.0 - 5.5 | 2.0 - 12 | 11 - 25 |
| 0.5 | 0.7 - 1.5 | 2.3 - 15 | 9.5 - 26 | 28 - 43 |

Nd,Dy-Fe,Co-B: $(BH)_{MAX} \approx 30$ MGOe

| | EXPOSURE TEMPERATURE IN AIR | | | |
|---|---|---|---|---|
| $-B_d/H_d$ | 75°C | 100°C | 125°C | 150°C |
| 3.2 | 0.24 | 0.41 | 0.47 | 0.55 |
| 1.0 | 0.24 | 0.53 | 0.75 | 1.00 |
| 0.5 | 0.44 | 0.89 | 1.00 | 3.60 |

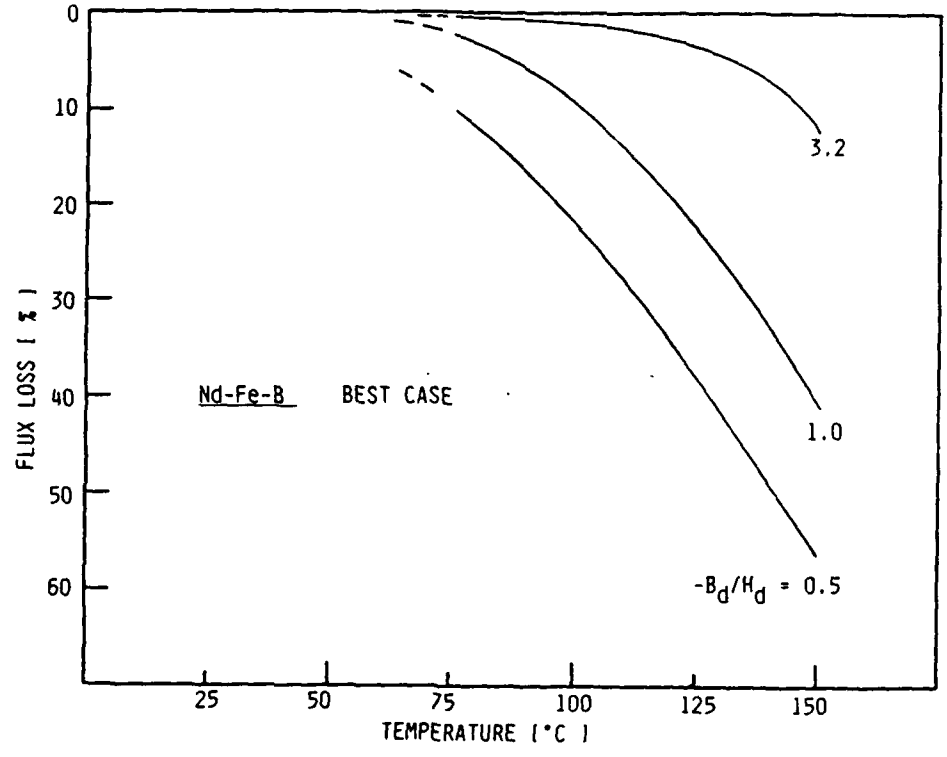


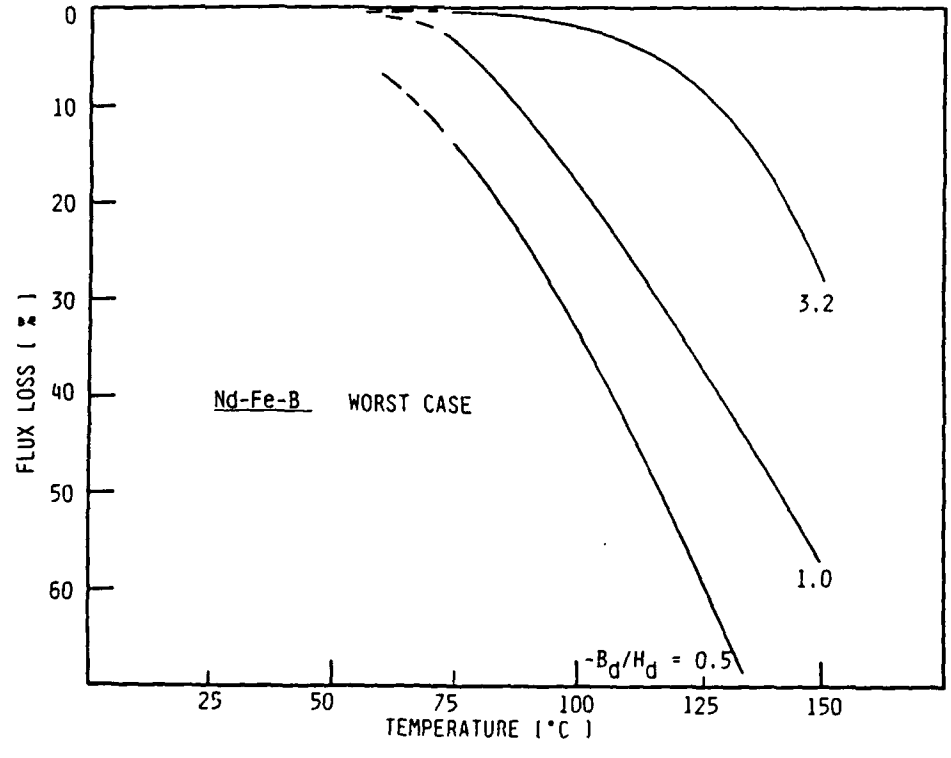


Figure 3 Best-and worst-case variation of initial irreversible loss in open-circuit remanent flux for sintered Nd-Fe-B magnets as a function of permeance and temperature.

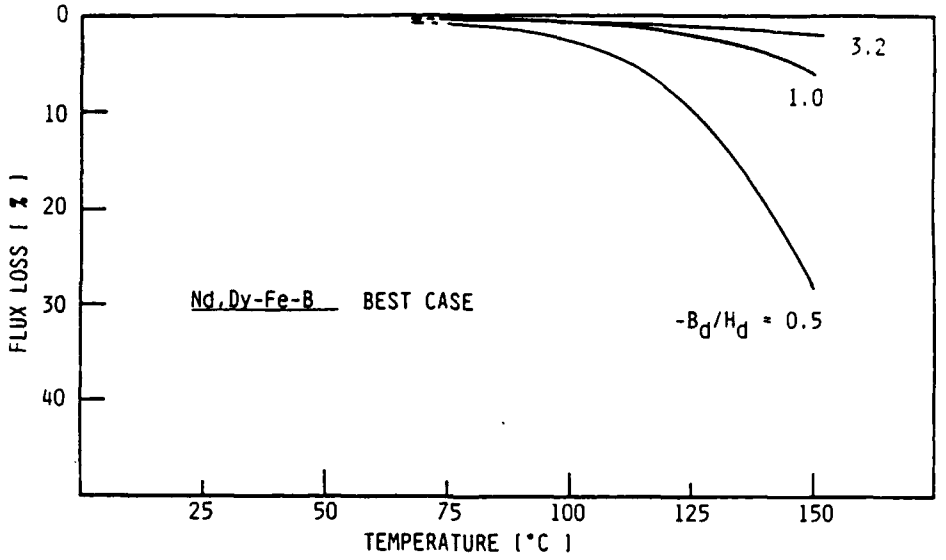


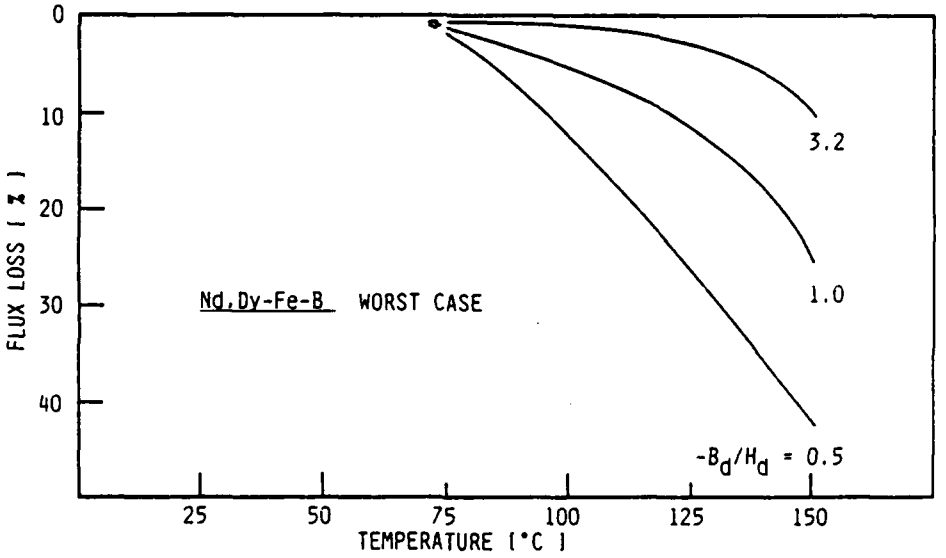


Figure 4 Best- and worst-case variation of initial irreversible loss in open-circuit remanent flux for sintered Nd,Dy-Fe-B magnets as a function of permeance and temperature.

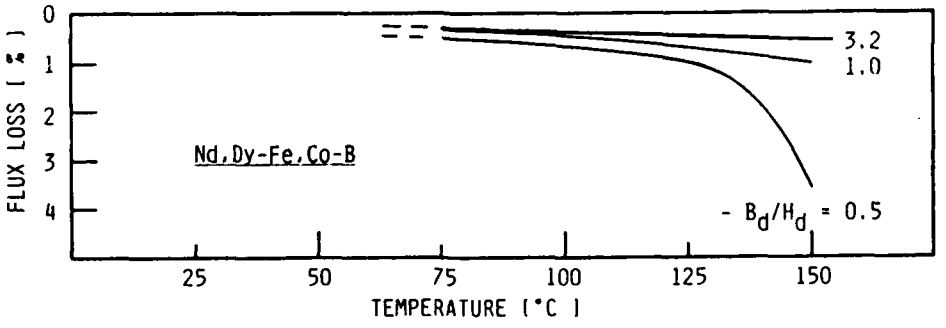


Figure 5 Variation of initial irreversible loss in open-circuit remanent flux for sintered Nd,Dy-Fe,Co-B magnets as a function of permeance and temperature.

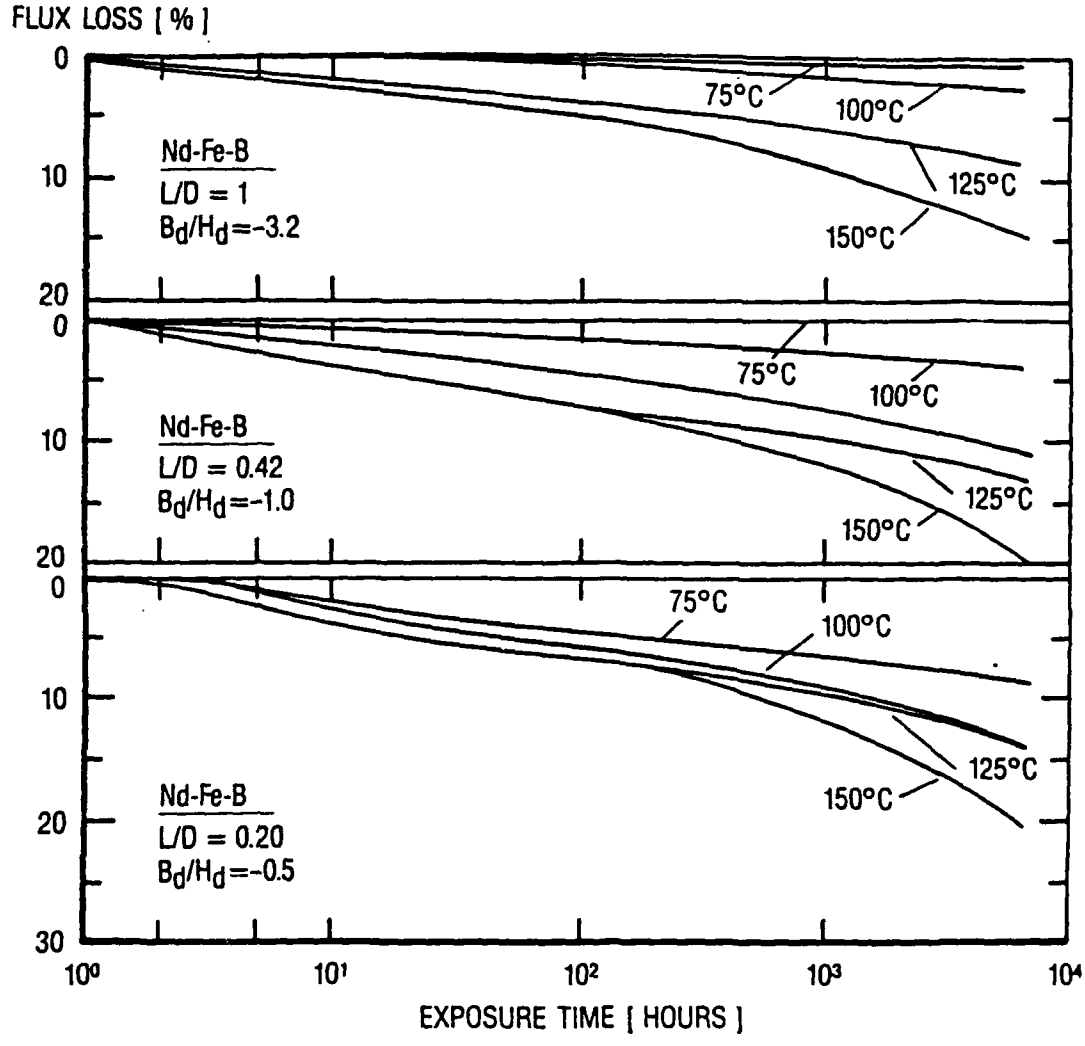


Figure 6 Long-term stability (>5,000 hours) of open-circuit remanent flux of Nd-Fe-B permanent magnet alloys as a function of elevated temperature exposure between 75° and 150° C, and unit permeance $B_d/H_d$ of -3.2, -1 and -0.5.

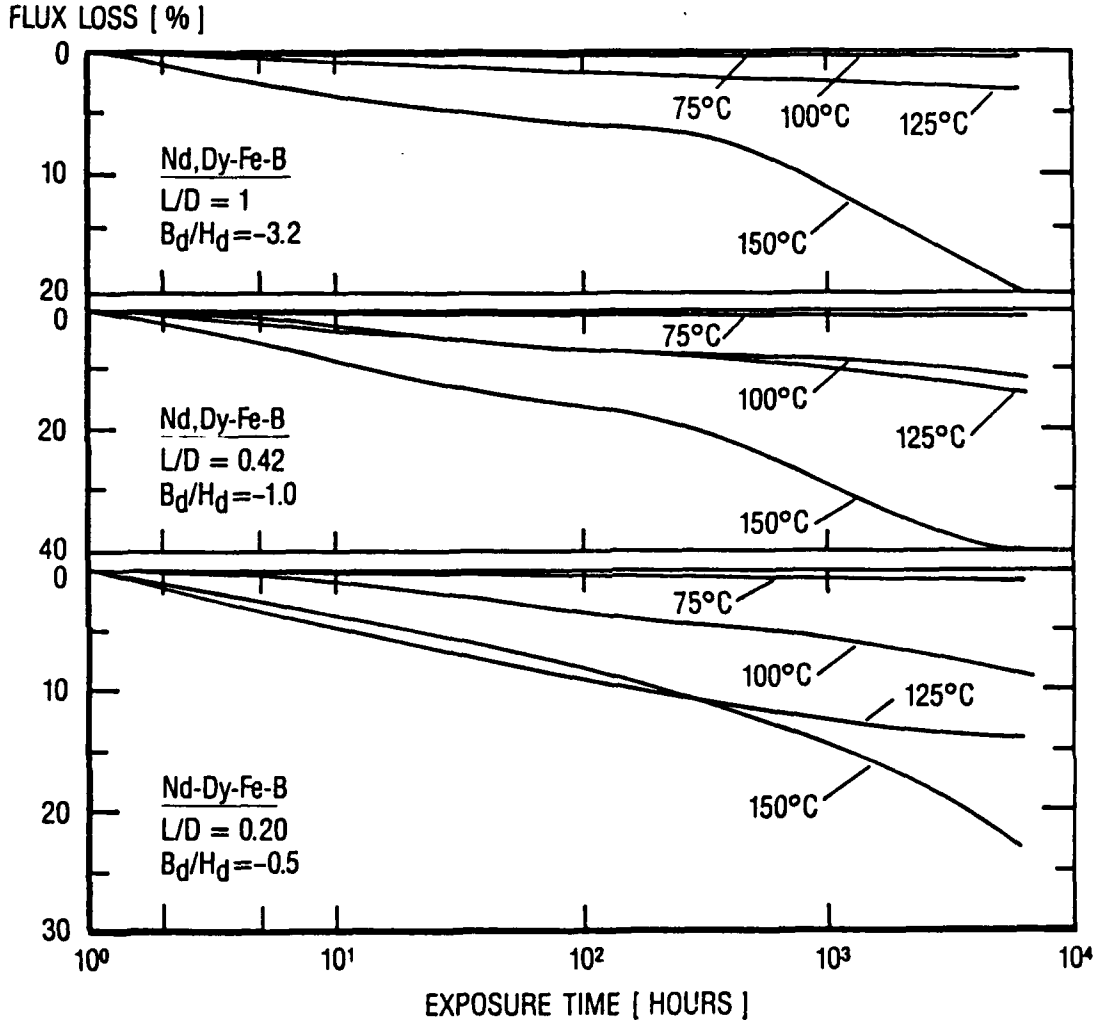


Figure 7 Long-term stability (>5,000 hours) of open-circuit remanent flux of Nd,Dy-Fe-B permanent magnet alloys as a funtion of elevated temperature exposure between 75° and 150° C, and unit permeance $B_d/H_d$ of -3.2, -1 and -0.5.

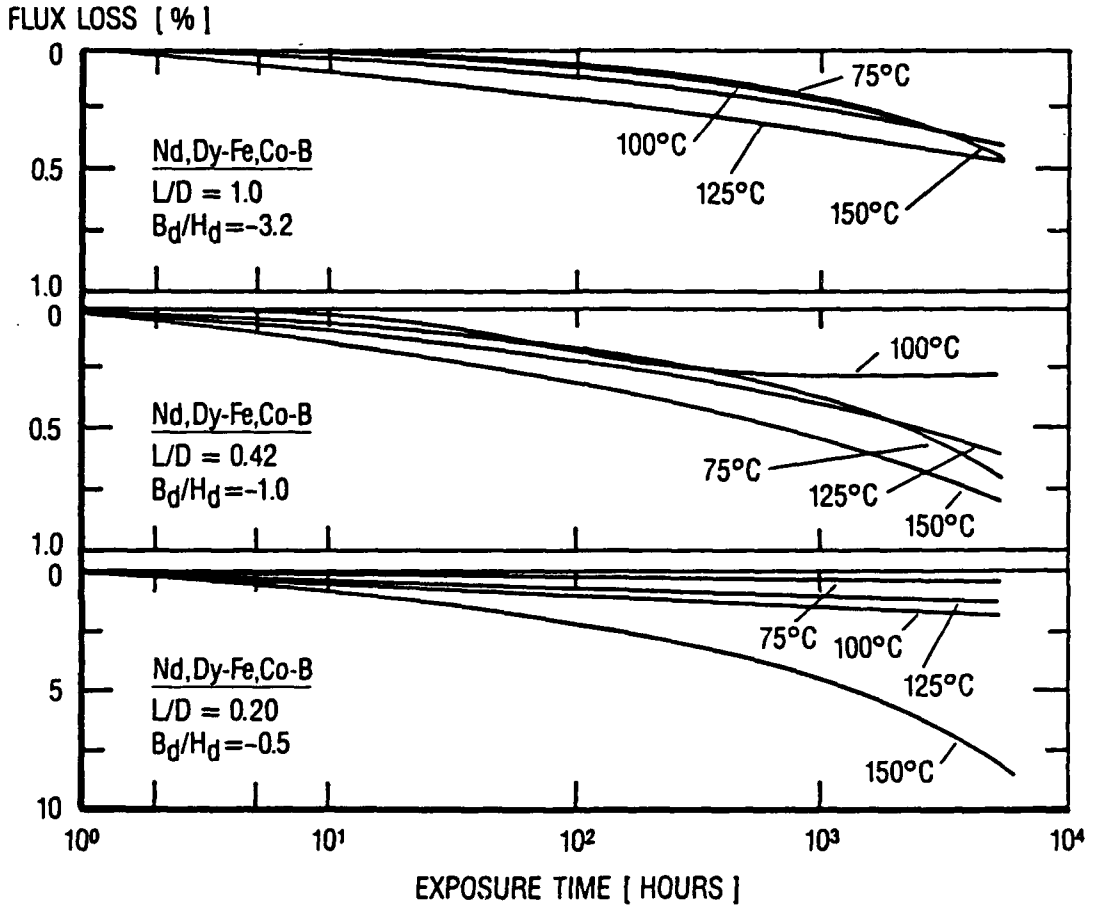


Figure 8 Long-term stability (>5,000 hours) of open-circuit remanent flux of Nd,Dy-Fe,Co-B permanent magnet alloys as a funtion of elevated temperature exposure between 75° and 150° C, and unit permeance $B_d/H_d$ of -3.2, -1 and -0.5.

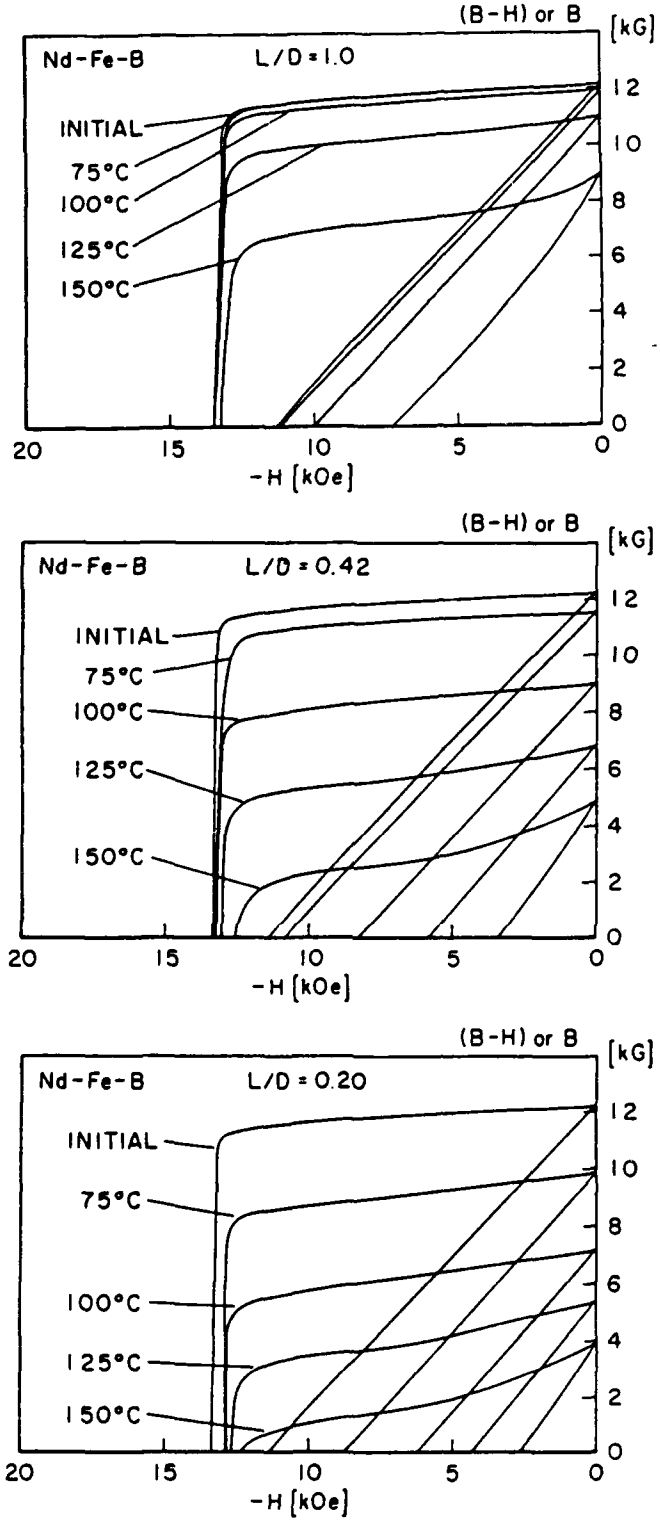


Figure 9 Thermally induced changes in the intrinsic and normal demagnetization curves after long-term aging (>5,000 hours) of Nd-Fe-B sintered magnets as a function of type, temperature, and sample L/D ratios pertaining to an open-circuit permeance B/H = -3.2, -1.0, -0.5.

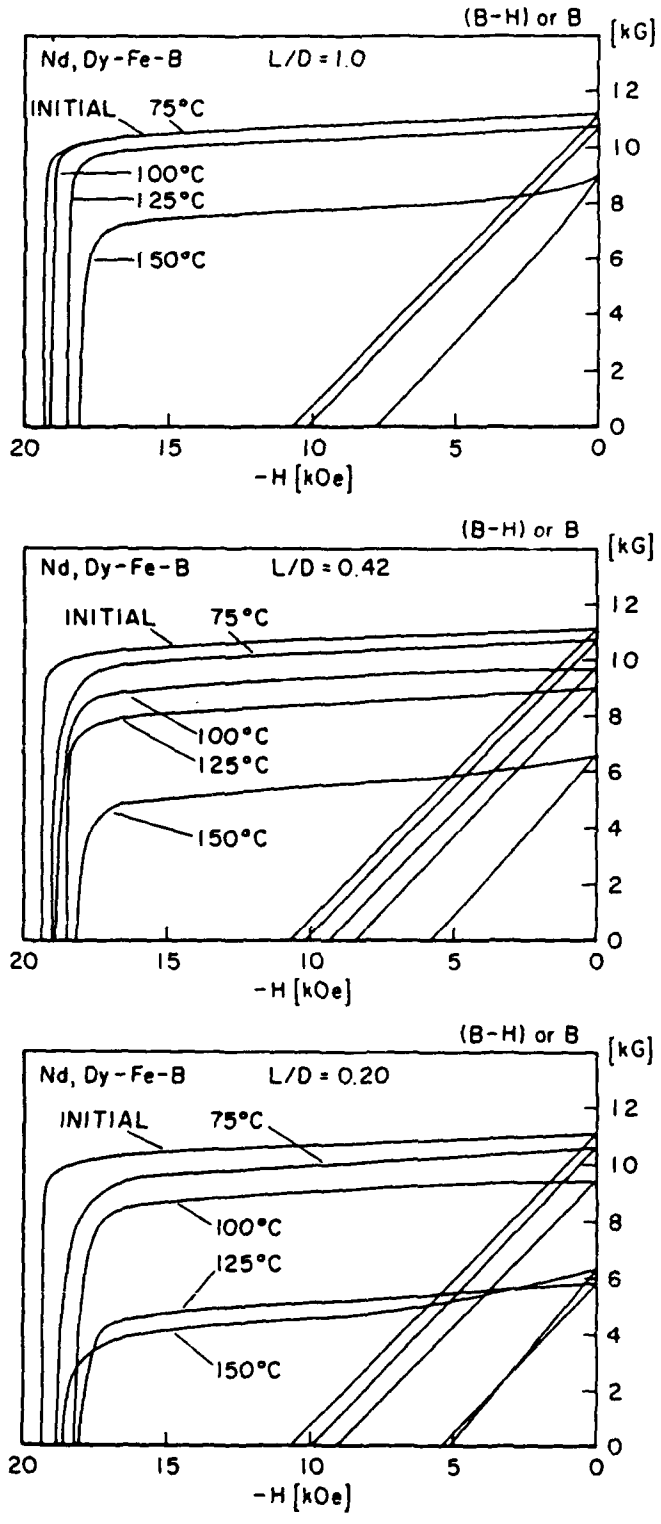


Figure 10 Thermally induced changes in the intrinsic and normal demagnetization curves after long-term aging (>5,000 hours) of Nd,Dy-Fe-B sintered magnets as a function of type, temperature, and sample L/D ratios pertaining to an open-circuit permeance B/H = -3.2, -1.0, -0.5.

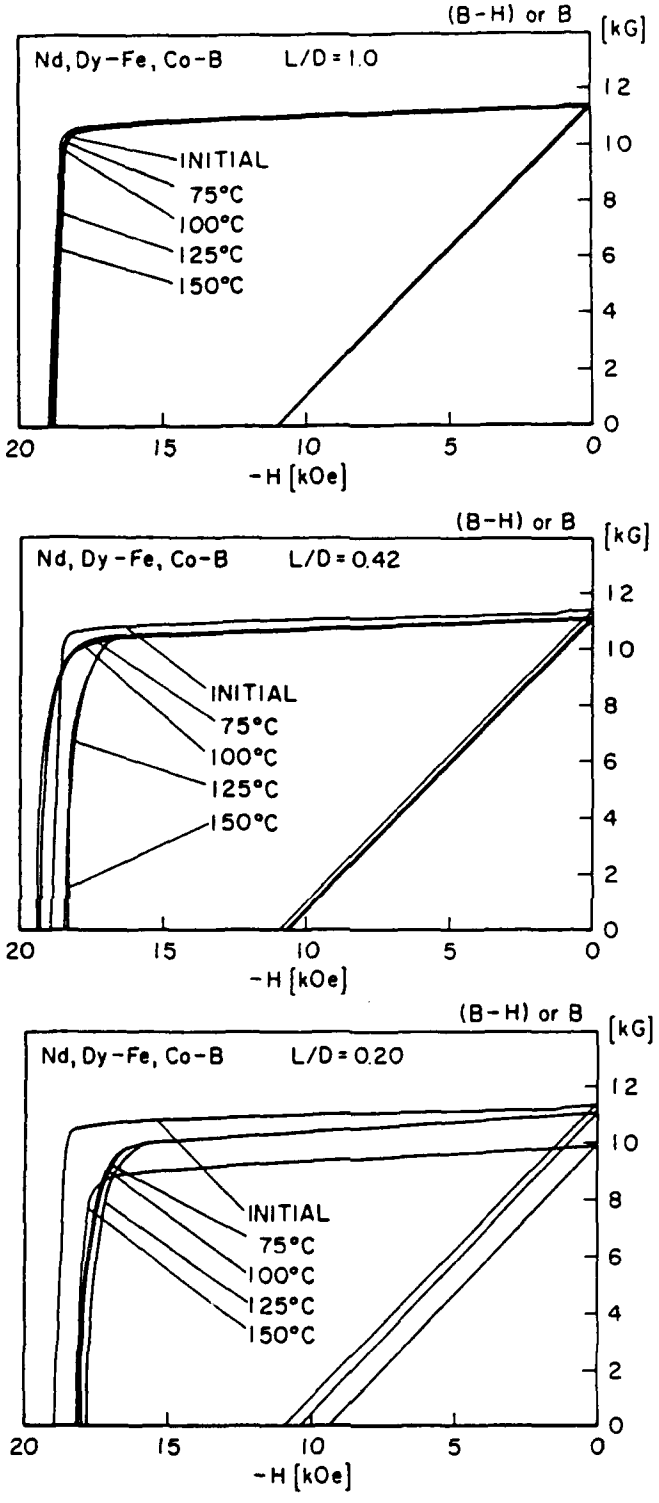


Figure 11 Thermally induced changes in the intrinsic and normal demagnetization curves after long-term aging (>5,000 hours) of Nd,Dy-Fe,Co-B sintered magnets as a function of type, temperature, and sample L/D ratios pertaining to an open-circuit permeance B/H = -3.2, -1.0, -0.5.

TABLE 3 PERCENT RECOVERABLE IRREVERSIBLE LOSS AFTER LONG-TERM THERMAL AGING FOR 5000 HOURS AND REMAGNETIZATION.[1]

Nd-Fe-B: $(BH)_{max} \approx 35$ MGOe

| Manufacturer and Type | 2) $-B_d/H_d$ | Property | Exposure Temperature [°C] 75 | 100 | 125 | 150 |
|---|---|---|---|---|---|---|
| Sumitomo Special Metals Neomax-35 | 3.2 | $B_r$ | 98 | 98 | 99 | 90 |
| | | $_MH_c$ | 100 | 100 | 100 | 100 |
| | 1.0 | $B_r$ | 100 | 100 | 100 | 100 |
| | | $_MH_c$ | 98 | 98 | 98 | 95 |
| | 0.5 | $B_r$ | 100 | 100 | 100 | 100 |
| | | $_MH_c$ | 95 | 94 | 100 | 92 |
| Crucible Magnetics Crumax-35 | 3.2 | $B_r$ | 100 | 100 | 100 | 100 |
| | | $_MH_c$ | 100 | 100 | 100 | 100 |
| | 1.0 | $B_r$ | 100 | 100 | 100 | 100 |
| | | $_MH_c$ | 100 | 100 | 96 | 95 |
| | 0.5 | $B_r$ | 100 | 100 | 100 | 100 |
| | | $_MH_c$ | 96 | 97 | 95 | 95 |

1) Percent recoverable based on initial salient magnetic property values.
2) Permeance values correspond to L/D ratios of 1.0, 0.42, and 0.20, respectively.

TABLE 4 PERCENT RECOVERABLE IRREVERSIBLE LOSS AFTER LONG-TERM THERMAL AGING FOR 5000 HOURS AND REMAGNETIZATION.[1]

Nd,Dy-Co,Fe-B: $(BH)_{max} \approx 30$ MGOe

| Manufacturer and Type | 2) $-B_d/H_d$ | Property | Exposure Temperature [°C] 75 | 100 | 125 | 150 |
|---|---|---|---|---|---|---|
| Hitachi Magnetics Hicorex Nd-94S | 3.2 | $B_r$ | 99 | 99 | 99 | 99 |
| | | $_MH_c$ | 100 | 99 | 99 | 90 |
| | 1.0 | $B_r$ | 100 | 100 | 100 | 99 |
| | | $_MH_c$ | 100 | 100 | 97 | 96 |
| | 0.5 | $B_r$ | 99 | 100 | 100 | 99 |
| | | $_MH_c$ | 96 | 96 | 95 | 96 |

1) Percent recoverable based on initial salient magnetic property values.
2) Permeance values correspond to L/D ratios of 1.0, 0.42, and 0.20, respectively.

TABLE 5 PERCENT RECOVERABLE IRREVERSIBLE LOSS AFTER LONG-TERM THERMAL AGING FOR 5000 HOURS AND REMAGNETIZATION.[1]

Nd,Dy-Fe-B: $(BH)_{max} \approx 30$ MGOe

| Manufacturer and Type | 2) $-B_d/H_d$ | Property | Exposure Temperature [°C] 75 | 100 | 125 | 150 |
|---|---|---|---|---|---|---|
| Sumitomo Special Metals Neomax-30H | 3.2 | $B_r$ | 100 | 98 | 98 | 98 |
| | | $_MH_c$ | 100 | 100 | 100 | 100 |
| | 1.0 | $B_r$ | 100 | 100 | 100 | 97 |
| | | $_MH_c$ | 100 | 95 | 94 | 98 |
| | 0.5 | $B_r$ | 100 | 100 | 100 | 100 |
| | | $_MH_c$ | 100 | 92 | 94 | 95 |
| Crucible Magnetics Crumax-30A | 3.2 | $B_r$ | 100 | 99 | 99 | 99 |
| | | $_MH_c$ | 100 | 98 | 99 | 97 |
| | 1.0 | $B_r$ | 97 | 97 | 99 | 99 |
| | | $_MH_c$ | 99 | 80 | 99 | 64 |
| | 0.5 | $B_r$ | 98 | 97 | 98 | 98 |
| | | $_MH_c$ | 94 | 94 | 94 | 97 |
| Crucible Magnetics Crumax-30B | 3.2 | $B_r$ | 100 | 99 | 99 | 99 |
| | | $_MH_c$ | 100 | 100 | 100 | 100 |
| | 1.0 | $B_r$ | 98 | 98 | 99 | 99 |
| | | $_MH_c$ | 98 | 98 | 97 | 95 |
| | 0.5 | $B_r$ | 100 | 100 | 100 | 100 |
| | | $_MH_c$ | 97 | 93 | 98 | 93 |
| Hitachi Magnetics Hicorex Nd-94EA (Parallel Pressed) | 3.2 | $B_r$ | 99 | 99 | 99 | 99 |
| | | $_MH_c$ | 100 | 100 | 100 | 100 |
| | 1.0 | $B_r$ | 98 | 98 | 100 | 99 |
| | | $_MH_c$ | 100 | 94 | 97 | 95 |
| | 0.5 | $B_r$ | 96 | 98 | 99 | 97 |
| | | $_MH_c$ | 90 | 95 | 95 | 91 |
| Hitachi Magnetics Hicorex Nd-94EB (Transverse Pressed) | 3.2 | $B_r$ | 99 | 98 | 99 | 98 |
| | | $_MH_c$ | 100 | 99 | 96 | 100 |
| | 1.0 | $B_r$ | 99 | 98 | 97 | 97 |
| | | $_MH_c$ | 95 | 98 | 88 | 90 |
| | 0.5 | $B_r$ | 99 | 97 | 97 | 91 |
| | | $_MH_c$ | 90 | 95 | 89 | 90 |

1) Percent recoverable based on initial salient magnetic property values.
2) Permeance values correspond to L/D ratios of 1.0, 0.42, and 0.20, respectively.

## 4.2. Task B: Nd-Fe-B Magnet Preparation and Property Optimization

In the Spring of 1985, we began to prepare sintered magnets from ternary Nd-Fe-B alloy in our laboratory, simultaneously with the first characterization efforts on commercial prototype magnets, using the same techniques and equipment that had worked for Sm-Co 1-5 and 2-17 magnets, namely; crushing in a steel mortar, grinding in a small double-disc pulverizer and a small attritor mill; sifting, handling and compacting the fine powders in air, then outgassing, sintering, and heat treating in an excellent high vacuum/argon/hydrogen tube furnace system. The vehicle was a single alloy prepared and kindly provided to us by the nearby laboratory of Delco Products, a GMC Division which had also begun working on rare-earth magnets. The magnet fabrication parameters, such as particle sizes, sintering, and heat-treating temperatures and times, were gleaned from the early publications and a patent application by SSMC.

We succeeded quickly, after only a few attempts, in preparing magnet samples with 29 MGOe energy product that also had otherwise respectable magnetic properties at RT. We concluded that it was basically easier to make sintered Nd-Fe-B than Sm-Co-based magnets. However, we also encountered several difficulties, which indicated that certain techniques that are quite adequate for Sm-Co are unsatisfactory when working with Nd-Fe-based alloys: it proved difficult to get good density in sintering, and the micron-particle powders showed an increased propensity to spontaneously ignite or at least heat up. This also implied that cleaner grinding and handling methods were needed than for Sm-Co, and that fine powders that are to be stored for some time at RT should be kept in a good vacuum or a highly oxygen and moisture-free protective atmosphere. Indeed, early troubles with poor reproducibility of properties achieved in sintering could be traced to unpredictable particle surface oxidation during storage. The iron alloys are also much tougher and harder to crush or coarse-grind than Sm-Co.

When the existence of these new difficulties was realized, we devoted much effort and considerable funds to improving our laboratory facilities for magnet fabrication. In the next subchapter, 4.3., we discuss what was done in this regard. A delay of nearly a half year was caused in the magnet preparation and alloy modification tasks by the need to acquire, install, and learn how to use a number of new laboratory tools. During this time we also concentrated on the effort discussed about the characterizing magnets obtained from other laboratories.

The magnet fabrication work resumed in the Spring of 1986; with the help of the new powder handling equipment and improved powder metallurgical techniques the abovementioned difficulties had by then been largely overcome. We could now reproducibly make good magnets

from ternary Nd-Fe-B alloys, with well over 30 MGOe energy product, a good demagnetization curve shape and improved density. Similar results could be achieved using the Delco Products material and a ternary alloy produced by Dr. A.E. Ray at the University of Dayton by induction melting and chill casting. The Task-B objective of reproducing the results reported in 1983/84 from Japan, and of developing a good laboratory methodology for making sintered Nd-Fe-B-type magnets, had thus been achieved, although considerably later than we had originally hoped. Data for the magnetic properties of our ternary Nd-Fe-B magnets are included in several places in later sections herein, reporting the results of alloy modification work; this alloy was included as a terminal or reference composition in several of the alloy series investigated.

### 4.3 Requisite Development of Processing Methods and Laboratory Facilities

The following equipment was acquired, modified as necessary, and installed to improve our powder metallurgical fabrication capabilities. Some improvements were needed to make our techniques adequate for use with Nd-Fe-B type alloys. The purpose of others was to make available alternative methods of fine powder grinding (an attritor mill) and of compaction (an isostatic press) which have become common production tools in the rare-earth magnet industry. Using these in our development work will facilitate the transfer of any useful new technology into commercial production.

Two vacuum storage chambers for powders were built to our specifications and equipped with a fast high-vacuum pumping system and provisions for backfilling with protective gas. A separate new chamber that has only a mechanical roughing pump is used for the quick drying of powders milled in an organic fluid. A vacuum glove box, available in the laboratory but long unused, was also refurbished and put back into operation.

For better comminution of the alloy into the requisite fine powders of several micron particle size (with the added capability of working on a somewhat larger scale than in the past) we acquired three new grinding machines designed for laboatory use:

(1) a jaw crusher for producing millimeter-size grains from alloy ingots,
(2) a roller mill capable of reducing these grains further to particles in the 10 to 100 μm range suitable as feed material for the final pulverizing step,
(3) a fluid-energy (jet) mill for the production of fine powders suitable for compaction and sintering. The mill we bought has a 2-inch diameter grinding chamber and is the smallest such unit built.

The funds for items 1 and 2 had been budgeted under this contract. The jetmill, item 3, was purchased with funds under another Army-sponsored project--an ARO grant under which concurrent work was done on 2-17 type Sm-Co magnets that requires similar equipment and methods. The coarse grinding devices 1 and 2 were modified to allow feeding, crushing and collecting the alloy under a protective gas blanket, usually dry nitrogen gas. For the roller mill, which imparts a lot of energy to the powder and heats the particles so that they sometimes ignite, a collection pan was built that can be cooled with liquid nitrogen to prevent fires in the mill. The jet mill was installed inside a low-pressure glove box which must be filled with nitrogen gas to prevent aspiration of air into the grinding chamber. Dry and oxygen-free nitrogen is also used as the working fluid. A special manifold had to be built which permits the use of up to six pressure cylinders and which has valves, pressure reducers and flowmeters to permit the needed control of the flow rate and pressure of the gas jets.

Using the jet mill properly is not a simple matter and requires much experience. Considerable time and material were invested in learning how to produce useful powders and good sintered magnets from them. Since we had much more experience making magnets from this alloy than from Nd-Fe-B, 2-17 Sm-Co alloys were used as the learning vehicle for this. We eventually succeeded in making magnets with higher energy and better loop shape in this way, compared with those made from ball- or attritor-milled powders. The advantages of the jetmill are that it yields dry powder which is not contaminated with toluene, alcohol, or acetone, and, therefore, does not require a separate drying step, and that the powder can have a very narrow particle size distribution. However, that latter result--and its good reproducibility--hinges on achieving a steady-state operation of the mill. This requires a reasonably long operating time; our very small mill consumes some 100 gram of powder before it yields reliably reproducible powder properties. We, therefore, still often resort to using the traditional ball-milling methods in preliminary evaluation experiments, where only a small quantity of alloy powder (typically 50 to 100 g) is available for each mill run.

Another newly acquired tool was an isostatic press. This was also purchased with ARO grant funds and was used under both programs. Isostatic compaction (at room temperature) of pulse-premagnetized powders can yield better grain alignment and greater density after sintering than diepressing does, hence more anisotropic magnets with somewhat higher remanence and energy product. Working together with a local industrial laboratory we successfully developed procedures for making Nd-Fe-B magnets in sample sizes up to 1-1/4" x 1-1/4" x 8" long and 2-1/8" diameter x 6" long. A typical mold size used frequently in the present program was 1-1/4" square x 3/4", magnetized in the short direction. After sintering, four hysteresigraph samples of our standard 0.5" cube size could be cut from such a piece and subjected to different heat treatments or other process variations.

## 4.4 Task C: Sintered Magnets from Cobalt-Modified Alloys

The next step in the original proposal specified a study of the effects of a partial replacement of Fe by Co, and the development of a reasonably optimized recipe for making high-coercivity sintered magnets from such a Co-modified alloy. In the meantime, work along these lines had been done in several laboratories in the United States, Japan, Austria, and China, with good agreement on the effects: cobalt substitution for iron up to 100 percent was possible in the 2-14-1 phase; Co initially raises the Curie temperature at a rate of about 1.0 to 1.2°C per atomic percent (referred to total transition metal content), with the rate decreasing steadily as the Co content increases; the saturation magnetization was found to increase slightly and be almost independent of the Co content up to about 25 percent, then it begins to decrease. Sintered magnets could be prepared in a very similar way to Co-free magnets, but their intrinsic coercive force dropped rapidly with increasing Co content, so that more than a 10 to 15 percent Co substitution seemed out of the question. It was also well-known at that time that the partial replacement of Nd by Dy in an otherwise ternary Nd-Fe-B magnet had the effect of substantially raising the coercivity. Thus, it seemed that dysprosium additions to Nd-Fe-Co-B might be used to partially or completely offset the adverse effect of Co on $H_c$. It had, furthermore, been reported that aluminum additions had a similar effect to dysprosium, dramatically raising the intrinsic coercive force at room temperature.

With view toward improving the elevated temperature properties of magnets, the introduction of cobalt in the alloy should be beneficial, because it reduces the magnitude of the (negative) temperature coefficient (TC) of the saturation and thus, potentially, the TC of the remanence, $\alpha(B_r)$. But at, say, 12 percent Co (again of the total transition metal content), the coercivity reduction is so severe that at 150°C such magnets are indeed less suited for tube applications than those without Co. On the other hand, dysprosium substitution for Nd leaves the Curie point unchanged, so that the coercivity increase in the 150 to 200°C temperature range is not what it might be if $T_c$ were higher.

In view of these reports we decided not to spend much time working with cobalt or dysprosium additions alone. Instead, we wanted to proceed as quickly as possible to work with multiple substituents, starting with compositions that had Dy in addition to Co, and then investigating the potential of Al for improving the elevated-temperature behavior. When Al proved disappointing for this purpose, we looked into several alternatives, namely, Nb, Ti and Zr. The influence of erbium substituting for part of the rare earth was also investigated.

We quickly succeeded in preparing sintered magnets with several levels of Co addition, essentially reproducing the results achieved in other laboratories. In coordination with Hitachi/HML workers, who also supplied some of their samples for this work, we then settled

on a standard level of Co for the further investigations. This was $x = 0.12$ in terms of the alloy formula written as $Nd\ (Fe_{.92-x}Co_xB_{.08})_{5.5}$ or about 10 percent by weight of the total alloy. Magnets of this quaternary composition were found to have a main-phase Curie temperature of 435°C, in fair agreement with earlier reports, and a room temperature "saturation" of 12500 *Gauss*, measured at 15 kOe applied field with a vibrating sample magnetometer.

## 4.5. Sintered Magnets from Dy- and Er-Substituted Alloys

The alloy was now further modified by replacing some of the Nd by a heavy rare earth (HRE), with the intent of reducing the absolute value of the temperature coefficients, $\alpha(B_r)$ and $\beta(_MH_c)$. The different compositions were achieved conveniently by blending several master alloys in the form of ballmilled powders in the appropriate ratios, then magnetizing and isostatically compacting the blends, and sintering and heat treating the compacts. No (Nd,B)-rich "sintering aid" was used.

We first systematically investigated the effects of Dy substitution for up to 20 percent of the Nd. The results are reported in Appendix D. Briefly, the intrinsic coercive force at RT is raised from 7 to about 18 kOe, $\alpha(B_r)$ is lowered from -0.126 percent per °C for ternary Nd-Fe-B to -0.09 by the Co addition alone, and further to -0.068 by 20 percent Dy (all TC's are 0-150°C). $\beta(H_c)$ is almost unchanged near -0.55 percent per °C. There is the expected slight sacrifice of $B_r$ and $(BH)_{max}$.

The introduction of erbium reduces the coercivity again, as might be expected from the fact that Er favors easy-basal-plane anisotropy in the 2-14-1 compound, so that small amounts of Er must lower the anisotropy field. Within the 20 percent HRE level (of the total rare earths, TRE), we traded off Dy for Er. When the whole 20 percent was erbium (no Dy), the coercivity was down to 5 kOe, i.e., even a little less yet than for the Co alloy without any heavy RE. However, a small Er content, $\sim$ 4 percent of TRE, can be benefical: $B_r$ and $(BH)_{max}$ are slightly increased, $\alpha$ is reduced to -0.048 and $\beta$ to -0.46 percent per °C, while the RT coercivity remains acceptably high, at $\sim$ 12 kOe. All in all, Dy substitution alone is better for magnets that have to operate above 100°C at low permeance values; the said small Er content is better near room temperature because of the higher remanence and energy, and the lower temperature coefficients. Good square second-quadrant demagnetization curve shapes were obtained in all cases under the correct heat treatments as described in Appendix D.

## 4.6 Effects of Additional Minor Alloying Elements - Al, Nb, Zr, and Ti - on the Magnetic Properties of Sintered "Nd-Fe-B"

Next we explored the effects of small additions of aluminum on the properties of sintered magnets which were already modified with both Dy and Co. The hope was that one would be able to further

increase the $_{M}H_{c}$ in such a way that the hard-magnetic properties in the 100 to 200°C regime would be improved, too, especially the flux stability on heating and the reversible temperature coefficients. If aluminum had this desirable effect, it should then be possible to reduce the content of the expensive dysprosium.

This study is documented in Appendix E. The results were disappointing. Small Al additions do indeed bring a strong further increase of the intrinsic coercive force at room temperature, from 16 kOe without Al up to 19-24 kOe (in different samples) at 3 wt. percent Al. But this advantage is quickly lost on heating, since the $_{M}H_{c}$ drops off much more rapidly with increasing temperature: $\beta$ rises from 0.63 to nearly 0.9 percent per °C, and the coercivity above 140°C is indeed lower with Al than without. This is reflected in higher irreversible flux losses on thermal cycling to above this temperature. Curie point, remanence and its TC, and the energy product at RT are all adversely affected. It was our conclusion that aluminum may be a desirable additive for magnets to be used near the normal RT, but that it quickly loses its benefits at higher operating temperatures, and it seriously degrades the flux stability in the range where TWT magnets have to function. Al-modified magnets, thus, are not useful for such applications.

Keeping in mind the important improvements in coercity which zirconium additions brought to the 2-17 type Sm-Co magnets, we next explored the effects of adding minor amounts of Zr and of the similar elements, Nb and Ti, to sintered "Nd-Fe-B" magnets. Again, we tried to hold on to previously attained improvements of the elevated temperature behavior by working with Co and Dy-containing alloys, modifying them further with these transition elements. The generic formula of the alloys prepared under this subtask is $(Nd_{.88}Dy_{.12})\ (Fe_{.80-x}Co_{.12}B_{.08}M_{x})_{5.5}$, where M = Zr, Nb or Ti, and $x < 0.072$, corresponding to <6 atomic percent of M in the alloy. Procedures and results are documented in Appendix F.

It was indeed found that small additions of either of the three M-elements increase the coercive force, but that the benefit was significant only for niobium (Nb), where the optimal amount of three at percent raises $_{M}H_{c}$ from 11.5 to 17 kOe. Additions in excess of 3 percent Nb, or of 1 at percent of Zr or Ti, cause the coercivity to drop precipitously. It could be shown that this is due to a destabilization of the 2-14-1 phase with the accompanying formation of a magnetically soft 2-17 phase. In contrast to the effect found with aluminum, the increase of $_{M}H_{c}$ caused by Nb is maintained at higher temperatures ( $\alpha$ and $\beta$ between 0 and 150°C are almost unaffected), the Curie point remains nearly constant, and there is only a very minor reduction of saturation and $B_{r}$ at 3 percent Nb. We were able to prepare magnets with excellent loop squareness. In summary, a 3 at percent addition of Nb ($x = 0.036$) improves the utility of such magnets for TWT and similar applications at about 150°C.

Pursuing the questions of phase stability somewhat further, it was found that a slight increase in the neodymium (and total RE) content prevented the formation of the 2-17 phase and allowed the increase in the addition of niobium to at least 4 atomic percent without an adverse effect on coercivity and demagnetization curve shape. However, there is no practical advantage in doing this, as it slightly reduces remanence and energy product while increasing the alloy cost. This is discussed in some detail in the attached publication, Appendix G, which also summarizes the principal results of all the earlier substitution studies, with Co, Dy, Er, Al, and the Nb.

## 4.7 Scientific Contributions to the Understanding of the Physical Origins of High Coercivity

Controlling the intrinsic coercive and its temperature dependence is a central problem in improving permanent magnets in general, and particularly of the rare earth-iron-based magnets that concerned us in this present development effort. Coercivity is closely tied to the metallurgical microstructure of the magnets, and it is sensitively dependent on its very fine-scale features that are often beyond the resolution of even the best electron microscopes and microanalyzers now available. While the objective of this contract effort was defined in fairly applied terms--to improve the utility of Nd-Fe-B for elevated temperature applications--we conducted a number of experiments that were aimed primarily at a better understanding of the physical mechanisms that cause, or sometimes prevent, usefully high coercive forces. Some of the work described here and in the Appendices A and B is in this category.

Another set of basic-science experiments is described in Appendix H. While there is considerable disagreement among physicists--especially theoreticians--about the nature of the events controlling magnetization reversal, and thus the coercivity in rare earth magnets, we have long believed that the pinning of domain walls by (at or within) secondary magnetic phases in the grain boundary regions is the most important mechanism controlling coercivity in the $SmCo_5$-type sintered magnets, as well as those of the Nd-Fe-B family. A group at the Japanese Hitachi Metals Research Laboratory (Tokunaga, Harada, et al.) had recently done careful measurements of $_MH_c$ near the Curie point of the 2-14-1 phase in (Nd,Dy)(Fe,Co,B) sintered magnets, also interpreting their results in terms of a thin, and probably metastable, boundary layer of a ferromagnetic phase the exact composition and structural nature of which are still in question. We obtained their samples, which were of two different compositions and had been given several different heat treatments.

We devised an experiment that we believe is capable of probing for local magnetic properties, such as secondary-phase Curie points and the temperature dependence of the initial permeability, which reflects that of magnetization and anisotropy. This is done by means

of a low-field thermomagnetic analysis in the fully magnetized versus the thermally demagnetized states. The results are shown and discussed in Appendix H. In our interpretation, they offer further confirmation that a thin, coherent ferromagnetic layer covering the main-phase grains in Nd-Fe-B-type sintered magnets is responsible for their high coercive force. This appears to have its Curie point 50-80°C below that of the main phase, at the point where $_{M}H_{c}$ reaches near-zero values on heating. The chemical and crystallographic nature of this phase is still an open question. The practical significance of such information is that one can attempt to change the coercive force and its temperature variation by selectively tampering with the magnetic grain boundary phase, e.g., by heat treatments or by alloying additions that will selectively go into this phase.

## 4.8 Samples Supplied to the Sponsoring Laboratory

The contract specified that samples of alloys which had technological or scientific interest should be provided to the U.S. Army Electronics Technology and Devices Laboratory for further evaluations. In September 1986 we sent two samples of an experimental Nd,Dy-Fe-B sintered magnet material obtained from Hitachi Metals, Ltd, Japan (through the courtesy of Mr. M. Tokunaga); these had been ground by us into spheres of $\sim$ 1/8" diameter for use in magnetometer measurements.

In July 1988 another 14 samples (2 each of 7 compositions) were sent to the ETD Laboratory. These were cut into cubes of 2.5 mm edge lengths, with one edge parallel to the easy axis of magnetization. They were sintered magnets prepared in our laboratory in the course of the contract work, heat treated to near-optimum condition. The seven compositions were as follows:

$Nd(Fe_{.80}Co_{.12}B_{.08})_{5.5}$

$(Nd_{.80}Dy_{.20})\ (Fe_{.80}Co_{.12}B_{.08})_{5.5}$

$(Nd_{.88}Dy_{.12})\ (Fe_{.80}Co_{.12}B_{.08})_{5.5}$

$(Nd_{.75}Dy_{.20}Er_{.05})\ (Fe_{.80}Co_{.12}B_{.08})_{5.5}$

$(Nd_{.88}Dy_{.12})\ (Fe_{.788}Co_{.12}B_{.08}Zr_{.012})_{5.5}$

$(Nd_{.88}Dy_{.12})\ (Fe_{.764}Co_{.12}B_{.08}Nb_{.036})_{5.5}$

$(Nd_{.88}Dy_{.12})\ (Fe_{.764}Co_{.12}B_{.08}Al_{.036})_{5.5}$

## 5. CONCLUSIONS

The original ternary Nd-Fe-B composition has very poor elevated temperature properties and is not suitable for use under the operating conditions of most military microwave devices. It also has some problems in the cryogenic regime, below about -120°C. It must thus be considered essentially a room-temperature magnet for uncritical applications in consumer electronics. Partial replacement of Fe by Co raises the Curie temperature and reduces the temperature coefficients of saturation and coercivity. However, this also lowers the intrinsic coercive force at room temperature, cutting it in half at the otherwise useful Co content of $\sim$ 10 at percent. Thus, Co-containing magnets are still not useful in the 100° to 200°C range.

Dysprosium substituted for part of the neodymium has the opposite and desirable effect of substantially raising ${}_{M}H_{C}$, and (Nd,Dy)FeB magnets have become commercial products because of this. These two effects can be superimposed, and magnets containing some Co plus Dy are indeed magnetically more stable in the range of 80-150°C than either Nd-Fe-B or its single-element modifications. Such magnets are now also beginning to be available commercially.

Aluminum additions can also strongly increase the coercivity at room temperature, but aluminum raises the magnitude of the temperature coefficient $\beta$. Our work with (Nd-Dy)-(Fe-Co,B) alloys modified with Al shows that above about 130-140°C their coercive force is indeed lower than that of aluminum-free magnets. Since Al also reduces $T_C$, $M_S$, and $(BH)_{max}$, it is not a beneficial additive for our purpose. (But again, for moderate temperature uses in consumer products it may prove quite practical to add Al instead of the costly and rare Dy.)

By way of further modifications of the five-component alloys containing Co and Dy, we explored the effects of Nb, Ti, and Zr additions. Nb up to $\sim$ 3 at percent is clearly benefical by increasing ${}_{M}H_{C}$ at room and elevated temperatures while leaving Curie point and saturation unaffected. For instance, a magnet of composition $(Nd_{.88}Dy_{.12})(Fe_{.764}Co_{.12}B_{.08}Nb_{.036})_{5.5}$ has rather useful demagnetization curve properties and fair flux stability at $B/H \geq -1$, at least up to 150°C. It is better at 150°C than the equivalent Nb-free magnet, although not as good as a magnet tried that had nearly twice as much Dy and half the Co. A number of different tradeoffs of properties, cost, and materials availability appear possible.

With regard to understanding the physical origins of the high coercive force and its relationship to the metallurgical microstructure, some new insights were gained from magnetic domain studies, investigations of the temperature function of the intrinsic coercive force, and

low-field ac permeability measurements. It seems that at least one metastable ferromagnetic grain-boundary phase exists in the sintered magnets which can strongly pin domain walls locally after high-field magnetization, but which loses its pinning effectiveness as its Curie temperature is approached. This suggests that the most promising approach to improving the terribly strong temperature variation of $_{M}H_{c}$ is to try to tamper with the properties of this phase by proper alloying additions and heat treatments.

Attempts to improve the reversible temperature coefficient by alloying-in heavy rare-earth elements, namely, Dy and Er, alone or combined, were not particularly successful. Dysprosium affects mostly the coercivity and reduces $\alpha$ only in a minor way. Erbium favors easy-axis anisotropy, so it reduces $_{M}H_{c}$, and only small amounts can be tolerated in the magnet. A little Er reduces $\alpha$, but full temperature compensation, as it was achieved in $(Sm,Er)(Co,Fe,Cu,Zr)_{7.2}$ magnets, is impossible here. And the irreversible flux losses on heating above $\sim$100°C are indeed increased by the presence of Er in the alloy.

# APPENDIX A

## HIGH-AND-LOW TEMPERATURE PROPERTIES OF SINTERED Nd-Fe-B MAGNETS

# High and Low Temperature Properties of Sintered Nd-Fe-B Magnets

K. J. Strnat, D. Li, and H. Mildrum
University of Dayton, Dayton, Ohio

## ABSTRACT

Permanent magnet properties of sintered Nd-Fe-B were measured over the approximate temperature range from -200° to +200° C. The intent was twofold: to provide design data for engineers, and to assess the effects of the reported low-temperature spin reorientation in $Nd_2Fe_{14}B$ on the properties of sintered magnets. Commercial Neomax 35 and a low-coercivity sintered body were the vehicles for this study. Easy and hard-axis magnetization curves are reported for the temperature range. The temperature dependence of the anisotropy is extracted from these, and this as well as demagnetization curve anomalies at low temperatures are interpreted. The temperature dependence of salient magnet properties is presented. Reversible and irreversible flux losses on heating are reported.

## INTRODUCTION

Since they were first announced in 1983 [1,2], permanent magnets based on boron-modified rare earth-iron alloys have received a great deal of attention by design engineers as well as by materials scientists and physicists. It is expected that the new R-Fe-B compositions will considerably broaden the application range of rare-earth magnets in general, replacing Sm-Co in some of its present applications, but also finding uses in products where Sm-Co is either too expensive or too supply-limited. While it remains to be seen if the expectations for a much lower price can be realized, it is certainly true that the raw material availability is much greater if iron is used instead of cobalt, and neodymium instead of the samarium. (Later perhaps also Pr, Ce and/or La.)

The first commercial prototype magnets, now in limited production, are based on the ternary intermetallic compound $Nd_2Fe_{14}B$, with a slight excess of Nd and B over this stoichiometric ratio. They are prepared by powder metallurgy, including sintering. The best laboratory samples have record energy products in the range of 40 to 45 MGOe [3,4]. Commercial products with energies between 25 and 35 MGOe

**********

Paper No. VIII-8 at the 8th International Workshop on Rare Earth Magnets and Their Applications, Dayton, Ohio, 6-8 May, 1985. (Proceedings Book: University of Dayton, Magnetics, KL-365, Dayton, Ohio 45469, USA).

Address inquiries to: K. J. Strnat, University of Dayton, Magnetics Laboratory, KL-365, Dayton, Ohio 45469.

D. Li (Li Dong) is on leave of absence from the Central Iron and Steel Research Institute of Beijing, China.

are becoming available from several sources. In the present investigation we used one of these, Neomax 35, as a typical example. It has a moderately high intrinsic coercive force of 12 to 15 kOe. For reasons explained below we also needed a magnet with much lower coercivity, which we prepared ourselves.

With regard to applications requiring elevated operating or bake-out temperatures, Nd-Fe-B magnets have much less desirable properties than Sm-Co-based magnets. The temperature coefficient of $B_r$ at 20°C is 2.5 to 3 times greater than for $SmCo_5$ or 2-17 magnets, respectively. ${}_MH_c$ declines at a rate of 0.86 % per °C, i.e., nine times faster than $B_r$, or at 2.6 to 3.1 times the ${}_MH_c$ rate of typical 1-5 or 2-17 Sm-Co-based magnets. Ways of improving this behavior have been described. They involve the re-introduction of cobalt to raise the Curie temperature, or additions of the heavy rare-earth metal, dysprosium, to increase the coercivity. Since both measures increase the cost and limit the materials supply again, the large-scale user will try to work with the unmodified Nd-Fe-B where possible. To make such economic decisions intelligently, a designer must know the temperature variation of all magnetic design parameters in detail. One purpose of our study of Neomax 35 was to provide this information for the Co- and Dy-free magnets now available.

Increasingly, magnets are also used in devices that have to function at cryogenic temperatures. Recent measurements on single crystals of the 2-14-1 compound of Nd-Fe-B [5] and on polycrystalline cast or sintered magnet alloys [6,7,8] revealed a change in the anisotropy on cooling, beginning between 150 and 200 K. This has been interpreted as a spin reorientation in which the easy direction tilts away from the c-axis. It is certainly important to some magnet users to know which effects - reversible and irreversible upon reheating - this may have on the flux the magnet provides in the circuit. We can now report the first results of a low-temperature magnet property study, presented in the form of demagnetization curves measured down to liquid nitrogen temperature.

## SAMPLES

Most measurements reported in this paper were made on four samples cut from larger sintered magnets. Their salient permanent-magnet properties at room temperature (RT) are given in Table I. Samples A, B and D were Neomax 35, kindly provided by Dr. Sagawa of the Sumitomo Special Metals Comp. Sample A was a cube of ~8 mm edge length, used for hysteresigraph measurements; B was a small cylinder (2.35 Diameter x ~2 mm long) with the easy axis along a diameter. Sample C was a ~3 mm cube of a low-coercivity magnet sintered by us. B and C were magnetometer samples. Sample D, for pull-coil measurements of losses, was an axially magnetized cylinder of 6.2 mm dia. x 6.5 length.

Table I: Salient PM Properties at 20°C of Samples Used in this Study.

| Sample | Open circuit B/H | B (kG) | $_BH_C$ (kOe) | (BH)max (MGOe) | $H_k$ (kOe) | $_MH_C$ (kOe) |
|---|---|---|---|---|---|---|
| A | -2 | 12.2 | 11.1 | 34.8 | 12.3 | 15.1 |
| B | -1.96 | 12.3 | 10.6 | 32.0 | 7.8 | 12.2 |
| C | -2 | 12.6 | 3.3 | 15.8 | 1.6 | 3.8 |
| D | -0.6 | 12.6 | 11.7 | 36.9 | 13.1 | 13.5 |

## EXPERIMENTAL PROCEDURES

Closed-circuit measurements with a DC hysteresigraph on Sample A yielded the demagnetization curves from -40° to +200°C and the first-quadrant hard-axis (HA) magnetization curves at +20° and +200°C. The demagnetization curves with field in the grain alignment direction, ("easy axis", EA), and the HA first-quadrant curves, shown for several temperatures from +25° down to -194°C, were measured on Sample B with a vibrating sample magnetometer (VSM) in open circuit. They were corrected by shearing. The DC field in the VSM was limited to 15 kOe. The sample was pulse charged with 100 kOe along the EA at room-temperature before plotting each curve. The temperature was allowed to stabilize for 2 minutes. The VSM field-sweep time was 2.5 minutes for each curve. The hard-axis curves are remagnetization curves after DC demagnetization of the sample along the EA.

The thermomagnetic analysis (TMA) curves were measured on powder of 105 - 177 μm particle size with a 5 kHz field of about 1 Oe amplitude. The average temperature sweep rate was 1.3°/min.

The plot of reversible and irreversible losses during thermal cycling to elevated temperatures up to 275°C is for Sample D. The open-circuit remanent flux, at B/H=-0.6, was measured with a tightly fitting pull coil and an integrating digital voltmeter.

## RESULTS AT ELEVATED TEMPERATURES

Figure 1 shows a set of easy-axis demagnetization curves for Neomax 35, measured in closed circuit. Figure 2 is a plot of the temperature variation of the salient properties, $B_r$, $_MH_C$, $_BH_C$ and $(BH)_{max}$, extracted or calculated from the above. This information was previously published [9] and is included here for the sake of completeness. The temperature range overlaps with that of our low-temperature VSM measurements. Note that the intrinsic coercive force drops much more rapidly on heating than $B_r$ does, aiming at near-zero values at 250°C, well below the 312°C Curie point of the 2-14-1 phase.

We performed an AC thermomagnetic analysis (TMA) on Neomax 35 (Figure 3). Taking the point of inflection above the narrow upper maximum as the Curie temperature of the main phase, we found $T_c$=316°C on heating, 312°C on cooling, in good agreement with the values reported by others. (A small thermal hysteresis is unavoidable with this method. There is no other sharp peak in the temperature range covered, 20 to 380°C, to indicate the Curie point of any other well-defined ferromagnetic compound. However, there is a broad maximum some 70 to 80° below the $T_c$ of $Nd_2Fe_{14}B$. This may indicate the existence of a secondary magnetic phase (in the grain boundaries?) with gradual local property fluctuations over short distances of the order of the lattice dimensions. These could be due to a degree of atomic disorder (and thus compositional and lattice parameter variations), e.g., stacking faults, or coherency strains at an epitaxial interface with the 2-14-1 main phase grains. If such a non-equilibrium phase had a magnetic ordering temperature near 250°C, its "Curie point" should be ill defined, and the "local $T_c$" would cover a range of temperatures, causing the kind of broad permeability maximum observed.

Note that this μ-maximum occurs in the same region in which the coercivity drops to near zero. It is tempting to speculate - as we previously did for "$SmCo_5$" sintered magnets [10] - that such a phase exists and is important in controlling the magnet's coercivity by pinning domain walls in the grain boundary areas. In any case, such a peak does not normally occur in a single-phase ferromagnet. (See e.g. the TMA curve for pure nickel superimposed in Fig. 3.) But we did find one for Sm-Co alloys in the range between $Sm_2Co_7$ and $SmCo_5$, where the compositions of "$SmCo_5$" magnets lie.

A maximum of μ vs. T is associated with low crystal anisotropy (this is indeed the reason for the peak below $T_c$!). One could thus look for an anisotropy minimum in the 2-14-1 phase. However, there is no other evidence of any anisotropy anomaly near 200°C - neither in our work nor in published results of other authors who have investigated this temperature range [5,6].

We also measured the changes of the open-circuit remanent flux (OCRF) during temperature cycling between RT and various levels up to T=275°C. The results are shown in Figure 4. This was done at a low operating permeance, B/H=-0.6 G/Oe, with a TWT tube application in mind. The so-called "losses" are percentage changes from the initial RT value: the term "total loss" refers to the flux reduction during heating to T; the portion of the flux that returns on cooling to RT is the "reversible loss"; the difference which is not recovered simply by cooling is called the "irreversible loss." It can be seen from the figure that the irreversible loss becomes noticeable above 50°; at 150°C the flux loss is more than half; and above 265° the sample becomes completely and permanently demagnetized in its own self-demagnetizing field, because the coercive force disappears.

The shape of the reversible loss curve, with losses peaking near 125°, is initially puzzling. It can be understood as follows: Well below $T_c$ the reversible loss increases on heating, reflecting the temperature variation of the spontaneous magnetization, the Brillouin function (as indeed the moment of each domain must, all the way up to $T_c$). But as an increasing volume fraction of domains reverses by thermal activation on further heating, this drop of the domain magnetization partially cancels out when averaged over a large number of domains. Finally, at 265°, no bulk magnetization is left. The partial remagnetization on cooling which the term "reversible loss" implies could then occur only if domain walls shifted to favor one set of domains. Obviously, this is not the case. Direct observations of domain patterns during thermal cycling support this explanation [11,12].

Further measurements we made at elevated temperatures include the hard-axis magnetization curves at 20° and 200°C shown in Figure 5. They will be discussed in conjunction with similar measurements made below room temperature.

## MEASUREMENTS MOSTLY BELOW ROOM TEMPERATURE

We wanted to study the temperature dependence of the crystal anisotropy of $Nd_2Fe_{14}B$, especially in the range below about 200 K where the existence of a spin reorientation has been reported. Since we had no single crystals available, we worked with field-pressed and sintered bodies.

Sets of magnetization curves measured on single crystals, with the magnetizing field applied parallel and normal to the c-axis, are the best vehicles for determining the anisotropy constants of highly anisotropic materials such as Nd-Fe-B. Sintered magnets with a strong grain texture closely approximate single crystal behavior with regard to the uniaxial component of the anisotropy. But any possible anisotropy in the basal plane cannot be observed at all, and the high coercivity of a good magnet interferes with the accurate determination even of the uniaxial constants, $K_1$ and $K_2$. With the magnetizing field applied at right angle to the grain-alignment direction (the "c-axis"), the observed magnetization change should be due mostly to a rotation of the domain magnetization against anisotropy forces. Any misaligned grains, however, can also contribute magnetization by wall motion, which manifests itself as an additional curvature of the "hard-axis" curve that might be misinterpreted as being due to $K_2$.

We measured such M vs. H curves with H perpendicular to the c-axis at a number of temperatures between +200 and -194°C. They are reproduced in the Figures 5 and 6. In each case, the sample was first fully saturated in a field along the c-axis, a demagnetization curve was plotted (not shown), and the sample demagnetized in a negative field. Then it was rotated through 90° and the hard-axis curve measured with the VSM. (All curves were sheared.) From the fact that near

RT the "curves" are practically straight lines through the origin, we conclude that grain alignment is excellent and the wall-motion error negligible. It follows, then, that the curvature observed at higher as well as lower temperatures should indeed be due to $K_2$ or higher-order anisotropy parameters. The c-axis magnetization/demag. curves were only used to determine the spontaneous magnetization, Ms(T), so that anisotropy field values could be obtained by extrapolating tangents to an intercept with the $M_s$-horizontal.

In all these curve manipulations we must keep in mind that the available maximum field of 15 kOe is generally only a small fraction of the field strength needed to saturate (except at 200°C, where 15 kOe achieves $M_s/2$). This means that our extrapolations are dangerously long, and that we do not see the high-field portions where the curvature due to $K_2$ manifests itself strongly. We can, therefore, only obtain estimates for $K_1$ and no useful $K_2$-values at all from these curves. In the temperature range where the HA-lines are straight, we get the following, reasonably reliable, values for $K_1=M_sH_a/2$:

| T (°C) | $4\pi M_s$ (kG) | $H_a$ (kOe) | $K_1$ ($10^7$ erg/cm$^3$) |
|---|---|---|---|
| -28 | 13.45 | 65.0 | 3.5 |
| +24 | 12.73 | 59.2 | 3.0 |
| +60 | 11.83 | 54.5 | 2.6 |

In order to have some numbers for a description of the temperature variation of the HA magnetization curve shape, we define two other "anisotropy constants," K' and K", *in the following manner:* For K' we draw a tangent to the steepest section of the curve, shift it parallel into the origin, and extrapolate it to saturation at an "anisotropy field", $H_a'$. For K" we do the same thing with the tangent at the high-field end of the HA magnetization curve, near 15 kOe. In each case, $K=M_sH_a/2$. Figure 7 is a temperature plot of these two K parameters. In the range where K' and K" are nearly the same, either can be interpreted as approximating $K_1$; but at the lower temperatures, especially, their physical meaning is quite unclear. It is interesting, though, that both K's have a maximum value at about -70 to -80° where the spin reorientation is said to begin on cooling. The steep portion of the M vs H curve at the lowest temperatures can be interpreted as the motion of walls between tilted domains, with easy directions tilted away from the c-axis direction. This would be followed by domain rotation against very high anisotropy forces as the field exceeds about 5 kOe. However, other interpretations are possible. It is conceivable that the spin reorientation takes place only in a portion of the magnet volume (K' would represent its uniaxial anisotropy constant) while another, as yet unidentified, fairly major phase would continue to become "harder" on cooling. (See trend of K" .)

We also measured demagnetization curves along the alignment axis at the low temperatures. These are shown in Figure 8. This Neomax-35 sample B exhibited a low-field step in the demagnetization curve, and thus a fairly low $H_k$-value, even at RT. On cooling, $H_k$ first rises, but then the step becomes much more pronounced near liquid nitrogen temperature. The coercive force remains very large (<16 kOe) - too high to measure with our VSM - throughout this temperature range. $H_k$ vs. T is plotted in Figure 9. The $H_k$ has a maximum near -75°C (~200 K) and sharply decreases on further cooling.

In order to follow the temperature dependence of the intrinsic coercive force through the entire temperature range, we needed a sample with a sufficiently low coercivity at room temperature so that $H_c$ would not exceed 16 kOe even at $LN_2$ temperature. This was found in an experimental composition having higher iron content.

For this poorer sintered magnet, Sample C, we were able to follow the trend of both, $H_k$ and $_MH_c$, all the way down to -194°C. These results are also shown in Fig. 9. Again, $H_k$ has a pronounced maximum near -75°C and drops on further cooling. The intrinsic coercive force levels off for a 50° interval just below this temperature and then resumes its steep increase with decreasing temperature. It is likely, but not certain, that the $_MH_c$ vs. T curve of higher-coercivity magnets will show the same features.

## CONCLUSIONS

While Nd-Fe-B magnets have much higher values of remanence and energy product at room temperature than Sm-Co magnets, these advantages are lost on heating to only moderately high temperatures in the 100° to 150°C range, because of the much higher temperature coefficients. (See [9].) Also, due to the rapid drop of the intrinsic coercive force, the irreversible flux losses become very severe there, especially at low operating permeance. However, after thermal demagnetization by brief heating above the Curie point the losses are almost fully recoverable by remagnetizing. This means that full charging of the magnets by heating them to about 275°C, applying a low field and cooling in it is quite feasible.

On cooling below room temperature, the magnets first get better in the sense that $_MH_c$ increases rapidly, $B_r$ and $(BH)_{max}$ more moderately. However, near -75°C $_MH_c$ levels off, and below about -100°C a low-field "step" develops in the second-quadrant demagnetization curve which gets quickly worse on cooling. This is the consequence of an anomaly in the crystal anisotropy of $Nd_2Fe_{14}B$ in this temperature range. Designers of devices that have to operate in the cryogenic regime must therefore be cautioned to await further characterization of the low-temperature behavior of the Nd-Fe-based magnets. It is likely that these effects are reversible on heating, so that temporary excursions to low temperatures may not adversely affect the subsequent functioning of the magnets at room temperature. However, experimental proof of this thesis is still lacking.

ACKNOWLEDGEMENTS

This paper contains information generated under contracts with the U.S. Army Electronic Devices and Technology Laboratory, Ft. Monmouth, NJ (DAAK20-84-K-0458) and the U.S. Air Force Aerospace Propulsion Laboratory, WPAFB, OH (contract F33615-81-C-2012).

The Neomax 35® magnet samples were kindly provided by Dr. M. Sagawa of the Sumitomo Special Metals Co., Ltd., Osaka, Japan.

REFERENCES

1. M. Sagawa, et al., J. Appl. Physics 55 (1984) 2083. (1983 MMM Conf.)
2. J. J. Croat, et al., J. Appl. Physics 55 (1984) 2078. (1983 MMM Conf.)
3. K.S.V.L. Narasimhan, Paper AB-01 at the 30th MMM Conf., Nov. 1984.
4. M. Sagawa, et al., IEEE Trans. Magnetics, MAG-20 (1984) 1584.
5. M. Sagawa, et al., Paper AB-04 at the 30th MMM Conf., Nov. 1984. To be published in J. Appl. Physics 56, April 1985.
6. S. Sinnema et al., J. Magnetism and Mag. Materials 45 (1984)
7. R. Grossinger et al., Paper VIII-6, this proceedings.
8. H. Oesterreicher, F. Spada and C. Abache, Mat. Res. Bull. 19 (1984) 1069.
9. D. Li, H. F. Mildrum and K. J. Strnat, Paper CC-02 at the 30th MMM Conf., Nov. 1984. To be published in J. Appl. Physics 56, April 1985.
10. S. Liu, K. J. Strnat and H. F. Mildrum, Proc. 6th Int'l. Workshop Rare Earth-Co Perm. Mag., (ed. J. Fidler) Tech. Univ. Vienna, Austria, 1982, p. 631. (Also Refs. 20, 21 in that paper.)
11. D. Li and K. J. Strnat, Paper CC-03, 30th MMM Conf., Nov. 1984.
12. D. Li and K. J. Strnat, Paper X-7, this proceedings.

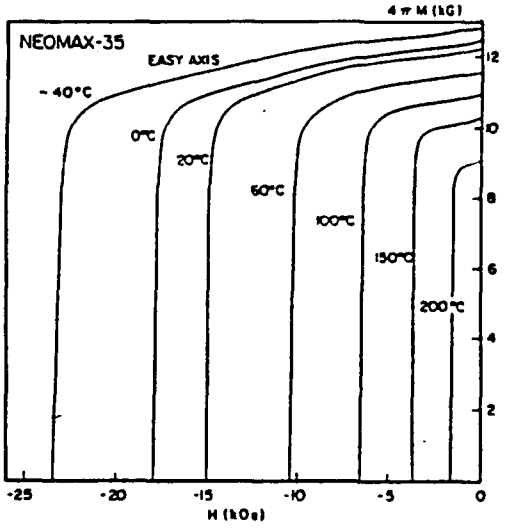


Fig. 1: Neomax-35 sintered Nd-Fe-B magnet. Easy-axis demagnetization curves between -40 and +200°C, measured after 100 kOe pulse charging at RT. Closed-circuit measurements with hysteresigraph on Sample A.

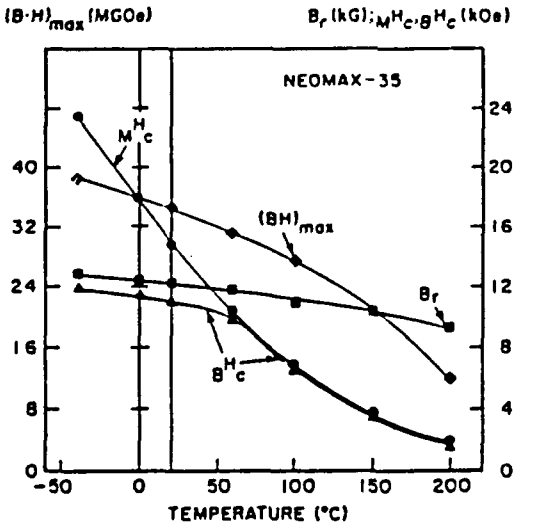


Fig. 2: Neomax-35: Temperature dependence of salient PM properties from -40° to +200°C. (Derived from Figure 1.)

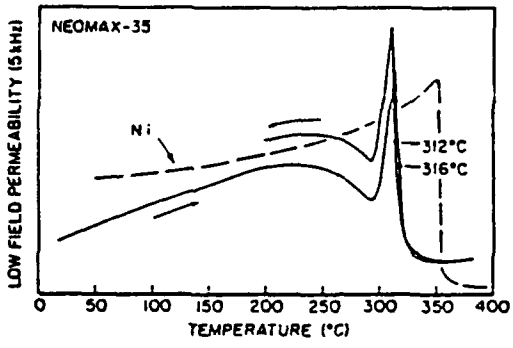


Fig. 3: Thermomagnetic analysis of Neomax-35 above RT. A TMA result for pure nickel is shown for curve-shape comparison.

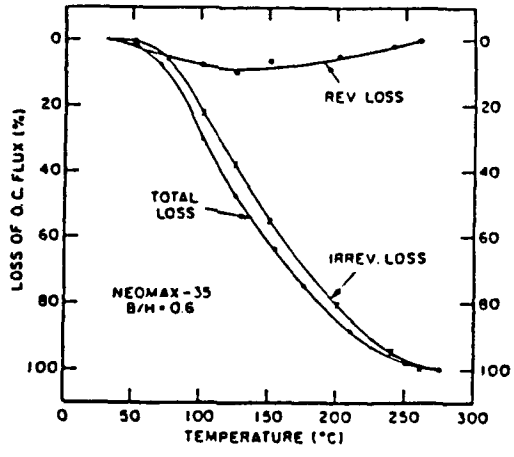


Fig. 4: Neomax-35, Sample D, $B/H \approx -0.6$. Open-circuit remanent flux losses during short term heating/cooling cycles above room temperature.

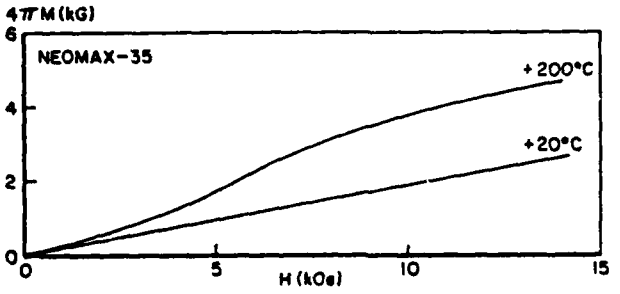


Fig. 5: Neomax-35: Remagnetization curves at 20° and 200°C with field along room-temperature hard axis. Measured in closed circuit with hysteresigraph on Sample A.

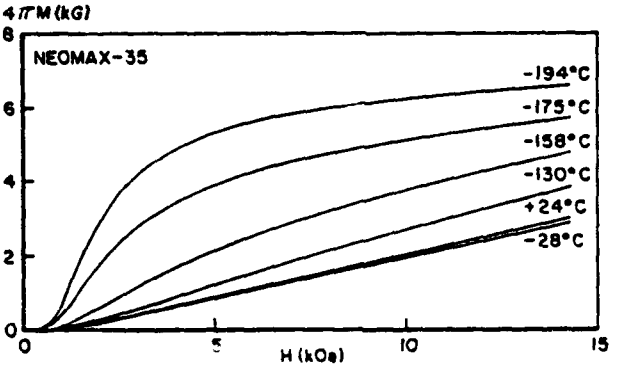


Fig. 6: Neomax-35: Remagnetization curves at various temperatures below RT, field along the RT hard axis. Measured in open circuit with magnetometer on Sample B; curves sheared

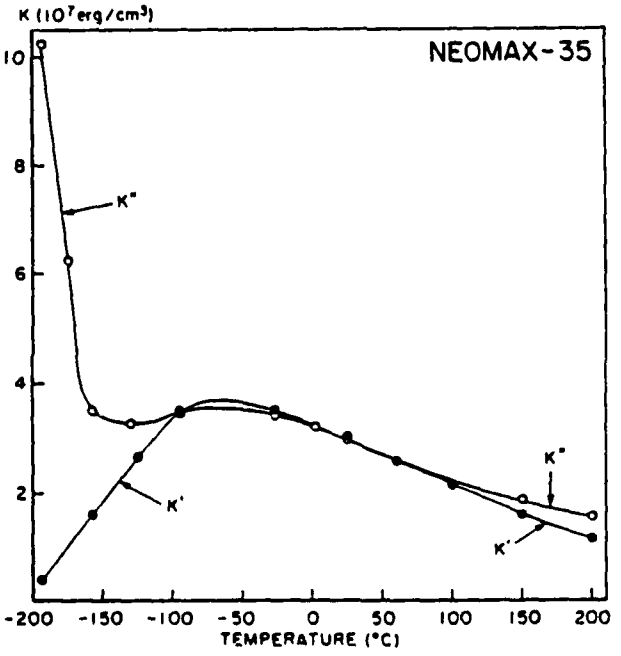


Fig. 7: Temperature dependence of anisotropy parameters K' and K". (For definition see text.) Derived from data in Figures 5 and 6.)

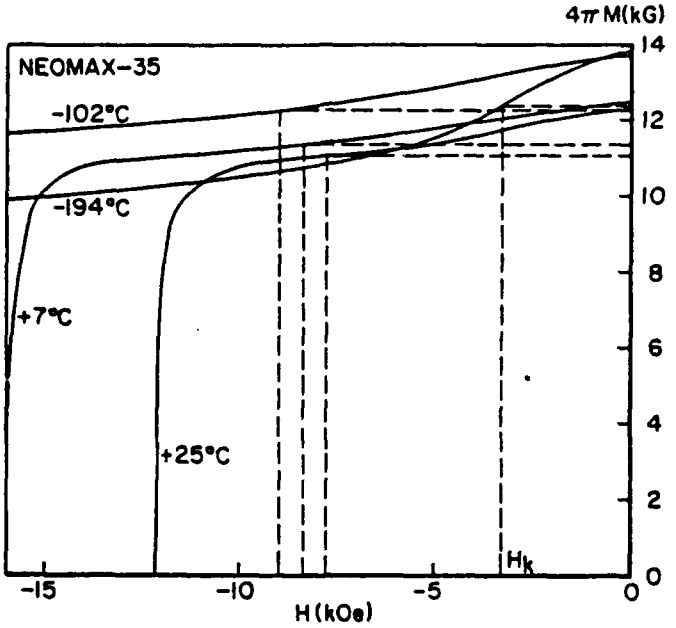


Fig. 8: Neomax-35: Intrinsic demagnetization curves at several temperatures below RT. Measured with VSM on Sample B, sheared.

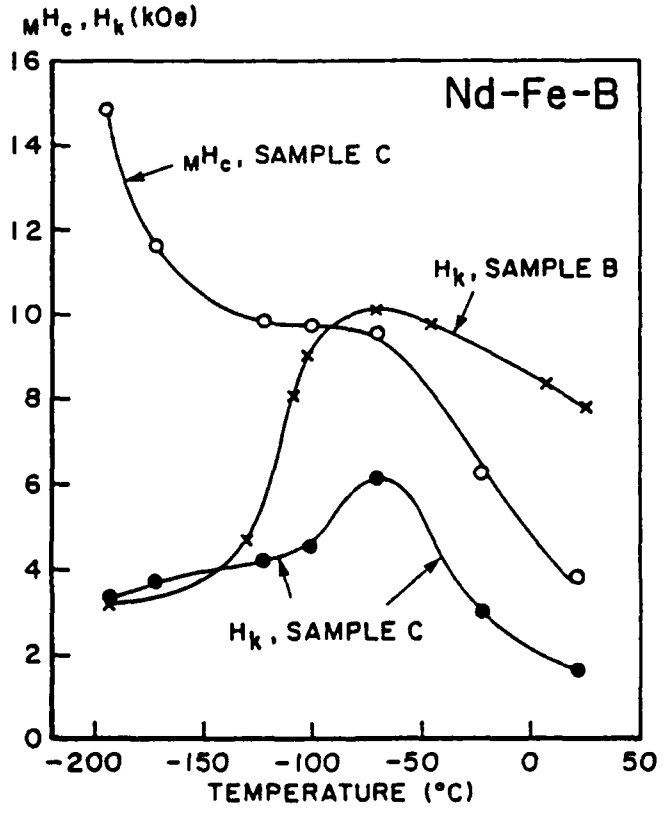


Fig. 9: Temperature variation of the intrinsic coercive force, $_{M}H_{c}$, and the knee field, $H_{k}$ at 0.9 $B_{r}$. For Neomax-35 (Sample B, from Fig. 8) and for a low-$H_{c}$ sintered magnet (Sample C).

# APPENDIX B

## DOMAIN BEHAVIOR IN SINTERED Nd-Fe-B MAGNETS DURING FIELD-INDUCED AND THERMAL MAGNETIZATION CHANGE

# Domain behavior in sintered Nd-Fe-B magnets during field-induced and thermal magnetization change

D. Li[a] and K. J. Strnat[b]
*University of Dayton, School of Engineering, Dayton, Ohio 45469*

On sintered Nd-Fe-B permanent magnets, magnetic domain pattern changes in applied fields and at elevated temperatures were observed by the Kerr effect. Patterns on pole and side faces were recorded for different magnetization states in fields up to 17 kOe at 20 °C, and remanent patterns at temperatures up to $T_C$. They are qualitatively interpreted. On pole faces, most grains are multidomain even at remanence. But the surface domains seen are not characteristic of the magnet interior. Side faces show mostly single-domain grains at remanence. These images appear to reflect bulk behavior. Walls are strongly pinned at grain boundaries but move easily in the main magnetic phase, a behavior analogous to that of sintered $SmCo_5$.

## I. INTRODUCTION

M. Sagawa *et al.*[1] first prepared sintered Nd-Fe-B permanent magnets having record high room-temperature energy products. The new magnets are said to comprise a main phase of tetragonal crystal structure, $Nd_2Fe_{14}B$, and two minor phases, namely, tetragonal $Nd_2Fe_7B_6$ and a fcc Nd-rich phase of 95 at. % Nd, both located along grain boundaries or at corners.[2] Hard magnetic properties, such as the coercivity, are structure sensitive and thus strongly dependent on heat treatment and on the nature and distribution of secondary phases. The objective of this work, like that of our other recent studies on Sm-Co magnets,[3,4] is to provide more experimental data for a comprehensive interpretation of the magnetization change mechanisms in sintered rare-earth magnets.

## II. SAMPLES AND EXPERIMENTAL PROCEDURES

We used two sintered magnets received from the Sumitomo Special Metals Co. One magnet was a cube (~8 mm) of NEOMAX-30H[5] with these properties at 20 °C: $B_r = 11.26$ kG, ${}_MH_c = 21.6$ kOe, and $(BH)_{max} = 30$ MGOe. The second was an axially aligned cylinder (6.2 mm diam × 6.5 mm long) of NEOMAX-35 with $B_r = 12.63$ kG, ${}_MH_c = 13.4$ kOe, and $(BH)_{max} = 36.9$ MGOe. For the domain observations, the cylinder was sectioned into two samples by spark cutting.

Magnetic domains were observed by the magneto-optic Kerr technique. During the microscopic examination, a variable magnetic dc field could be applied at room temperature, or the temperature could be raised in the absence of a field. We also compared the 20 °C Kerr images on side faces (containing the easy axis) with Bitter patterns and confirmed that they showed essentially the same domain structures. The samples were in a nearly closed magnetic circuit during the observations in fields. Maximum available fields in the fixtures were ~10 kOe for observations on "pole faces" (cut normal to the easy magnetization axis) and ~17 kOe for side-face images.[3] The cylindrical sample could be raised to ~350 °C in a vacuum hot stage (in $1.4 \times 10^{-4}$ Torr) for open-circuit observations without an applied field. It was magnetized in a 100 kOe pulsed field before heating. The average heating rate from room temperature to $T_C$ was ~6 °C per min. Demagnetization curves were measured with an integrating dc hysteresigraph.

## III. RESULTS AND DISCUSSION

### A. Magnetization curve measurements

Figure 1 shows, for the two magnet types studied, intrinsic demagnetization curves at 20 °C, several recoil lines, first-quadrant remagnetization curves after a recoil through the origin, and virgin curves from the thermally demagnetized state. Dots indicate the magnetization states for which domain photos are presented. (*Figure numbers indicated.*) Note that the recoil lines for a low-coercivity grade 35 are strongly curved, yet almost reversibly traced, with no significant loop area. The recoil/remagnetization line through the origin shows an unusual two-step shape, suggesting that two clearly differentiated mechanisms of domain-wall motion

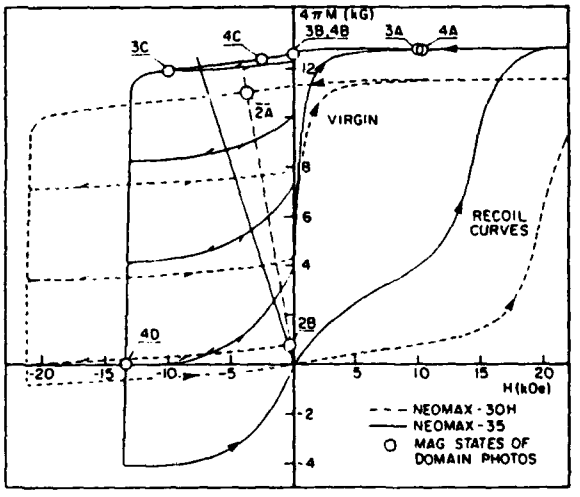


FIG. 1. Magnetization and demagnetization curves for magnets studied. Circles indicate states for which domain patterns are shown, with reference to the figure number.

[a] Visiting scientist, on leave from the Central Iron and Steel Res. Inst., Beijing, China.

[b] Work supported by the U. S. Army Research Office, Durham, NC.

 0021-8979/85/014143-03$02.40  

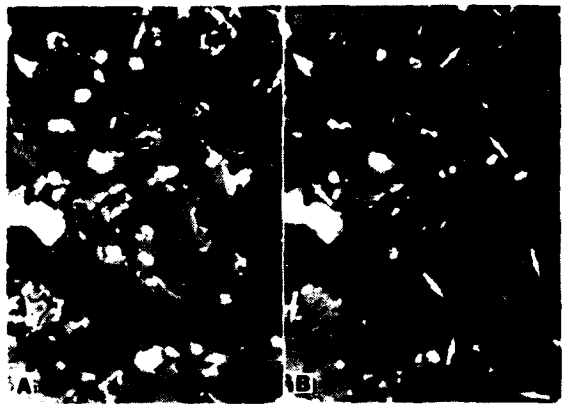


FIG. 2. Domain patterns on pole face in open circuit ($B/H \approx 2$) for NEOMAX-30H. (A) Saturated with 100 kOe pulse. (B) Nearly demagnetized with $H = -{}_M H_c$. Arrows show fully reversed grains.

are active, apparently involving different volume regions of comparable size.

### B. Domain patterns in variable fields at room temperature

Figure 2 shows patterns for NEOMAX 30-H on a pole face. In the open-circuit remanent state (2A), about 85% of the field-of-view is already multidomain grains containing a much larger proportion of reversed (dark) area than would correspond to the ~3% magnetization drop from saturation. We are clearly observing surface spikes and lamellar domains which form to reduce the magnetostatic energy and are not characteristic of the sample interior. After near-demagnetization by a field equal to ${}_M H_c$, Fig. 2(B) shows almost all multidomain grains. Patterns within individual grains look rather different in detail from Fig. 2(A). However, a few of the smaller grains are still fully magnetized in the original direction, while others have been fully reversed without going through a stable multidomain state. (See arrows pointing to grains turned uniformly darker relative to their surroundings.)

All subsequent photographs were taken on the lower-$H_c$ NEOMAX 35. The limited field strength of the electromagnet on our microscope was too low to produce significant pattern changes on the 30-H material, while it could fully reverse and essentially saturate the grade 35 samples. The sequence of pictures in Fig. 3 was taken after saturating the cylindrical sample with a + 100 kOe pulse and transferring it open-circuit to an iron-pole-piece fixture. The bulk of the sample is then subjected to dc fields progressing from + 10 kOe [Fig. 3(A)] to zero ($B_r$ point) [Fig. 3(B)], to − 10 kOe [Fig. 3(C)] and back to zero. These fields, all $H < {}_M H_c$, change the magnetization very little away from positive saturation (cf. Fig. 1). It seems therefore surprising that in Fig. 3(A) most grains already show multidomain patterns. This is again a surface effect which makes such pole-face images of questionable value for judging interior domain processes. (Also note that the fixture pole piece has an opening for the objective lens, so that, in the field-of-view, value and direction of the applied field are uncertain.) Removal of the field [Fig. 3(B)] brings only reversible width increases of the white "squiggle" domains. But a further slow change of $H$ from about − 1.5 to − 10 kOe [Fig. 3(C)] causes additional grains to burst suddenly into multiple domains (see arrows). This observation was also made on $SmCo_5$ magnets[3] and indicates that wall pining is much weaker in the main-phase grains than along the grain boundaries.

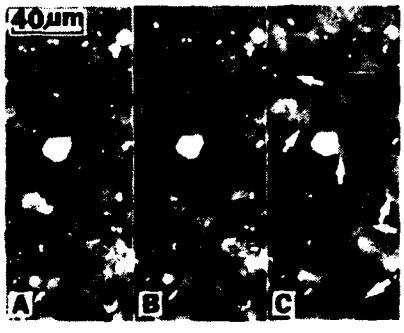


FIG. 3. Field-induced domain changes on pole face, NEOMAX-35. Arrows show reversed grains: (A) In + 10 kOe after 100 kOe pulse. (B) $H = 0$, $B_r$ state. (C) − 10 kOe.

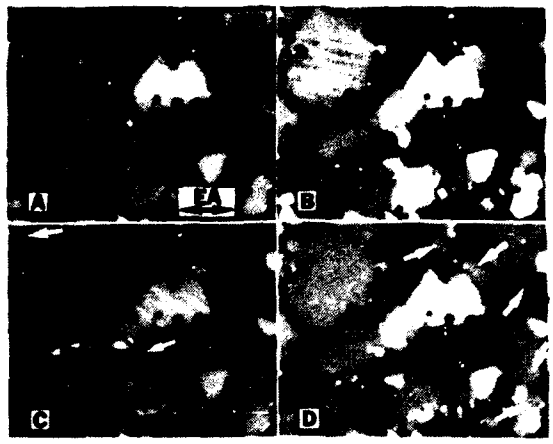


FIG. 4. Field-induced domain changes on side surface, NEOMAX-35. Arrows indicate pattern changes. (A) In + 10.4 kOe after + 100 kOe pulse. (B) $H = 0$, $B_r$ state. (C) $H = -2.5$ kOe, (D) $H = -13.4$ kOe, ${}_M H_c$ state.

A different behavior is seen on the side surfaces which contain the (average) easy axis. In the highest available field of + 17 kOe, i.e., $H \approx 1.3\,{}_M H_c$, no reverse domains are seen. This clearly saturated state persists down to about + 10 kOe [Fig. 4(A)]. When $H$ is further reduced, spike-shaped domains appear in some (primarily the larger) grains, originating mostly on visible grain-boundary lines that are nearly perpendicular to the easy $c$ axis ( = spike axis). The small reversed (darker) area seems consistent with the small measured drop in average magnetization at the remanence point [Fig. 4(B)] and at $H = -2.5$ kOe [Fig. 4(C)]. In this field range, most of the magnetization change is by gradual and reversible expansion of these spikes; but some new sets of spikes may "nucleate" at another boundary of the same grain at a higher reversed field, suddenly popping into a finite equilibrium size. In some places dual sets of spikes start simultaneously, at the same field strength, into two clearly separated grains from an intervening second-phase strip of several microns width. Spikes that had first appeared by the

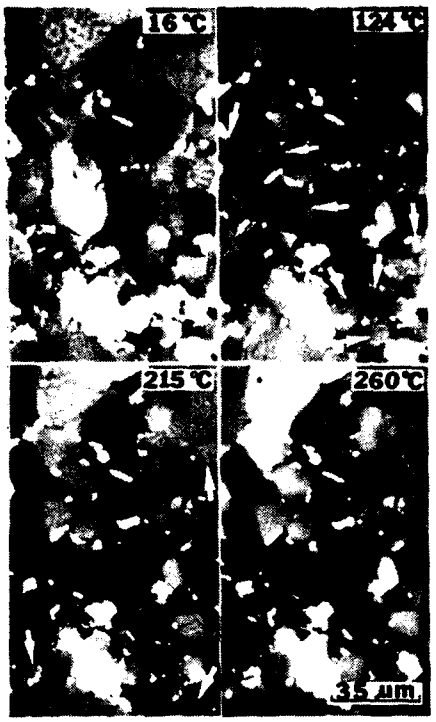


FIG. 5. Pole-face domain patterns at elevated temperatures. Open-circuit remanent state after 100 kOe pulse. NEOMAX-35, $B/H \simeq 0.6$. Arrows indicate pattern changes.

"popping" can be gradually suppressed and made to disappear completely into the grain boundary of their origin by reversing the field-change direction. On reversing it once more, they reappear from the same "nuclei" and now grow gradually as the local driving field increases. However, if the "suppression field" exceeds a critical level, the process becomes irreversible, and popping will again occur only after a finite field change, at the original nucleation field.

We interpret these observations to mean that what occurs is not true nucleation but the expansion of residual reversed domains from localized pinning sites. For $SmCo_5$ magnets we had previously concluded that this pinning often does not take place at the grain interface per se, but inside a magnetic minor phase which contains graduated pinning sites that are more effective pins than the intermediate grain-boundary region.[4,6] Given the present knowledge of phase compositions in the Nd-Fe-B magnets, however, one cannot identify such a magnetic pinning phase in this case. As the negative applied field is further increased through the steep flank of the $B_i/H$ curve, the multidomain grains become fully saturated and many small grains reverse their magnetization suddenly without forming stable domain walls. Because in the side-face images the large crystallographic contrast between grains masks the small shade differences due to the Kerr effect, these reversals are best seen in dynamic observations. In still pictures they must be identified by the changed contrast of a reversed grain relative to its surroundings. In Fig. 3(D) the arrows indicate some such reversals that occurred between $-2.5$ and $-13.4$ kOe; but note that a few grains had "flipped" even between 0 and $-2.5$ kOe [arrows in Fig. 3(C)].

### C. Domain changes during thermal demagnetization of NEOMAX 35

To provide a bulk-property reference, the open-circuit flux was measured at 25 °C after thermal cycling to progressively elevated temperatures (up to 275 °C). The irreversible loss reached 100% at 265 °C, indicating that positive and negative domains had achieved an equilibrium throughout the magnet. Independent measurements of hysteresis loops[7] had also indicated that the coercivity drops to zero at this temperature, about 50 °C below $T_C$. Corresponding remanent domain-pattern changes on a pole face at elevated temperature are shown in Fig. 5. Again, most grains are multidomain even at room temperature. When $T$ is raised, previously saturated grains burst suddenly into "flower patterns." This process is essentially complete at or below 215 °C. Reversed domain "nucleation" is certainly facilitated by the increase in thermal energy; but the principal cause of the thermally activated multidomain formation is probably a rapid weakening of the grain-boundary pin strength with increasing temperature. On further heating, the up/down magnetization balance shifts gradually toward equilibrium in all grains, while general patterns and domain spacings remain almost unchanged. Kerr contrast diminishes close to the Curie temperature and domains fade out completely around 265 °C. The old patterns reappear near 265 °C on cooling from 313 °C.

[1]M. Sagawa, S. Fujimura, M. Togawa, H. Yamamoto, and Y. Matsuura, J. Appl. Phys. 55, 2083 (1984).
[2]M. Sagawa, S. Fujimura, M. Togawa, H. Yamamoto, Y. Matsuura, and K. Hiraga, IEEE Trans. Magn. MAG-20, 1584 (1984).
[3]K. J. Strnat, D. Li, and H. F. Mildrum, J. Appl. Phys. 55, 2100 (1984).
[4]S. Liu, K. J. Strnat, and H. F. Mildrum, *Proceedings of the 6th International Workshop on Rare Earth-Co Permanent Magnets*, edited by J. Fidler, (Technical University, Vienna, Austria, 1982), p. 631.
[5]NEOMAX is a registered trademark of the Sumitomo Special Metals Co., Ltd.
[6]K. J. Strnat, AIP Conf. Proc. No. 5, 1047 (1971).
[7]D. Li, H. Mildrum, and K. Strnat (these Proceedings).

# APPENDIX C

## ELEVATED-TEMPERATURE BEHAVIOR OF SINTERED "Nd-Fe-B Type" MAGNETS

I-MAG-24/2/2/22163

# Elevated Temperature Behavior of Sintered "Nd-Fe-B Type" Magnets

H.F. Mildrum
G.M. Umana

Reprinted from
IEEE TRANSACTIONS ON MAGNETICS
Vol. 24, No. 2, March 1988

C-2

# ELEVATED TEMPERATURE BEHAVIOR OF SINTERED "Nd-Fe-B TYPE" MAGNETS

H.F. Mildrum and G.M. Umana
Magnetics Laboratory, School of Engineering
University of Dayton, OH 45469, USA

ABSTRACT: The effects of elevated temperature air exposure at 75°, 100°, 125° and 150°C on the performance of sintered "Nd-Fe-B type" permanent magnets has been investigated. The observations include a comparison of the initial and final demagnetization curves after long term aging in excess of 5000 hours, initial irreversible losses on heating, and the stability of open-circuit remanent flux as a function of time, temperature and operating point permeance.

Test samples were obtained from four magnet producers. The results reported may be considered to be typical for present commercial production magnets made from ternary Nd-Fe-B and from alloys modified with dysprosium and cobalt.

Test results indicate that there are very restrictive operational limits imposed by a combination of elevated temperatures $\geq$ 125°C, and unit permeance values $\leq$ 1.

## Introduction

Permanent magnets made from rare earth-iron-boron alloys have rapidly gained technological and economic significance in new device applications. These include sintered magnets based on the ternary alloy and more recently alloys containing dysprosium and cobalt.

In many permanent magnet devices elevated temperatures are incurred. It is important for the design engineer to know what "irreversible losses" of the useful flux to expect upon first heating, and subsequent aging losses incurred at elevated temperatures.

This paper reports such data with regard to temperature, time and unit permeance dependency of characteristic demagnetization curves before and after aging, and long-term stability of remanence.

Three types of commercially available materials, Nd-Fe-B, Nd,Dy-Fe-B, and Nd,Dy-Fe,Co-B, offered by magnet producers were used in this investigation.[1-4]

## Experimental Procedure

A total of eight different brand types of commercial magnets provided by four manufacturing firms were utilized in this study. All magnets received were prepared from large production bars by the manufacturers. The actual test magnet samples are axially magnetized cylinders ~ 6.35 mm in diameter and lengths corresponding to open-circuit unit permeances $B_d/H_d$ = -3.2, -1.0 and -0.5.

All magnets were pulse magnetized with a 100 kOe peak field prior to measurement with a d.c. Hysteresigraph for samples with L/D ratios $\geq$ 1, and an Oscillating Sample Magnetometer (OSM) for L/D ratios < 0.42 and 0.2. Initial intrinsic and normal demagnetization curves plotted indicate consistent salient property data.

Irreversible and long-term losses in flux were measured with a close fitting pull-coil, precision integrating digital voltmeter (± 0.005% accuracy and resolution to ± 0.1 μV-sec) to measure the open-circuit remanent flux (OCRF). All magnets were pulse magnetized prior to determining the initial reference value at 25°C. Subsequent measurements were routinely obtained at elapsed time intervals of thermal exposure, after cooling to room temperature and recording the change in remanent flux. A computer program stores the integrated signal and then proceeds to systematically correct the data for instantaneous background noise and sample temperature (± 0.1°C) at the time of measurement, using the reversible temperature coefficient of induction for each type. Corrected data is then normalized and further processed by the program to yield specific information such as the "initial irreversible loss" in one hour, and subsequent aging losses (referred to the value at one hour) at any point in time.

## Results and Discussion

Irreversible losses: Table 1 summarizes the overall range of so-called "irreversible losses," i.e. the reduction of open-circuit remanent flux as a consequence of short-term heating at specific temperature and unit permeance for each type magnet alloy evaluated. The exposure temperatures were within the reported operating range.

In practice, if one were to consider a 5% irreversible loss as acceptable, the operational temperature range and size of the magnet would have to be limited to values shown in the un-shaded areas. In examining the data, particularly for cobalt containing magnets, it would be erroneous to assume that even higher operating temperatures could be tolerated because of the low initial irreversible flux loss. In any given circuit design, one must also take into consideration the overall detrimental effect thermal exposures >100°C have on the characteristic loop squareness ($H_k$), intrinsic coercivity ($_MH_c$) and induction (B), and consequently the stability of the operating point.[5-7]

We can also conclude from the data that the degree of irreversible loss at an elevated temperature is inversely proportional to the magnitude of $_MH_c$ in each material type group.

Long-term aging: The results of long-term aging are shown as composite plots of normalized flux loss (from 1 hour) versus exposure time in Figure 1. These plots clearly illustrate the direct relationship between flux loss in time and the two variables, temperature and permeance. Examining all eight groups indicates as a rule that the degree of loss is also dependent upon the magnitude of $_MH_c$ and $H_k$. That is, magnets of the same material type exhibiting higher values for the magnetic parameters cited will incur lower losses.

Effects on demagnetization curves: Composite plots of typical intrinsic and normal demagnetization curves (Figure 2) measured before and after aging clearly illustrate the effect of long-term exposure and magnet geometry. Combined effects due to irreversible and long-term losses at high permeance and moderate temperature conditions ($\leq$ 100°C) are acceptable for all material types evaluated.

0018-9464/88/0300-1623$01.00©1988 IEEE

We also observe as a rule that values of $_{M}H_{C}$ remain nearly constant (< 10% change in the worst case) even after 5000 hours exposure. The slope of intrinsic demagnetization curves also remain nearly constant. From an application standpoint, the primary difficulty to contend with is the sustained loss in magnitude of induction and loop squareness for the restraints indicated. Beyond these limits extreme care should be exercised in selecting the appropriate material for optimum performance.

## Summary

The test results indicate that ternary magnets operating at a high permeance incur acceptable irreversible losses (< 3.0% at 75°C to 125°C) in the first hour of exposure. As the permeance decreases or the temperature increases, severe losses were observed. This was also the case for magnets with dysprosium additions. Conversely, a dysprosium plus cobalt addition drastically improved the initial loss (< 0.5%) at these same temperatures. Long-term elevated temperature losses also follow the same trend, that is, Nd-Fe-B magnets with and without dysprosium exhibit a higher rate of loss as the permeance decreases and/or the temperature increases. The losses incurred by magnets containing a cobalt addition are substantially less.

TABLE 1: RANGE OF INITIAL IRREVERSIBLE LOSS (1 HOUR) OF OPEN CIRCUIT REMANENT FLUX, AS A FUNCTION OF PERMEANCE AND ELEVATED TEMPERATURE*

Nd-Fe-B: $(BH)_{MAX} \approx 35$ MGOe

| $-B_d/H_d$ | EXPOSURE TEMPERATURE IN AIR | | | |
|---|---|---|---|---|
| | 75°C | 100°C | 125°C | 150°C |
| 3.2 | 0.4 - 0.5 | 1.0 - 2.0 | 3.0 - 8.0 | 12 - 27 |
| 1.0 | 1.6 - 2.1 | 9.0 - 18 | 22 - 38 | 41 - 57 |
| 0.5 | 9.5 - 14 | 22 - 33 | 37 - 60 | 56 - 66 |

Nd,Dy-Fe-B: $(BH)_{MAX} \approx 30$ MGOe

| $-B_d/H_d$ | EXPOSURE TEMPERATURE IN AIR | | | |
|---|---|---|---|---|
| | 75°C | 100°C | 125°C | 150°C |
| 3.2 | 0.1 - 0.6 | 0.4 - 0.7 | 1.0 - 2.2 | 1.5 - 10 |
| 1.0 | 0.3 - 0.7 | 1.0 - 5.5 | 2.0 - 6.3 | 11 - 42 |
| 0.5 | 0.7 - 1.5 | 2.3 - 20 | 9.5 - 30 | 28 - 43 |

Nd,Dy-Fe,Co-B: $(BH)_{MAX} \approx 30$ MGOe

| $-B_d/H_d$ | EXPOSURE TEMPERATURE IN AIR | | | |
|---|---|---|---|---|
| | 75°C | 100°C | 125°C | 150°C |
| 3.2 | 0.24 | 0.41 | 0.47 | 0.55 |
| 1.0 | 0.24 | 0.53 | 0.75 | 1.00 |
| 0.5 | 0.44 | 0.89 | 1.00 | 3.60 |

* Unshaded areas represent design limits for temperature and permeance that would incur operational losses < 5 percent.

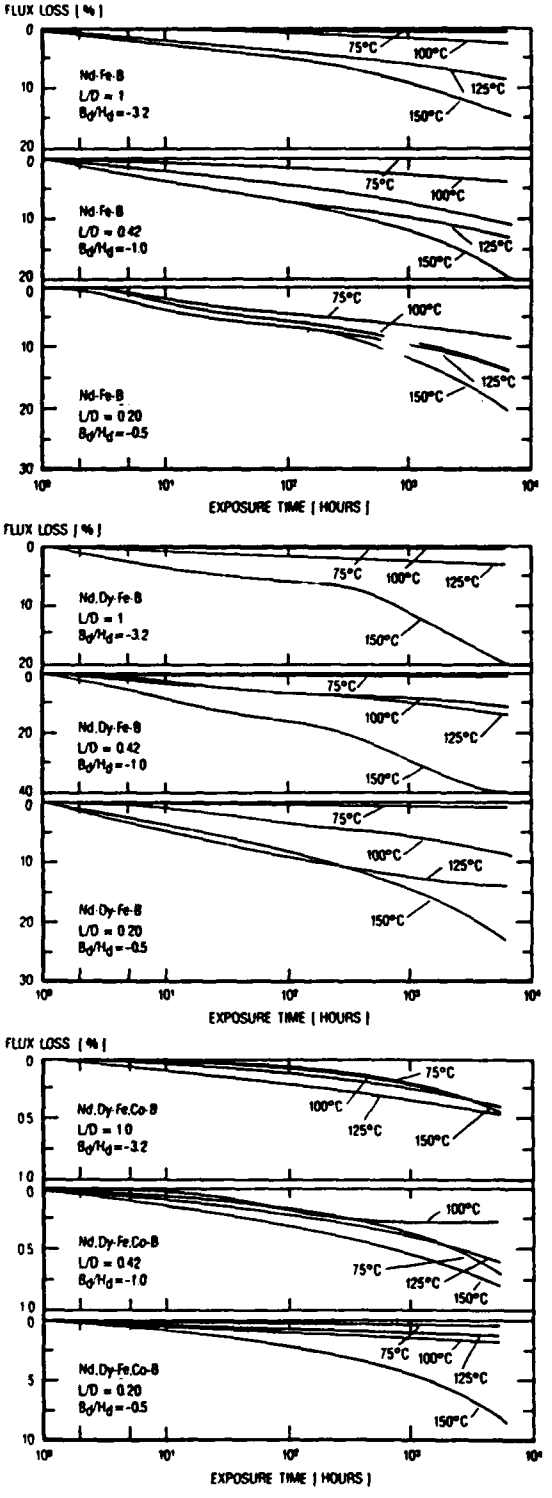


Fig. 1 Long term stability (> 5,000 hours) of open circuit remanent flux of three commercial Neodymium type permanent magnet alloys, as a function of elevated temperature exposure between 75° and 150°C, and unit permeance $B_d/H_d$ of -3.2, -1 and 0.5.

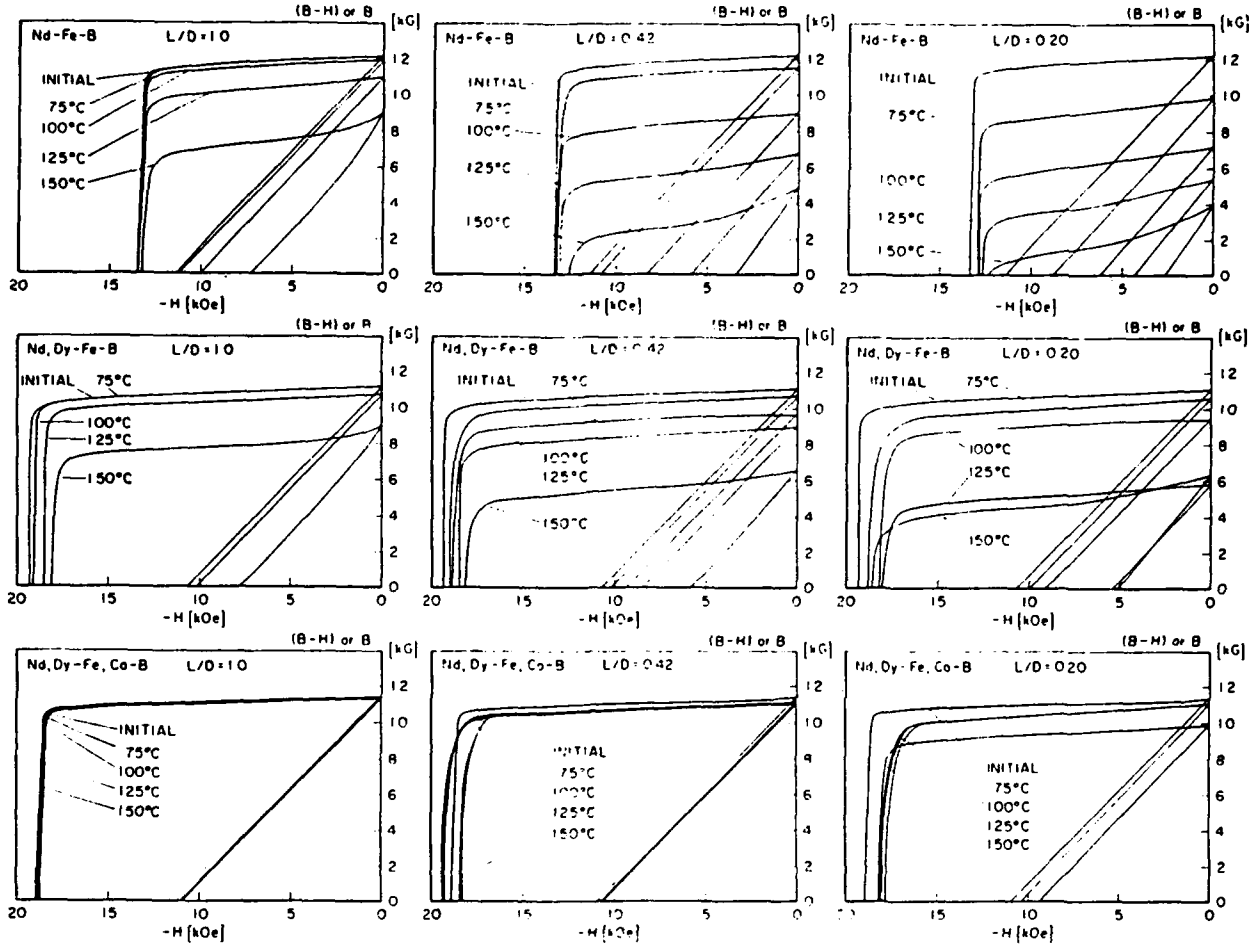


Fig. 2 Thermally induced changes in the intrinsic and normal demagnetization curves after long term aging (> 5,000 hours), as a function of Neodymium magnet alloy type, temperature, and sample L/D ratios pertaining to an open-circuit permeance B/H = -3.2, -1.0, -0.5.


## Acknowledgments

This work was performed with support from the U.S. Army Electronics Technology and Devices Laboratory under contract DAAK20-84K-0458.

We wish to thank the Hitachi Metals Research Laboratory, Sumitomo Metals Corporation of Japan, and Crucible Research Center, Hitachi Magnetics Corporation, USA, for contributing the test magnets used in this investigation.


## References


1. M. Sagawa et al., IEEE Trans. Magnetics MAG-20, 1984, p. 1584.
2. K.S.V.L. Narasimhan, J. Appl. Phys. 57, 1985, p.4081.
3. M. Tokunaga et al., IEEE Trans. Magnetics MAG-22, 1986, p. 904.
4. R.W. Lee et al., IEEE Trans Magnetics MAG-21, 1985, p. 1958.
5. D. Li et al., J. Appl. Phys. 57, 1985, p. 4140.
6. Y. Xiao, K.J. Strnat et al., "Effect of Minor Alloying Substituents (Nb,Ti,Zr) on the Temperature Dependence of the Permanent Magnet Properties of Sintered (Nd,Dy)-(Fe,Co)-B," Paper No. W8.2 to be presented at the 9th Int'l. Workshop on Rare Earth Magnets and their Applications, Bad Soden, FRG, August 31 - September 3, 1987.
7. Y. Xiao, K.J. Strnat et al., "Effects of Erbium Substitution on Permanent Magnet Properties of Sintered (Nd,Dy)-(Fe,Co)-B," to be published in IEEE Trans. Magnetics MAG-23, September 1987 issue.

# APPENDIX D

## EFFECTS OF ERBIUM SUBSTITUTION ON PERMANENT-MAGNET PROPERTIES OF SINTERED (Nd,Dy)-(Fe,Co)-B

# EFFECTS OF ERBIUM SUBSTITUTION ON PERMANENT MAGNET PROPERTIES OF SINTERED (Nd,Dy)-(Fe,Co)-B

Y. Xiao,* K.J. Strnat, H.F. Mildrum and A.E. Ray
School of Engineering and Research Institute
University of Dayton, Dayton, Ohio 45469

ABSTRACT: The effects of dysprosium and erbium on the temperature dependence of remanence and intrinsic coercivity in Co-containing Nd-Fe-B were studied. Sintered magnets were prepared and demagnetization curves measured at temperatures between -50 and 200°C. Curie temperatures and irreversible losses of open-circuit flux on heating were also determined. Dy increases the coercivity while Er decreases it. Both Dy and Er can improve the temperature coefficient of remanence and even that of the intrinsic coercivity. Simultaneous substitution of these two heavy rare earths can be beneficial for magnets used below 150°C, but Er lowers $H_c$ and increases the irreversible loss at higher temperatures.

## Introduction

Remanence, $B_r$, energy product, $(BH)_{max}$, and especially the intrinsic coercivity, ${}_MH_c$, of Nd-Fe-B magnets decline quickly with increasing temperature.[1] To make these magnets more useful above room temperature (r.t.), cobalt can be introduced to substitute for some of the iron.[2] This raises the Curie temperature, $T_c$, but at the expense of ${}_MH_c$. A modest dysprosium addition can nearly double the ${}_MH_c$, thus counteracting this adverse side effect of cobalt.[3] *Terbium is even better suited for enhancing the coercivity,*[4] but it is too scarce and expensive for most commercial uses. All the heavy rare earths (HRE)--Gd, Tb, Dy, Ho, Er and Tm--reduce the saturation, $B_s$, by coupling their magnetic moments antiparallel to the Fe moments.

$Er_2Fe_{14}B$ is known to have easy-base-plane anisotropy at r.t.[5,6] which is not favorable for developing coercivity. Therefore, erbium has not been considered as a substituent, even though it might be expected to reduce the temperature dependence of $B_r$ while keeping its magnitude higher than Tb, Dy or Ho do. $Er_2Fe_{14}B$ shows a higher saturation than $Dy_2Fe_{14}B$ or $Tb_2Fe_{14}B$ up to ~500 K, and its $B_s$ rises more strongly with increasing temperature in the range $0 \rightarrow 250$°K.[6] Hence one can expect Er substitution for Nd to improve the temperature coefficient, $\alpha$, of $B_r$ while retaining a relatively high remanence. Simultaneous substitution of Dy and Er might extend the range of such improvement to well above r.t., but at a sacrifice of $B_r$. The temperature coefficient, $\beta$, of ${}_MH_c$ should be adversely affected by Er because the anisotropy field of the 2-14-1 phase is reduced; but Dy should counteract this adverse side effect, too, and might allow one to maintain the ${}_MH_c$ near that of unsubstituted Nd-(Fe,Co)-B.

To test the above considerations, a set of experiments was designed, working in the alloy system $(Nd_{.80}Dy_{.20-x}Er_x)(Fe_{.80}Co_{.12}B_{.08})_{5.5}$ with x=0.04, 0.08, 0.12, 0.16, and 0.20. For control/reference purposes magnets with the compositions $Nd(Fe_{.80}Co_{.12}B_{.08})_{5.5}$ and $(Nd_{1-x}Dy_x)(Fe_{.80}Co_{.12}B_{.08})_{5.5}$, x=0.12, 0.16, and 0.20, were also prepared and examined.

## Experimental Procedure

Master alloys were made by arc and induction melting, and specific intermediate compositions by blending powders of these. Magnet samples were prepared by a conventional powder metallurgy process.[2] All samples were field-pressed, sintered at 1080°C for one hour in vacuum and quenched in argon gas; they were then reheated to 900°C/1 hr. in argon, furnace cooled, and they received a final heat treatment at 500°C for one hour. The magnetic properties reported are for the final state.

Demagnetization curves were measured on ~8 mm cubes in closed circuit at temperatures in the range -50 to +200°C with a DC hysteresigraph. Temperature coefficients, in % per °C, of $B_r$ and ${}_MH_c$ were determined from these curve sets. They are defined as follows:[7]

$$(T_1 \rightarrow T_2) = 100[B_r(T_2)-B_r(T_1)]/B_r(25°C)\cdot(T_2-T_1)$$
$$(T_1 \rightarrow T_2) = 100[{}_MH_c(T_2)-{}_MH_c(T_1)]/{}_MH_c(25°C)\cdot(T_2-T_1)$$

Before measurement at each of the different temperatures, the samples were fully remagnetized in a 100 kOe pulsed field at room temperature.

Irreversible flux losses during cycling to elevated temperatures, up to 200°C, were measured on 0.25" diameter cylinders of $p=B/H \approx -2$ in open circuit, using a tightly fitting pull coil and a fluxmeter. A thermal cycle took about 45 min., with 30 min. holding time at T. The Curie temperature of different alloy compositions was determined by a low-field thermomagnetic analysis (TMA) with a 5 kHz field of about 1 Oe amplitude; the average sweep rate was ~1°C/min.

## Results and Discussion

Ternary Nd-Fe-B magnets have excellent room-temperature values of $B_r$ and $(BH)_{max}$, with usefully high coercive force, ${}_MH_c$. However, the temperature coefficient $\alpha$ of $B_r$ in the temperature range $0 \rightarrow 150$°C is high, -0.126% per °C (3.5 to 4.1 times greater than for $SmCo_5$ or 2:17 magnets, respectively), which is often intolerable. ${}_MH_c$ declines at a rate of $\beta$=-0.86% per °C, i.e., ~2.6 to 3.1 times faster than for typical 1-5 or 2:17 magnets.[1] These higher temperature coefficients are usually attributed to the low $T_c \approx 312$°C.

Cobalt: In our experiments, introducing 10 at. % Co increased the Curie temperature to 435°C for $Nd(Fe_{.80}Co_{.12}B_{.08})_{5.5}$ magnets, lowering both temperature coefficients, $\alpha$ and $\beta$ to 0.09% and 0.54% per °C, respectively ($0 \rightarrow 150$°C).

Dysprosium: Additionally substituting some Dy for Nd, in $(Nd_{.80-x}Dy_x)(Fe_{.80}Co_{.12}B_{.08})_{5.5}$ magnets, caused more complex variations of the magnetic properties. The Curie point is slightly reduced by either Dy or Er. Some relevant values of $T_c$ are shown in Table 1.

Table 1: Some Curie Temperatures from Low-Field TMA

| Nominal Composition of Sintered Magnet | Curie Point $T_c$(°C) |
|---|---|
| $Nd(Fe_{.80}Co_{.12}B_{.08})_{5.5}$ | 435 |
| $(Nd_{.88}Dy_{.12})(Fe_{.80}Co_{.12}B_{.08})_{5.5}$ | 431 |
| $(Nd_{.80}Dy_{.20})(Fe_{.80}Co_{.12}B_{.08})_{5.5}$ | 424 |
| $(Nd_{.80}Er_{.20})(Fe_{.80}Co_{.12}B_{.08})_{5.5}$ | 432.5 |

0018-9464/87/0900-2293$01.00 © 1987 IEEE

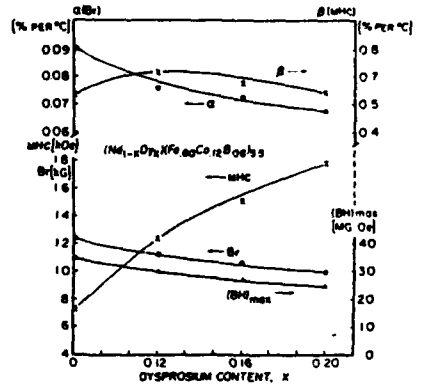


Figure 1. Variation of magnetic properties with Dy content for $(Nd_{1-x}Dy_x)(Fe_{.80}Co_{.12}B_{0.08})_{5.5}$ sintered magnets. $\alpha$ and $\beta$ were calculated for 0→150°C.

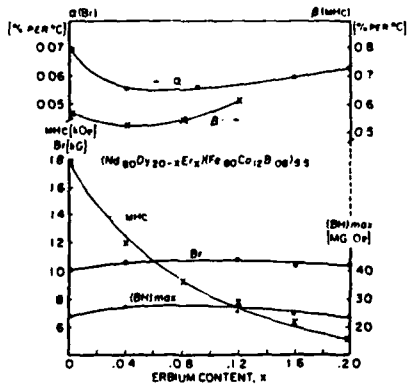


Figure 2. The influence of Er on the magnetic properties of $(Nd_{.80}Dy_{.20-x}Er_x)(Fe_{.80}Co_{.12}B_{.08})_{5.5}$. $\alpha$ and $\beta$ were calculated for 0→150°C.

The observed effects of dysprosium on $B_r$, $_MH_c$ and energy product (see Fig. 1) agree with previous results.[3] They will not be further discussed. $\alpha$(0→150°C) is monotonically decreased by Dy addition. One factor affecting $\alpha$ is the Curie temperature: Dy lowers $T_c$ a little, which might be expected to slightly increase $|\alpha|$; but $|\alpha|$ decreases! Thus the dominant influence must be the effect of the antiferromagnetically coupled Dy sublattice on the temperature variation of the saturation, $B_s$, which partly compensates for the rapid decrease of the Nd moment with increasing temperature. This is characteristic of many HRE-transition metal compounds.

The temperature variation of $_MH_c$ is more complicated. Explaining it is difficult as indeed the origins of coercivity in sintered magnets are still not satisfactorily clarified. $_MH_c$ is affected by the properties of minor secondary phases and their temperature dependence, and thus depends on the nature of all phases present and the partitioning of the different rare earths between them. Figure 1 shows that $\beta$ increases first with increasing Dy, then drops for x >0.12. (The function of $\beta$ vs. T does, of course, also depend on the temperature range for which is calculated.)

Erbium: The influence of Er in the alloy $(Nd_{.80}Dy_{.20-x}Er_x)(Fe_{.80}Co_{.12}B_{.08})_{5.5}$ is shown in Figure 2. $_MH_c$ decreases with increasing x. But the variations of remanence and of both temperature coefficients are more complicated: $B_r$ initially increases slightly with x, but it begins to decrease slowly at x≈0.12. Regarding the initial rise we note that $(Nd_{.80}Er_{.20})(Fe_{.80}Co_{.12}B_{.08})_{5.5}$ has a higher saturation (10.65 kG) than $(Nd_{.80}Dy_{.20})(Fe_{.80}Co_{.12}B_{.08})_{5.5}$ (namely, 10.3 kG). Also, small substitutions of Er for Nd in alloys without Dy, in the $(Nd_{1-x}Er_x)(Fe_{.80}Co_{.12}B_{.08})_{5.5}$ system change $4\pi M_s$ very little while the rate of drop increases for greater x (Table 2). In magnets with both, Dy and Er, the first of these effects may dominate at low Er content, the second for higher x.

Table 2. Effect of Erbium Substitution on Saturation

| $(Nd_{1-x}Er_x)(Fe_{.80}Co_{.12}B_{.08})_{5.5}$ | $4\pi M_s$(G) |
|---|---|
| x = 0 | 12500 |
| x = 0.04 | 12330 |
| x = 0.08 | 12000 |
| x = 0.20 | 10650 |

We find it difficult to understand why there are also minima in the curves of $\alpha$ vs. x and $\beta$ vs. x, both near x=0.04. However, it is a practically useful result that small substitutions of Er for Dy in $(Nd_{.80}Dy_{.20-x}Er_x)(Fe_{.80}Co_{.12}B_{.08})_{5.5}$ further reduce both temperature coefficients. Regarding the temperature variation of $B_r$, we conclude that Dy causes a minor but useful reduction of the slope of $B_s$ vs. T in the temperature range considered, 0→150°C, with Er having a synergistic effect when used together with Dy.--The slight reduction of $\beta$ by small Er additions was unexpected and remains unexplained. In order to confirm the reality of this minimum of $\beta$, another group of experiments was conducted using a higher HRE substitution, Dy+Er=25 at.% of total RE, in $(Nd_{.75}Dy_{.25-x}Er_x)(Fe_{.80}Co_{.12}B_{.08})_{5.5}$. Here, an even lower value of $\beta$=-0.46% was obtained for x=0.05 (compared to $\beta$=-0.53% per °C for x=0).

While substituting 0.04% Er for Dy further decreased $\beta$ compared with an Er-free magnet, the room-temperature coercivity is already relatively low (12.1 kOe) at the minimum of $\beta$. Nevertheless, the r.t. energy product is a maximum near the same value of x. It appears that B, $(BH)_{max}$ and both temperature coefficients can be improved by co-substituting several heavy rare earths, such as Dy plus Er, for some of the Nd in the Nd-HRE-Fe-Co-B system while keeping $_MH_c$ at an acceptable level.

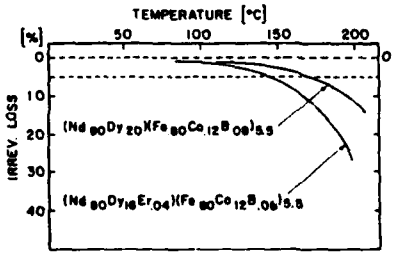


Figure 3. Irreversible flux losses at p=B/H= -2 during cycling between 25°C and the indicated elevated temperature. Tested were magnets with the compositions $(Nd_{.80}By_{.20})(Fe_{.80}Co_{.12}B_{.08})_{5.5}$ and $(Nd_{.80}Dy_{.16}Er_{.04})(Fe_{.80}Co_{.12}B_{.08})_{5.5}$

Figure 3 shows the results of irreversible loss measurements for a $(Nd_{.80}Dy_{.20})(Fe_{.80}Co_{.12}B_{.08})_{5.5}$ magnet and a $(Nd_{.80}Dy_{.16}Er_{.04})(Fe_{.80}Co_{.12}B_{.08})_{5.5}$ magnet. The irreversible loss was <5% up to T=175°C for $(Nd_{.80}Dy_{.20})(Fe_{.80}Co_{.12}B_{.08})_{5.5}$, and below 150°C for the $(Nd_{.80}Dy_{.16}Er_{.04})(Fe_{.80}Co_{.12}B_{.08})_{5.5}$ magnet. The losses are greater for the Er-containing magnet! Inspecting the demagnetizing curves in Figures 4 and 5 shows that at these temperatures the coercivity is near 5 kOe. In other words, it seems necessary to keep ${}_{M}H_{c}$ > 5 kOe at the peak temperature in order to have an irreversible loss below 5% at an operating permeance of p= -2.

## Summary

1. Substituting 10 at % Co for Fe in Nd-Fe-B magnets increases the Curie temperature to 435°C and lowers the temperature coefficient of $B_r$, $\alpha$(0→150°C), from -0.126 to -0.09% per °C.

2. Partially substituting Dy for Nd not only increases the coercivity but also further decreases the temperature coefficients of $B_r$ and ${}_{M}H_{c}$.

3. Substituting a small amount of Er for Dy ($x \approx 0.04$) in $(Nd_{.80}Dy_{.20-x}Er_{x})(Fe_{.80}Co_{.12}B_{.08})_{5.5}$ can further slightly improve the temperature coefficients of both, $B_r$ and ${}_{M}H_{c}$. The best temperature coefficients, $\alpha$ = -0.048% and $\beta$ = -0.46% per °C, were obtained in a sample with the composition $(Nd_{.75}Dy_{.20}Er_{.05})(Fe_{.08}Co_{.12}B_{.08})_{5.5}$.

4. It is necessary to have ${}_{M}H_{c}$>5 kOe at a given top temperature to keep the irreversible loss for p= -2 below 5%. This objective can be achieved either by raising ${}_{M}H_{c}$ or by reducing its temperature coefficient.


## ACKNOWLEDGMENT

This work was performed with support from the U.S. Army Electronics Technology and Devices Laboratory under contract DAAK20-84K-0458.


## REFERENCES


1. D. Li, et al., J. Appl. Physics, 57 (1985) 4140.
2. M. Sagawa, et al., IEEE Trans. Magnetics MAG-20 (1984) 1584.
3. M. Tokunaga, et al., IEEE Trans. Magnetics MAG-22 (1986) 904.
4. M. Tokunaga, et al., IEEE Trans. Magnetics MAG-21 (1985) 1964.
5. S. Sinnema, et al., J. Magnetism and Magnetic Materials 45 (1984) 333.
6. S. Hirosawa, et al., J. Appl. Phys. 59 (1986) 873.
7. H.F. Mildrum and K.M.D. Wong, Proc. 2nd Int'l. Workshop on Rare Earth Perm. Magnets and their Applic., Dayton, Ohio (1976) 35.


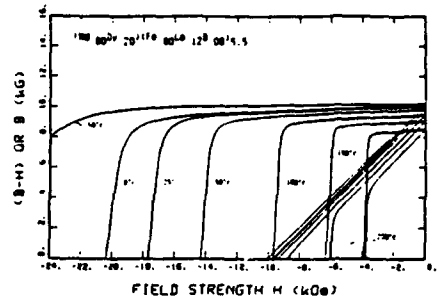


Figure 4. Demagnetization curves at several temperatures between -50°C and 200°C for a $(Nd_{.80}Dy_{.20})(Fe_{.80}Co_{.12}B_{.08})_{5.5}$ magnet.

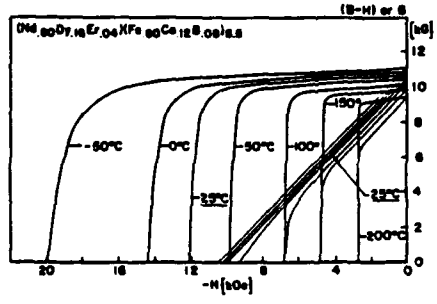


Figure 5. Demagnetization curves at several temperatures between -50°C and 200°C for a $(Nd_{.80}Dy_{.16}Er_{.04})(Fe_{.80}Co_{.12}B_{.08})_{5.5}$ magnet.


* Y. Xiao is on leave of absence from the Beijing University of Iron and Steel Technology, Beijing, P.R. of China.

# APPENDIX E

## ELEVATED TEMPERATURE PROPERTIES OF SINTERED MAGNETS OF (Nd,Dy)-Fe-B MODIFIED WITH COBALT AND ALUMINUM

# Elevated Temperature Properties of Sintered Magnets of (Nd,Dy)-Fe-B Modified with Cobalt and Aluminum

Y. Xiao, H.F. Mildrum, K.J. Strnat and A.E. Ray
School of Engineering, University of Dayton
Dayton, Ohio 45469

## ABSTRACT

The effect of small aluminum additions on the temperature dependence of remanence and intrinsic coercivity in Co- and Dy-containing Nd-Fe-B was studied. Sintered magnets were prepared and demagnetization curves measured at temperatures between -50 to +200°C. Curie temperatures and irreversible flux losses in open circuit were determined. Al increases the coercivity while decreasing remanence, energy product and Curie temperature. Other unfavorable side effects are the increase in temperature coefficients of $B_r$ and, especially, $_MH_c$. Substitution of Al is beneficial for magnets used at elevated temperature.

## INTRODUCTION

The rapid decline on heating of their remanence, $B_r$, the energy product, $(BH)_{max}$, and especially of the intrinsic coercivity, $_MH_c$, limits the application of ternary Nd-Fe-B magnets to below 100-150°C. To enable such magnets to operate at higher temperatures, different alloy modifications have been tried. Design engineers commonly describe the utility of magnets at elevated temperatures by two parameters: the temperature coefficient, $\alpha (B_r)$, of the remanent induction, and the irreversible flux losses in open circuit during a heating-cooling cycle. The losses must be tied to a specific operating point, e.g. by specifying the unit permeance, $p=-B_d/H_d$.

The large value of $|\alpha|$ for Nd-Fe-B magnets is due to the low Curie temperature, $T_c$, and the rapid decrease in Nd moment with increasing temperature, T. Hence, two approaches might result in a reduction of $|\alpha|$: raising the Curie temperature of the main phase of the magnet, or partially substituting heavy rare earths (HRE) for Nd. Cobalt is an effective alloying element for raising $T_c$. [1,2,3] Substitution of 18 to 20 at% Fe by Co enhances $T_c$ to above 500°C and thus lowers $\alpha$. However, this is at the expense of the intrinsic coercivity. A lower $_MH_c$, in turn, leads to an increase of the irreversible loss.

The irreversible losses are generally inversely related to the coercivity; and since $_MH_c$ usually decreases with increasing operating temperatures, the losses are indirectly related to the temperature coefficient of coercivity, $\beta (_MH_c)$. The physical parameters affecting the temperature dependence of the coercivity are not well known. One common practical approach to lowering the irreversible losses is simply to increase the intrinsic coercivity at room temperature. Then, even if $_MH_c$ is reduced by the same factor as in the absence of Dy on heating, a higher absolute value is left at T, and the flux loss is lower. A modest dysprosium addition can nearly double $_MH_c$ of a Nd-Fe-Co-B magnet and bring the irreversible loss to below 5% at 200°C [4]. However, the use of the expensive Dy significantly raises the cost of magnets, especially at higher dysprosium contents. Aluminum has also been found effective for enhancing the coercivity in both, Nd-Fe-B [5,6] and Nd-Fe-Co-B magnets.[7] It is much cheaper than Dy. But an unfavorable side effect of aluminum addition is that $B_r$ and $T_c$ decrease with increasing Al content.

Simultaneous substitution of Dy and Al for Nd and Fe, respectively, might be expected to offer a favorable compromise, yielding high coercivity

Mat. Res. Soc. Symp. Proc. Vol 96 · 1987 Materials Research Society

and a good remanence at elevated operating temperatures. Based on the above consideration, a set of experiments was designed, varying the Al content at a constant Dy substitution in the alloy system $(Nd_{0.88}Dy_{0.12})(Fe_{.80-x}Co_{.12}B_{.08}Al_x)_{5.5}$, where x=0.012, 0.024 and 0.036. For control and reference purposes, the properties of a corresponding Dy- and Al-free magnet of composition $Nd(Fe_{.80}Co_{.12}B_{.08})_{5.5}$ were also examined.

## EXPERIMENTAL PROCEDURE

Master alloys were prepared either by arc or induction melting, and specific intermediate compositions by blending powders of these. Sintered magnets were made by a conventional powder metallurgy process.[1] All samples were sintered at 1080°C for one hour in vacuum and rapidly cooled in argon gas; they were then reheated to 900°C/one hour in argon, furnace cooled, and they received a final heat treatment at 500°C for one hour. Magnetic measurements were made after the 900° anneal and in the final state.

Demagnetization curves were measured either on ~8mm cubes in closed circuit at temperatures in the range -50 to +200°C with a DC hysteresigraph, or on ~3mm cubes in open circuit in the same temperature range with a magnetometer. The temperature coefficients of $B_r$ and $_MH_c$ were determined from these curve sets. They are defined as follows: [8]

$$\left.\begin{aligned}\alpha(T_1\rightarrow T_2) &= 100[B_r(T_2)-B_r(T_1)]/B_r(25°C)\cdot(T_2-T_1)\\ \beta(T_1\rightarrow T_2) &= 100[{}_MH_c(T_2)-{}_MH_c(T_1)]/{}_MH_c(25°C)\cdot(T_2-T_1)\end{aligned}\right\}\ \text{in \% per °C}$$

Before measurement at each temperature, the samples were fully remagnetized in a 100 kOe pulsed field at room temperature.

Irreversible flux losses during cycling to several elevated temperatures, up to 200°C, were measured on 0.25" diameter cylinders of p=B/H≈-2 in open circuit, using a tightly fitting pull coil and a fluxmeter. The Curie temperature of different alloy compositions was determined by a low-field thermomagnetic analysis (TMA) with a 5 kHz field of about 1 Oe amplitude; the average sweep rate was 1°C/min.

## RESULTS AND DISCUSSION

Ternary Nd-Fe-B magnets combine excellent room-temperature (r.t.) values of remanence and energy product, with a usefully high coercive force. However, the temperature coefficients, $\alpha$ of $B_r$, and $\beta$ of $_MH_c$, in the temperature range 0-150°C are large, -0.126%°C and -0.71%°C, respectively. [9] These values are much higher than those of typical 1-5 and 2-17 Sm-Co magnets. The higher temperature coefficients are usually attributed to the low Curie temperature of $Nd_2Fe_{14}B$, $T_c$=312°C.

In our experiments, introducing 10 at% cobalt increased $T_c$ to 435°C, for $Nd(Fe_{.80}Co_{.12}B_{.08})_{5.5}$ magnets, lowering the $\alpha$ (0→150°C) to 0.09%per °C. By substituting some dysprosium for Nd, in $(Nd_{0.88}Dy_{.12})(Fe_{.80}Co_{.12}B_{.08})_{5.5}$, $\alpha$ could be further lowered to 0.077%, while increasing the coercive force, $_MH_c$, to 13 kOe. No significant change of $\beta$ ($_MH_c$) occurred compared to Nd-Fe-B.

The variation of remanence, coercive force, energy product and Curie temperature caused by addition of aluminum in $(Nd_{.88}Dy_{.12})(Fe_{.80-x}Co_{.12}B_{0.08}Al_x)_{5.5}$ is shown in Fig. 1. We see that $_MH_c$ rapidly rises with increasing x. For x = 0.036, i.e., 3 at% Al, the $_MH_c$ reaches 19 kOe. Contrary to this, $B_r$ decreases at the rate of 0.5 kG per 1 at% Al addition. Substituting Al initially does not change the Curie point. However, $T_c$ begins to decrease as the Al content exceeds 1 at%. This suggests that the initial small amounts enter only grain boundary phases, while Al in excess of ~1% is partitioned between the main phase, where it depresses $T_c$, and secondary phases.

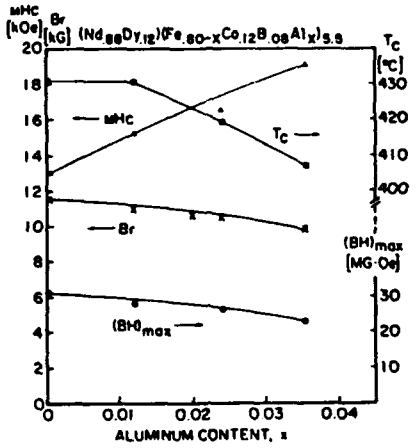


Fig. 1: Variation of magnetic properties with Al content for $(Nd_{0.88}Dy_{.12})(Fe_{.80-x}Co_{.12}B_{.08}Al_x)_{5.5}$ sintered magnets (x=0.012, 0.024, 0.036 correspond to 1, 2, 3 at.% Al, respectively).

The influence of Al on the temperature coefficients, $\alpha$ and $\beta$, is shown in Fig. 2. The magnitude of both increases with rising Al content. Especially $\beta$ gets rapidly worse. The value of $\beta$ = -0.89% for 3 at%, Al even exceeds the $\beta$ value of -0.71 observed on ternary Nd-Fe-B magnets. Although the r.t. coercive force is quite high, such a magnet does not permit a higher operating temperature because $_MH_c$ declines too fast with

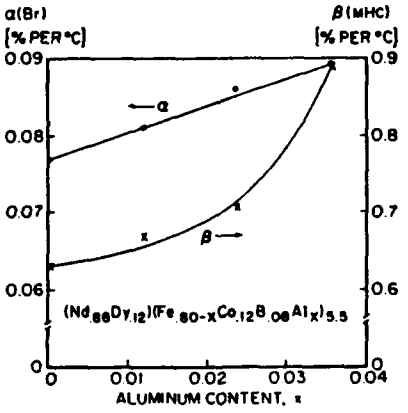


Fig. 2: The influence of Al on temperature coefficients $\alpha$ and $\beta$ for $(Nd_{.88}Dy_{.12})(Fe_{.80-x}Co_{.12}B_{.08}Al_x)_{5.5}$ sintered magnets $\alpha$ and $\beta$ were calculated for 0→150°C.

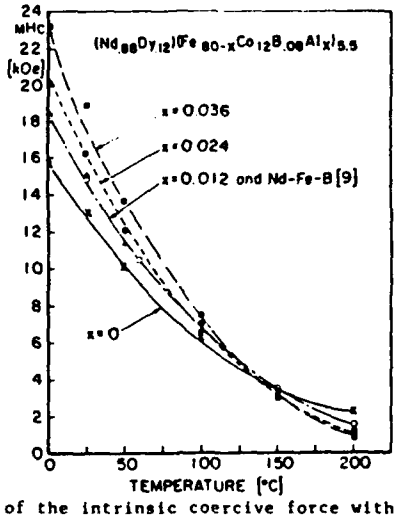


Fig. 3: Variation of the intrinsic coercive force with temperature for $(Nd_{.88}Dy_{.12})(Fe_{.80-x}Co_{.12}B_{.08}Al_x)_{5.5}$ with x=0, 0.012, 0.024, 0.036 and Nd-Fe-B magnets.

increasing temperature. This can be clearly seen in Fig. 3 where the temperature dependence of $_MH_c$ of magnets with different Al content is shown for the temperature range 0-200°C. The curve for Nd-Fe-B is included for comparison. The following facts can be observed:

1. For x=0 (no Al), the coercivity at r.t. is only 13 kOe, but at 200°C there is still 2.1 kOe left. In contrast, the sample with the highest Al content, x=0.036, possesses a 40% higher $_MH_c$ at room temperature, but it has only 1/3 as much coercive force left at 200°C than the x=0 magnet.

2. All the curves intersect around 140°C. Up to 140°C, the magnets with higher r.t. coercivity maintain a higher $_MH_c$.

We can conclude that, when the operating temperature is below ~140°C, the Al-containing magnets may also be expected to show lower irreversible losses. But above ~140°C, the Al additions have no benefit for the temperature stability. Direct measurement of irreversible losses for a $(Nd_{.88}Dy_{.12})(Fe_{.80}Co_{.12}B_{.08})_{5.5}$ magnet and a $(Nd_{.88}Dy_{.12})(Fe_{.764}Co_{.12}B_{.08}Al_{.036})_{5.5}$ magnet generally confirms this conclusion. (Fig. 4) The two curves of irreversible loss vs. T intersect near 150°C. But the gain in stability below this temperature is minimal, while the irreversible loss near 200°C is severely increased by the Al addition. Taking into account the concomitant sacrifices in $B_r$, $(BH)_{max}$ and $\alpha$, the minor improvement in irreversible loss at lower temperatures makes Al additions of questionable practical value. According to our results, substituting Al for some Fe increases the coercive force near r.t., but it does nothing to extend the useful operating temperature beyond the 140-150°C level up to which Nd-Dy-Fe-Co-B or even Nd-Dy-Fe-B magnets are useful. To allow further scrutiny of what is happening at the elevated temperatures, two complete sets of demagnetization curves measured at several temperatures for $(Nd_{.88}Dy_{.12})(Fe_{.80}Co_{.12}B_{.08})_{5.5}$ and $(Nd_{.88}Dy_{.12})(Fe_{.764}Co_{.12}B_{.08}Al_{.036})_{5.5}$ are shown in Fig. 5 and 6.

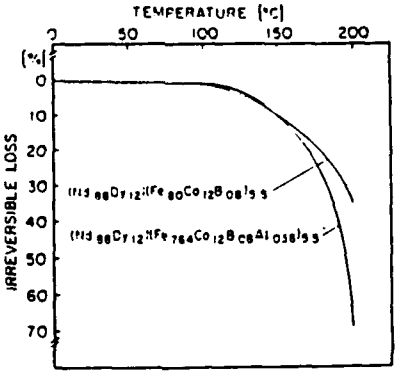


Fig. 4: Irreversible flux losses at p=B/H = -2 during cycling between 25°C and the indicated elevated temperature. Tested were magnets with compositions $(Nd_{.88}Dy_{.12})(Fe_{.80}Co_{.12}B_{.08})_{5.5}$ and $(Nd_{.88}Dy_{.12})(Fe_{.764}Co_{.12}B_{.08}Al_{.036})_{5.5}$.

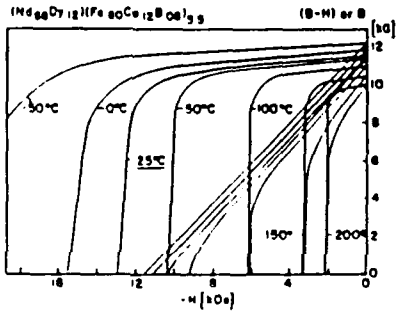


Fig. 5: Demagnetization curves at several temperatures between -50°C and 200°C for a $(Nd_{.88}Dy_{.12})(Fe_{.80}Co_{.12}B_{.08})_{5.5}$ magnet.

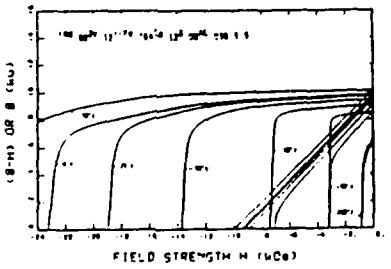


Fig. 6: Demagnetization curves at several temperatures between -50° and 200°C for a $(Nd_{.88}Dy_{.12})(Fe_{.764}Co_{.12}B_{.08}Al_{.036})_{5.5}$ magnet.

Before we summarize, we should briefly consider what these results tell us about the factors which affect the temperature coefficient of coercivity. $\beta$ does not seem to be directly related to the main-phase Curie temperature. (The temperature coefficient of induction is!) If $\beta$ were approximately inversely proportional to $T_c$, our (Co + Al)-containing magnet should have a lower $|\beta|$-value than Nd-Fe-B because its Curie point is higher by more than 100°C. But, on the contrary, it has a much higher $|\beta|$-value! Like ${}_{M}H_c$, the $\beta$ is likely to depend strongly on the temperature variation of the magnetic properties of secondary phases in the grain boundaries. The experiments described cannot yield any direct information about these.

## SUMMARY

1. Substituting 10 at.% Co for Fe increases the Curie temperature from ~310°C to 435°C and lowers the temperature coefficient of $B_r$, $\alpha(0\rightarrow150°C)$ to 0.09% per °C.

2. Partially substituting Dy for Nd in a Co-containing magnet of composition $(Nd_{.88}Dy_{.12})(Fe_{.80}Co_{.12}B_{.08})_{5.5}$ not only increases the coercivity, but it also decreases (i.e., improves) the temperature coefficient of $B_r$.

3. Additionally substituting Al for some of the Fe increases the coercivity, but it lowers the remanence and energy product. It raises the temperature coefficients, $\alpha(B_r)$ and, especially, $\beta({}_{M}H_c)$.

4. Such dual substitution of Co and Al is therefore not a good way of raising the useful operating temperature of magnets above 150°C. However, the magnets have attractively high coercive force near room temperature.

## ACKNOWLEDGMENT

This work was supported by the U.S. Army Electronics Technology and Devices Laboratory, Ft. Monmouth, New Jersey, under contract DAAK20-84-K-0458.

## REFERENCES

1. M. Sagawa et al., IEEE Trans. Magnetics MAG-20, (1984), 1584-1589.
2. T. Shibata et al., IEEE Trans. Magnetics MAG-21, (1985), 1952-1954.
3. Matsuura et al., Appl. Phys. Letters 46, 308 (1985).
4. M. Tokunaga et al., IEEE Trans. Magnetics MAG-22, (1986), 904.
5. M.(Maocai) Zhang et al., Proc. 8th Int'l. Workshop on REPM and their Applications, Dayton, OH, USA, May 1985, 541-552.
6. B.-M.(Bao-Min) Ma and K.S.V.L. Narasimhan, IEEE Trans. Magnetics MAG-22, (1986), 916-918.
7. T. Mizoguchi et al., IEEE Trans. Magnetics MAG-22, (1986), 919-921.
8. H.F. Mildrum and K.M.D. Wong, Proc. 2nd Int'l. Workshop on REPM and their Applications, Dayton, OH, USA, (1976), 35-54.
9. D. Li, K.J. Strnat and H.F. Mildrum, J. Appl. Physics, 57, (1985), 4140.
10. Y. Xiao et al., INTERMAG 1987, to be published in IEEE Trans. Magnetics, MAG-23 (Sep. 1987).

# APPENDIX F

## EFFECT OF MINOR ALLOYING SUBSTITUENTS (Nb,Ti,Zr) ON THE TEMPERATURE DEPENDENCE OF THE PERMANENT MAGNET PROPERTIES OF SINTERED (Nd,Dy)-(Fe,Co)-B

# EFFECT OF MINOR ALLOYING SUBSTITUENTS (Nb,Ti,Zr) ON THE TEMPERATURE DEPENDENCE OF THE PERMANENT MAGNET PROPERTIES OF SINTERED (Nd,Dy)-(Fe,Co)-B

Y. Xiao, K.J. Strnat, H.F. Mildrum and A.E.Ray
University of Dayton, School of Engineering, Dayton, Ohio 45469, USA

## ABSTRACT

Sintered bodies of $(Nd,Dy)(Fe,Co,B,M)_{5.5}$ were prepared, elevated-temperature magnetization curves measured, and the temperature dependence of permanent magnetic properties studied between -50° and 150°C. The effects of substituents M=Nb, Ti and Zr on $B_r$, $_MH_c$ and their temperature coefficients are reported. Small substitutions, especially of Nb, make the magnets more useful near 150°C. Larger amounts of M-element destabilize the 2-14-1 structure; formation of a 2-17 phase then severely degrades the coercivity.

## INTRODUCTION

It is well known that permanent magnets made from Nd-Fe-B alloys have excellent properties at room temperature, but their remanence ($B_r$) and, especially, their intrinsic coercive force ($_MH_c$) drop off rapidly on heating. This is true whether such magnets are processed by sintering or by the method of rapid quenching and further processing such as bonding or hot pressing. Making these magnets more useful at elevated temperatures in the 150-200°C range is at present an important objective of research and development, pursued in a number of laboratories worldwide.[1-7] The general approach is to modify the magnet alloy by introducing fourth, fifth and sixth component elements. However, even with a given alloy composition, it is possible to change the temperature variation of $_MH_c$ somewhat by altering details of the heat treatment, thus affecting the metallurgical microstructure in subtle ways.[2]

The users of the magnets--engineers designing devices and machines--often describe the temperature dependence of salient magnet properties in terms of temperature coefficients. The T.C. is a measure of the relative change of a quantity, often averaged over a certain temperature range, and normalized to the value at a reference temperature (which is usually room temperature). Considering the applied objective of this work, we also use temperature coefficients to discuss the consequences of certain alloying measures and to interpret the practical significance of our own results. We shall define two T.C.'s, for the common use-temperature range 0-150°C, using a linear approximation between these end points, and referencing to the value at room temperature (R.T.). A generalized temperature coefficient (T.C.) is then defined by the following equation, in which Q ("quantity") can represent $B_r$, or $H_c$, or any other property:

$$T.C.(T_1 \rightarrow T_2) = 100[Q(T_2) - Q(T_1)]/Q(25°C)\cdot(T_2-T_1) \text{ in \% per °C}$$

**********

Paper No. W8.2 at the 9th International Workshop on Rare-Earth Magnets and their Applications, Bad Soden, FRG, August 31 - September 2, 1987 (Proceedings Book by: Deutsche Physikalische Gesellschaft e. V., D-5340 Bad Honnef 1, FRG).

The T.C. of the remanence will be designated $\alpha(B_r)$. Note that often a modification of this quantity, using a flux density level, $B_d$, for a particular operating point in the second quadrant, is more useful to the design engineer, although $\alpha(B_r)$ is commonly reported by magnet producers. We also use a T.C. of the intrinsic coercive force, $\beta({}_MH_c)$. For the magnet types under study both quantities are negative, and the objective of the alloy modifications is to reduce the absolute value of $\alpha$ and $\beta$.

The large value of $\alpha$ for Nd-Fe-B is due to the low Curie temperature, $T_c$, and to the rapid decrease of the Nd moment with increasing temperature, T. Consequently, two approaches have been taken to reducing $\alpha$ : replacing some iron with cobalt, and substituting a heavy rare earth (Tb,Dy,Er) for some of the neodymium.[4,7] Magnets based on variations of the generic formula $(Nd,Dy)(Fe,Co,B)_x$ have been studied and products of this kind are now being commercially introduced.[2] The temperature coefficient of coercivity, $\beta$, is also an important practical parameter since it directly affects the irreversible losses of flux on heating. Its absolute value is typically one order of magnitude greater than that of $\alpha$. It is the rapid drop of ${}_MH_c$ with increasing temperature, and any loss of hysteresis loop squareness, which limit the utility of the Nd-Fe-B magnets at elevated temperatures much more severely than a low Curie point or a high value of $\alpha$. Unfortunately, the physical origins of the coercivity are still poorly understood, and so it is difficult to plan an effective approach to controlling and reducing $\beta$ by changing composition or microstructure. One commonly practiced measure is simply to increase the coercivity to guarantee that a higher ${}_MH_c$ value remains even at elevated T.

It was found that additions of dysprosium as well as aluminum can increase the room temperature coercive force up to 100%. Dy additions leave $\beta$ largely unchanged, and thus the top operating temperature at which irreversible losses remain tolerable is raised to 150°C for many applications. (Nd,Dy)-Fe-B magnets are therefore useful and have been in commercial production for some time. Cobalt, while raising the $T_c$ of the 2-14-1 main phase by $\sim$10°C per 1% substitution, reduces the coercive force, and this offsets its beneficial effect on the temperature variation of $B_r$. This can be counteracted by the simultaneous introduction of Dy and Co, and the "Nd-Fe" magnets with the best elevated temperature stability at present are of the type (Nd,Dy)(Fe,Co)-B.

However, it was also found that not all alloying elements which increase the R.T. coercivity will necessarily improve the stability at 150°C and above. A typical example is aluminum. In an earlier paper [6] we reported on the effect of aluminum additions to magnets of a reference composition $(Nd_{.88}Dy_{.12})(Fe_{.80}Co_{.12}B_{.08})_{5.5}$. Although a significant increase of the R.T. coercivity was obtained, the Al also strongly increased $\beta$, and above approximately 120°C the ${}_MH_c$ was in fact lower than without the Al.

All this suggests that a largely empirical search for other effective alloying elements is necessary. In this paper, we investigate the effect which substitutions of the elements niobium, titanium and zirconium for a part of the iron have on the magnetic properties and their temperature dependence. Specifically, we examined alloys of the nominal compositions $(Nd_{.88}Dy_{.12})(Fe_{.80-x}Co_{.12}B_{.08}M_x)_{5.5}$ where M=Nb, Ti, and Zr.

## EXPERIMENTAL METHODS

The procedures for preparing magnets and measuring their magnetic properties were previously described (6,7). Briefly, master alloys were prepared by arc or induction melting, intermediate compositions by blending powders of these. Magnet samples were made by ball milling, pressing in a transverse magnetic aligning field, vacuum sintering at 1080°C for one hour, followed by rapid cooling in argon gas, reheating to 900°C/1 hour in argon, furnace cooling and a final heat treatment at 500°C/1 hour.

Demagnetization curves were measured on cubes in a closed circuit with a DC hysteresigraph comprising a dual electronic integrator and a fixture permitting the heating and cooling of samples in the range -50 to +200°C.[8] The reported values of $B_r$ and $_MH_c$ and their temperature coefficients were determined from these curve sets.

Low-field AC thermomagnetic analysis was used to determine Curie points.[9] This method is discussed in more detail below.

## RESULTS AND DISCUSSIONS

Figure 1 shows the effects on the intrinsic coercive force of substituting each of the three elements, M=Nb, Ti and Zr. Note that an M-content of x=0.012 closely corresponds to 1 atomic % of the total alloy. The composition was altered in such 1% steps. In each case, small additions of M first bring a substantial increase in coercivity, up to a pronounced maximum beyond which $_MH_c$ drops rapidly with increasing x. Both the initial rate of increase and the rate of the drop after the peak are almost the same for the three elements. However, Nb is the most effective enhancer of the coercive force. The optimum 3 at.% substitution (x=0.036) increases $_MH_c$ by 50%, to a maximum of 16.8 kOe. For M=Zr and Ti the maximum occurs at 1% (x=0.012) and the $H_c$-gain is only about 12%. While we cannot explain the reason for the initial increase in coercivity, it is certainly a desirable effect. Especially Nb seems a useful modifier. To fully judge its utility and compare it with the effects of other elements, it is necessary to measure the influence on remanence, loop squareness and energy product, and to look at the reversible temperature coefficients of remanence and coercivity. Such measurements are reported.

The important question also arises why only small M-substitutions are helpful, and what causes the rapid deterioration of $_MH_c$ above a critical amount. An excess of M undoubtedly changes the microstructure in such a way that magnetization reversal becomes easy in some grains, possibly by introducing a soft magnetic phase that can serve to nucleate reverse domains at low fields. This question is addressed at the end of this paper.

Let us now inspect the variations of other magnetic perameters with Nb, Ti, and Zr additions. Figure 2 shows the composition dependence of the magnetization measured in a 23 kOe forward field in the first quadrant, the "saturation," $4\pi M_s$, and the zero-field remanence, $B_r$. As one would expect, these quantities are reduced by all these substituents. However, here, too, the Nb is the most useful, the flux density reductions being negligibly small up to the coercivity peak. Ti is worse; it reduces $B_r$ by $\sim$5% at the peak position (1 at.%) and by $\sim$30% at 3 at.% Ti. Zirconium reduces the remanence

but little at the $_{M}H_{c}$ peak, but then depresses it more rapidly than the Ti does.

Figure 3 shows room-temperature demagnetization curves of the three magnets with the highest coercive forces in each group. We see that the Nd and Zr additions not only enhance the $_{M}H_{c}$ but also maintain a good loop squareness (or high $H_{k}$ value). In contrast, the Ti-containing magnet has a very rounded demagnetization curve, which is undesirable.

Since niobium is by far the best of the three modifiers studied, the following discussion of other magnetic properties will be limited to the Nb-containing magnets. Figure 4 shows the variation with Nb content of $T_{c}$, $\alpha$ and $\beta$, and of the mass density, $\rho$, achieved in sintering. We see that $T_{c}$ remains essentially unchanged by the Nb additions, at $\sim$430°C. Only above x=0.06 (5 at.% Nb) a small decline is noticeable. At 10% (not shown) $T_{c}$ is down to 406°C. Both coefficients initially increase a little and then drop to values slightly below those of the Nb-free reference magnet: for 3 at.% Nb, $\alpha$ and $\beta$ are 0.075 and 0.57, respectively, compared to 0.077 and 0.63 per °C for the reference. We have previously measured still slightly lower values on a similar magnet with higher dysprosium content, $(Nd_{.80}Dy_{.20})(Fe_{.80}Co_{.12}B_{.08})_{5.5}$, namely, $\alpha$ = 0.068 and $\beta$ = 0.54 [7].

A set of demagnetization curves measured at seven different temperatures between -50°C and +200°C is shown in Figure 5. It is from such curves that the temperature coefficients were determined. Note that the $\alpha(B_{r})$ as defined here is not necessarily identical with the reversible T.C. measured in open circuit after a heating-cooling cycle. Even at the highest temperature, 200°C, the intrinsic demagnetization curve is fairly square ($H_{k} \approx {}_{M}H_{c}$) and $_{M}H_{c}$ > 3 kOe, which is 1 kOe higher than for the Nb-free reference magnet.

## THERMO-MAGNETIC PHASE ANALYSIS

Objective: We next wanted to learn something about the reason why the coercive force drops rapidly when the amount of substituent exceeds a critical value of $\sim$3% for Nd or $\sim$1% for Ti and Zr. If this is due to the formation of a soft magnetic "nucleation phase," the latter would have to have a Curie temperature above R.T., detectable by thermo-magnetic analysis (TMA).

Method: We employed a TMA technique which we have used in similar form for studying rare earth-transition metal alloys or magnets for over twenty years.[9,10] A $\sim$500 mg quantity of coarse alloy powder is made the core of an air-core transformer which can be heated and cooled. The primary is excited with a 5 kHz current that produces a field of $\sim$1 Oe amplitude. The voltage induced in the secondary, corrected for the air flux linkage, is amplified, synchronously rectified and plotted as a function of temperature while the sample is slowly heated and cooled. (Typically 0.5 to 2°C per minute in critical regions). In very hard magnetic materials, the 1 Oe field causes mostly small reversible domain wall motions and the resulting plot has essentially the shape of an initial permability curve, $\mu_{i}$ vs. T. The Curie temperature of a ferromagnetic phase is indicated by a "Hopkinson maximum" followed by a steep drop of $\mu$ on the high-T side. The point of inflection of that flank corresponds closely to $T_{c}$ obtained by much more time consuming

high-DC-field measurements with a magnetic balance. In a multiphase alloy, several such maxima and steep flanks will be observed at the Curie temperature of each phase that has a $T_c$ in the temperature range covered by the experiment.

Such "TMA spectra" were obtained for many of the magnet alloys studied, with all three substituents, Nb, Ti and Zr. Figure 6 shows a set of curves for five samples of the Nb series, with Nb contents up to 10 at.%. Generally, the conditions were the same, namely, a 1 Oe peak field and constant amplifier and recorder sensitivities; however, for Fig. (6-a) the field strength was doubled to increase the signal, and in (6-e) the recorder sensitivity was reduced by a factor 2.5 because the peaks were too high.

Results: The Curie point of the 2-14-1 phase is indicated by the upper sharp peak. The origin of the broad low-T maxima is not clear, but such "bulges" are always observed in rare earth-cobalt or iron sintered magnets, and their shape and position changes between heating and cooling. They may correspond to a secondary phase of ill-defined composition and therefore variable $T_c$. However, in materials with high magnetostriction, stress can also strongly influence $\mu_i$, so they may reflect random stresses induced during mortar grinding. Ignoring these low-T peaks, we can say that at zero and low Nb content the 2-14-1 is the only major phase in evidence. When the Nb content exceeds 5%, an indication of a second Curie point near 310°C appears. (Marked 1' in Figure 6-c). As the niobium increases, this low temperature peak and step 1' become more prominent, while peak 2 becomes even smaller. At 10 at.% Nb peak 2 disappears completely. Our interpretation is that niobium destabilizes the 2-14-1 phase and promotes the formation of another ferromagnetic phase with $T_c \approx 310°C$. At 10% Nb the 2-14-1 has completely disappeared and the only ferromagnetic phase with a $T_c$ above R.T. is this newly formed phase. (If we ignore a small step in the curve at ~350°C, marked 3, which seems to be the Curie point of another minor phase).

Experiments to identify this phase with $T_c \approx 310°C$ and to describe its properties are now in progress. Preliminary powder x-ray diffraction data indicate that it is a 2-17 intermetallic. To maintain metallurgical equilibrium, at least one other phase would have to form, probably one that is not ferromagnetic above R.T. There are additional lines in the x-ray spectrum which we have not yet identified. At 10 at.% Nb, there are no 2-14-1 lines. Easy and hard-axis magnetization curve measurements on the 10% Nb alloy are close toegher, indicating that there is little magneto-crystalline anisotropy. This is consistent with the fact that all $Nd_2(Fe,Co)_{17}$ phases have easy-plane symmetry at R.T.[11] Thus, the newly-formed phase may be inherently magnetically soft and not capable of developing high coercivity at all. It is certainly obvious that our present heat treatment is not proper for magnetic hardening.

It is also interesting to note that our "magnets" made of alloys with high Nb-content have lower density. It appears that the 2-17 phase, or the phase mixture which takes the place of the 2-14-1, prevents rapid shrinking during the sintering at 1080°C. It may be that this temperature is simply too low.

Analogous observations were made on the alloys containing Ti and Zr, indicating that there, too, the 2-14-1 phase becomes unstable at higher M-contents and a 2-17 phase forms in its place.

## SUMMARY AND CONCLUSIONS

1. The addition of small amounts of Nd, Ti or Zr can increase the coercive force of sintered magnets of composition $(Nd_{.88}Dy_{.12})(Fe_{.80-x}Co_{.12}B_{.08}M_x)_{5.5}$.

2. Nb is the most effective modifying element of these three. A 3 at.% Nb substitution for Fe can raise the room temperature coercivity about 50%, reducing the remanence only very slightly and keeping the temperature coefficients $\alpha$ and $\beta$ almost unchanged.

3. Niobium is thus a more suitable modifying element than aluminum if the objective is to improve the utility of the magnets at temperatures near 150°C.

4. Nb additions in excess of 3 at.%, and Ti or Zr additions of more than 1 at.%, destabilize the 2-14-1 phase and cause the formation of a 2-17 phase. This dramatically reduces the coercive force of sintered magnets.

## REFERENCES


1. M. Sagawa et al., IEEE Trans. Magnetics MAG-20 (1984), 1584.

2. M. Tokunaga et al., IEEE Trans. Magnetics MAG-22 (1986), 904.

3. M.(Maocai) Zhang et al., Proc. 8th Int'l. Workshop on REPM and their Applications, Dayton, OH, USA, May 1985, 541.

4. T. Mizoguchi et al., IEEE Trans. Magnetics MAG-22 (1986), 919.

5. B.-M.(Bao-Min) Ma et al., IEEE Trans. Magnetics MAG-22 (1986), 916.

6. Y. Xiao et al., Paper F.2.5 1987 MRC Spring Meet. To be published in MRC Proceedings (fall 1987).

7. Y. Xiao et al., Paper BC-05 1987 INTERMAG. To be published IEEE Trans. Magnetics MAG-23 (Sep. 1987).

8. Hysteresigraph HG-105 and temperature fixture TPF-1 of KJS Associates.

9. L.R. Salmans et al., Report AFML-TR-68-159, USAF Materials Laboratory, Wright-Patterson AFB, Ohio (1968).

10. K. Strnat et al., IEEE Trans. Magnetics MAG-2 (1966), 489.

11. A.E. Ray and K.J. Strnat, IEEE Trans. Magnetics MAG-8 (1972), 516.


## ACKNOWLEDGMENT


This work was supported by the U.S.Army Electronics Technology and Devices Laboratory, Ft.Monmouth, New Jersey under contract DAAK20-84-K-0458.

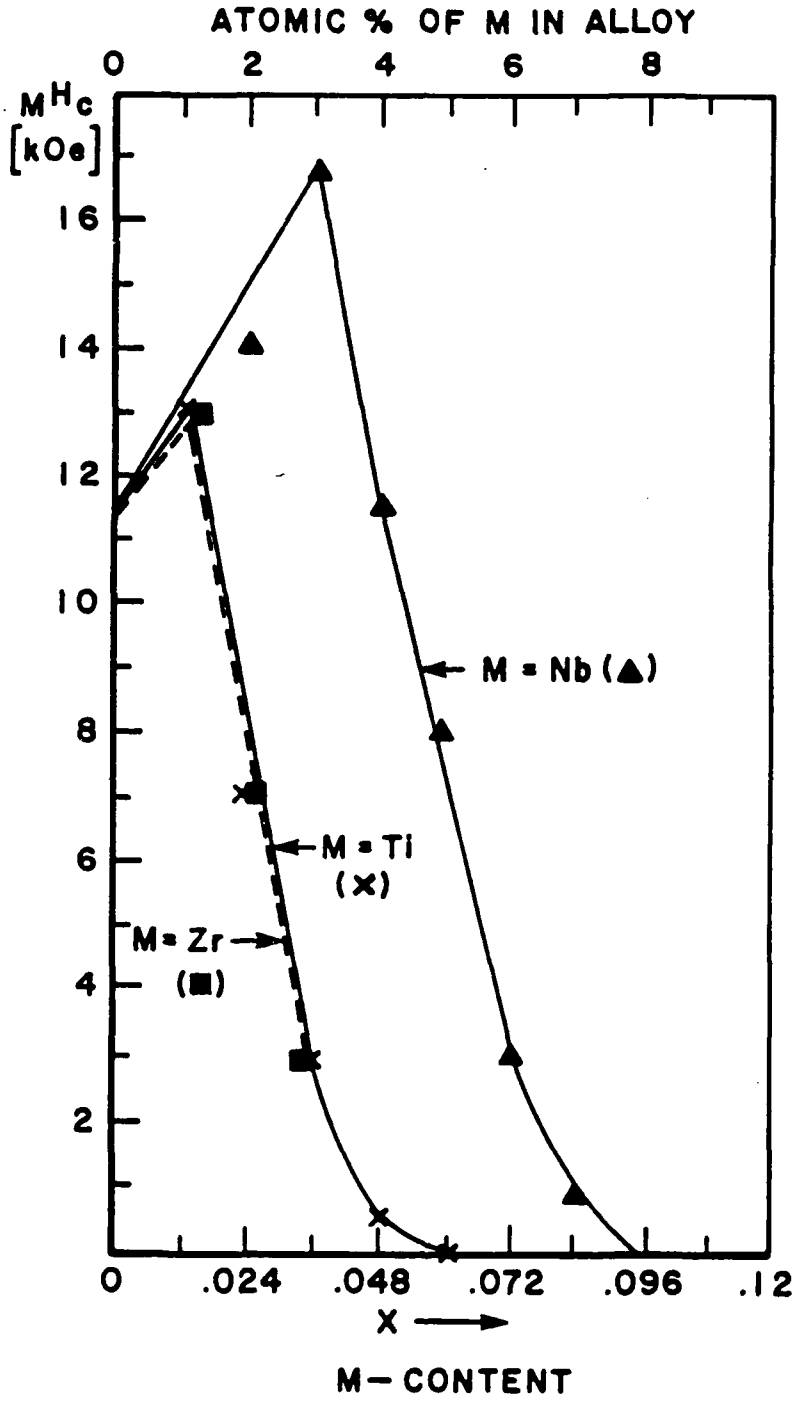


Fig.1: Dependence of the intrinsic coercive force on the amount of M(Nb,Ti or Zr)in sintered magnets of $(Nd_{.88}Dy_{.12})(Fe_{.88-x}Co_{.12}B_{.08}M_x)_{5.5}$ .

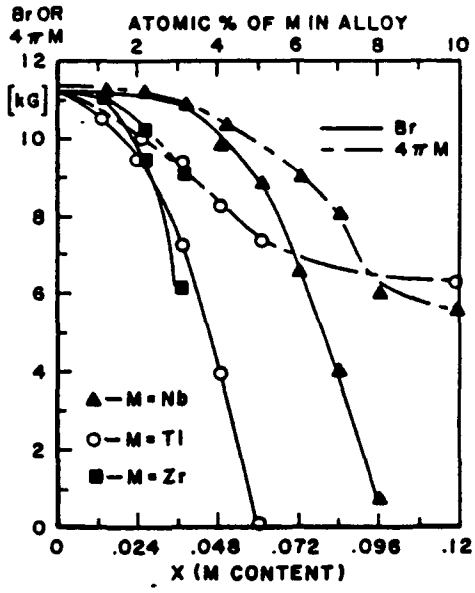


Fig.2: Variation of Br and $4\pi M$ (measured at 23kOe)with the M content in$(Nd_{.88}Dy_{.12})(Fe_{.80-x}Co_{.12}B_{.08}M_x)_{5.5}$ where M= Nb,Ti or Zr.

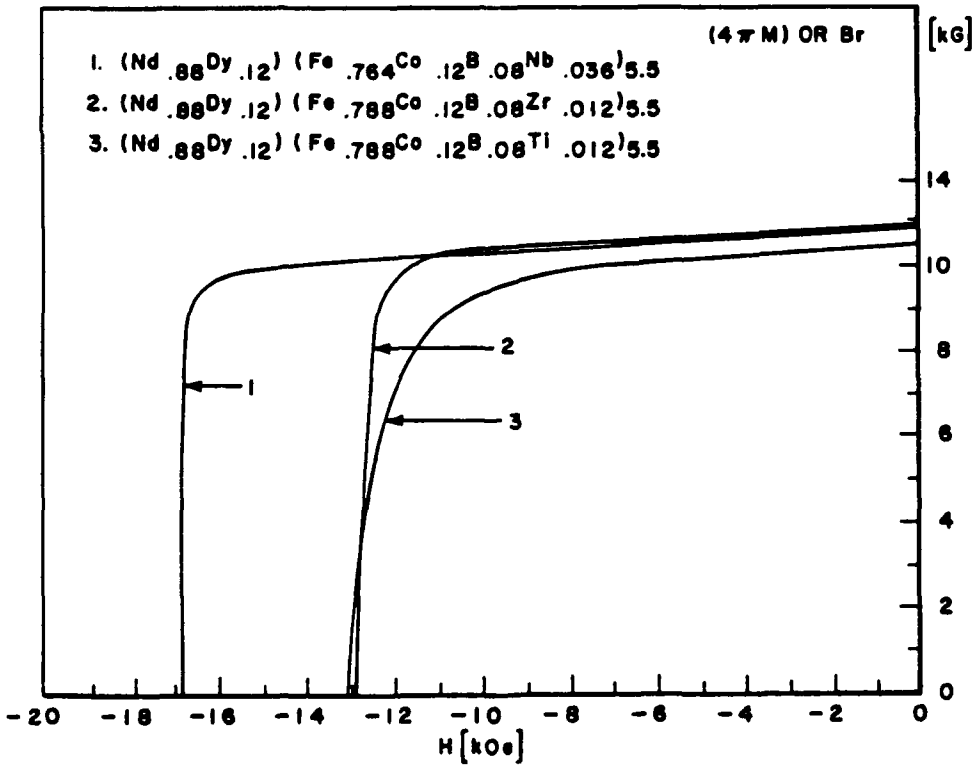


Fig.3: Demagnetization curves of three samples with optimum Nb,Ti and Zr content.

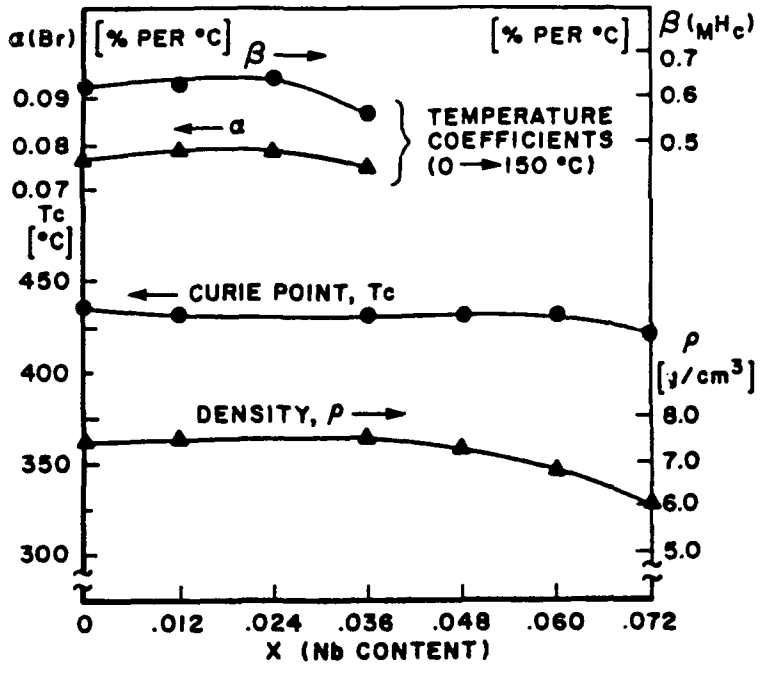


Fig.4: The variation with Nb content of the Curie temperature, $T_c$, the sintered density, $\rho$, and temperature coefficient $\alpha(B_r)$ and $\beta(_MH_c)$ (for temp. range 0→150°C in $(Nd_{.88}Dy_{.12})(Fe_{.80-x}Co_{.12}B_{.08}M_x)_{5.5}$

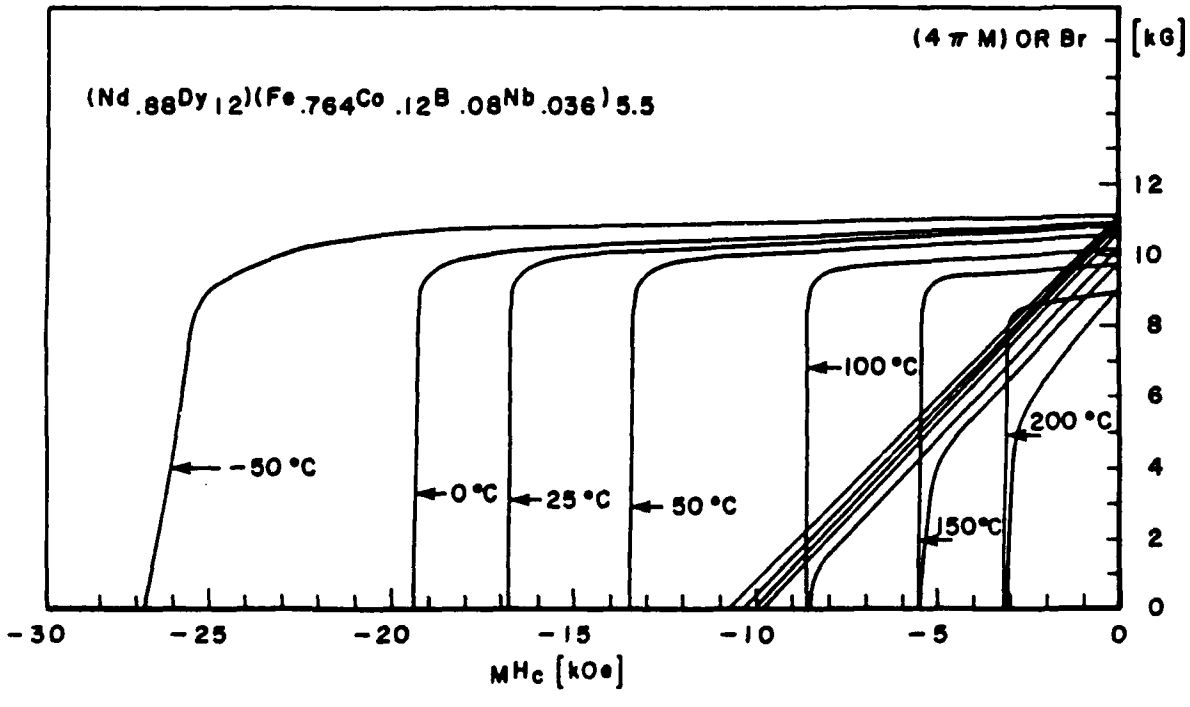


Fig.5: Demagnetization curves at several temperatures between -50 and 200°C for a sintered magnet of $(Nd_{.88}Dy_{.12})(Fe_{.764}Co_{.12}B_{.08}Nb_{.036})_{5.5}$ .

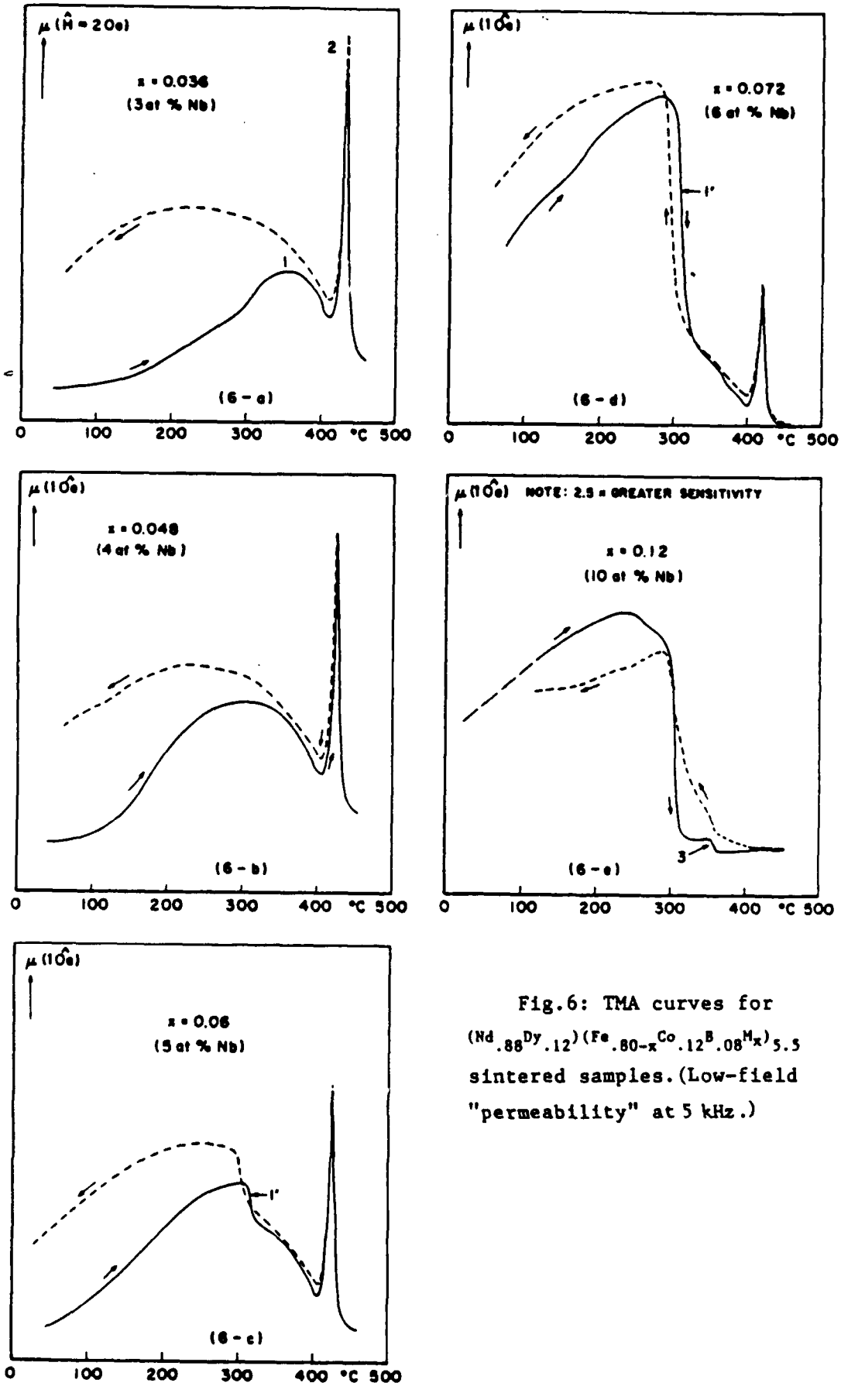


Fig.6: TMA curves for $(Nd_{.88}Dy_{.12})(Fe_{.80-x}Co_{.12}B_{.08}M_x)_{5.5}$ sintered samples. (Low-field "permeability" at 5 kHz.)

# APPENDIX G

THE EFFECTS OF VARIOUS ALLOYING ELEMENTS ON MODIFYING
THE ELEVATED TEMPERATURE MAGNETIC PROPERTIES
OF SINTERED Nd-Fe-B MAGNETS

# The effects of various alloying elements on modifying the elevated temperature magnetic properties of sintered Nd-Fe-B magnets

Y. Xiao, S. Liu, H. F. Mildrum, K. J. Strnat, and A. E. Ray
*University of Dayton, Dayton, Ohio 45469*

The effects of the alloying elements Co, Dy, Er, Al, and Nb on modifying the elevated temperature properties of sintered Nd-Fe-B–based permanent magnets have been studied in our laboratory. The results are summarized and analyzed. Small Nb additions increase coercivity and improve elevated temperature properties. Higher Nb additions lead to decomposition of the 2:14:1 phase into a 2:17 phase and a new magnetic phase with a Curie point around 350 °C. The effectiveness of Nb additions appears to be associated with the rare-earth content of the magnets.

## I. INTRODUCTION

An important objective of present research and development is making Nd-Fe-B magnets more useful at elevated temperatures. The general approach has been to modify the magnet alloy by introducing fourth, fifth, and sixth component elements. The elements selected for this objective should accomplish one or more of the following in the modified magnets:

(1) Raising the Curie temperature of the 2:14:1 phase;

(2) increase the coercivity significantly without an unacceptable decrease in remanence;

(3) reduce the temperature coefficient of remanence;

(4) reduce the temperature coefficient of coercivity.

A search conducted by several laboratories worldwide has identified some elements that qualify by these criteria.[1-5]

With the goal of enabling the magnets to be useful in the temperature range 150–200 °C, Nd-Fe-B alloys, modified with Co, Dy and/or Er, Al and Nb, Zr, or Ti have been investigated in our laboratory.[6-8] In this paper we briefly summarize and analyze these results and report some new results regarding Nb additions.

## II. EXPERIMENTAL METHODS

The procedures for preparing sintered magnets and evaluating their magnetic properties were previously described.[6,7] Demagnetization curves were measured on 1-cm cubes in a closed circuit with a dc recording hysteresigraph comprising a dual electronic integrator and a fixture permitting the heating and cooling of the samples in the range $-50-+200$ °C. The values of $B_r$ and ${}_MH_c$ and their temperature coefficients were determined from curve sets obtained with this equipment. The temperature coefficients $\alpha$ of $B_r$ and $\beta$ of ${}_MH_c$, quoted in this paper, are defined as follows:

$$\alpha(T_1 \to T_2) = 100[B_r(T_2) - B_r(T_1)]/[B_r(25\,^\circ\text{C})(T_2 - T_1)], \quad (1)$$

$$\beta(T_1 \to T_2) = 100[{}_MH_c(T_2) - {}_MH_c(T_1)]/[{}_MH_c(25\,^\circ\text{C})(T_2 - T_1)]. \quad (2)$$

They are inherently negative for our alloys, and to improve the magnets, the absolute values of both $\alpha$ and $\beta$ should be reduced.

Low-field ac thermomagnetic analysis (TMA) was used to determine the Curie temperatures of the magnetic phases present. Metallography and x-ray diffraction were also employed to study the magnet alloys.

## III. RESULTS AND DISCUSSION

Data related to the temperature dependence of some modified Nd-Fe-B magnets prepared in our laboratory, as well as some magnets for reference, are listed in Table I. The ternary Nd-Fe-B magnets have temperature coefficients, $\alpha$ and $\beta$, which are 3.0–3.6 times greater than those of commercial $SmCo_5$ or 2:17 types. The higher-temperature coefficients of the Nd-Fe-B magnets are usually attributed to the low Curie temperature of the $Nd_2Fe_{14}B$ phase. Therefore, raising the Curie temperature of this phase has been an important approach for improving the thermal stability Nd-Fe-B magnets. But this is not enough; a high intrinsic coercive force, ${}_MH_c$, and good hysteresis loop squareness must also be maintained throughout the use temperature range.

### A. Cobalt

The most effective element for raising the Curie temperature of the 2:14:1 phase is cobalt. Substitution of 10 at. % Co for Fe in ternary Nd-Fe-B magnets raises the Curie point from 316 to 435 °C while reducing $\alpha$ from $-0.126\%/^\circ\text{C}$ to $-0.09\%/^\circ\text{C}$, and $\beta$ from $-0.86\%/^\circ\text{C}$ to $-0.54\%/^\circ\text{C}$. However, Co additions have adverse side effects. It is well known that Co reduces ${}_MH_c$ in ternary Nd-Fe-B magnets; when Co and Dy additions are combined it also reduces the effectiveness of the Dy for increasing ${}_MH_c$ and decreasing $\beta$ in Nd-Dy-Fe-B magnets. For example, compare our samples 9 and 4. Both have identical Dy contents, but sample 9 has only half the Co content of sample 4. Room-temperature coercivities of ${}_MH_c = 22$ kOe can be developed in sample 9 (5 at. % Co), but only 16 kOe in sample 4 (10 at. % Co). Due to the lower $\beta$, $-0.47\%/^\circ\text{C}$ for sample 9, compared to $-0.54\%/^\circ\text{C}$ for sample 4, the coercivity of sample 9 remains higher at 150 °C, ${}_MH_c = 7.80$ kOe, than for sample 4, ${}_MH_c = 6.05$ kOe. The adverse effects of higher cobalt substitutions on coercivity and $\beta$ are to a large extent

 0021-8979/88/083516-03$02.40  

TABLE I. Property values describing the elevated temperature behavior of sintered Nd-Fe-B magnets modified with Co, Dy, Er, Al, and Nb in different combinations.

| No. | Composition of magnet | $T_c$ (°C) | $\alpha$ (%/°C)[a] (0–150 °C) | $\beta$(%/°C)[b] (0–150 °C) | ${}_MH_c$ (kOe) (at 150 °C) | $B_r$ (kG) (at 150 °C) | $(BH)_{max}$ (MGOe) (at 150 °C) |
|---|---|---|---|---|---|---|---|
| 1 | Nd-Fe-B (Neomax-35)[c] | 316 | −0.126 | −0.86 | 3.60 | 10.3 | 21.0 |
| 2 | $Nd(Fe_{0.90}Co_{0.12}B_{0.08})_{5.5}$ | 435 | −0.09 | −0.54 | 2.30 | 10.42 | 14.7 |
| 3 | $(Nd_{0.88}Dy_{0.12})(Fe_{0.80}Co_{0.12}B_{0.08})_{5.5}$ | 431 | −0.077 | −0.63 | 3.43 | 9.67 | 20.5 |
| 4 | $(Nd_{0.80}Dy_{0.20})(Fe_{0.80}Co_{0.12}B_{0.08})_{5.5}$ | 424 | −0.068 | −0.54 | 6.05 | 9.08 | 19.4 |
| 5 | $(Nd_{0.80}Dy_{0.16}Er_{0.04})(Fe_{0.80}Co_{0.12}B_{0.08})_{5.5}$ | 425 | −0.058 | −0.53 | 4.57 | 9.51 | 22.2 |
| 6 | $(Nd_{0.88}Dy_{0.12}(Fe_{0.764}Co_{0.12}B_{0.08}Nb_{0.036})_{5.5}$ | 433 | −0.075 | −0.57 | 5.60 | 9.59 | 21.4 |
| 7 | $(Nd_{0.88}Dy_{0.12})(Fe_{0.764}Co_{0.12}B_{0.08}Al_{0.036})_{5.5}$ | 407 | −0.087 | −0.89 | 3.30 | 8.54 | 14.8 |
| 8 | $(Nd_{0.75}Dy_{0.20}Er_{0.05})(Fe_{0.80}Co_{0.12}B_{0.08})_{5.5}$ | [e] | −0.048 | −0.46 | 4.80 | 9.82 | 21.2 |
| 9 | $(Nd_{0.80}Dy_{0.20})(Fe_{0.86}Co_{0.06}B_{0.08})_{5.5}$[d] | 380 | −0.087[f] | −0.47 | 7.80 | 9.55 | 25.3 |

[a] Temperature coefficient of $B_r$.
[b] Temperature coefficient of ${}_MH_c$.
[c] Sample from Sumitomo Special Metals Co. Ltd., Japan; measured at the University of Dayton.
[d] Sample from Hitachi Metals, Ltd., Japan; measured at the University of Dayton.
[e] Not measured.
[f] 22–150 °C.

offset by the positive effects on $\alpha$ and $T_c$. These results suggest that, for operation at elevated temperatures, the Co content, particularly in combination with Dy, is important for obtaining an optimal balance between $\alpha$ and $\beta$.

### B. Dysprosium and erbium

Dy very effectively enhances the coercive force of both Nd-Fe-B and Nd-Fe-Co-B magnets, as well as decreasing both $\alpha$ and $\beta$. A 3 at. % Dy addition reduces $\alpha$ and $\beta$ to −0.065% and −0.54%, respectively, in the $(Nd_{0.80}Dy_{0.20})(Fe_{0.80}Co_{0.12}B_{0.08})_{5.5}$ magnet (sample 4, Table I). These values are only about twice as large as those for $SmCo_5$ or 2:17 magnets. Substitutions of Er, especially in combination with Dy, can further reduce $\alpha$ and $\beta$ (samples 5 and 8). But ${}_MH_c$ at elevated temperatures is also lowered to such an extent that Er cannot be considered an attractive alloying element for improving the temperature stability of Nd-Fe-B magnets above 100 °C.[2]

### C. Aluminum

Al is more effective than Dy in increasing ${}_MH_c$ at room temperature. However, it increases both $\alpha$ and $\beta$, especially $\beta$. Comparing samples 3 and 7 in Table I, a 3 at. % Al addition increases $\beta$ from −0.63% to −0.89%, which is even larger than that of the ternary Nd-Fe-B magnet. Consequently, a cosubstitution of Al and Co does not improve the properties of the permanent magnets above 150 °C.[6]

### D. Niobium

In Ref. 8 we reported that a small Nb addition brings a substantial increase in coercivity. Substituting 3 at. % Nb ($x = 0.036$) for Fe in $(Nd_{0.88}Dy_{0.12})(Fe_{0.80-x}Co_{0.12}B_{0.08}Nb_x)_{5.5}$ increases ${}_MH_c$ from 11.5 to 16.8 kOe. An interesting and important feature of small Nb additions is shown in Fig. 1. Up to 3 at. %, Nb does not change $B_r$, $T_c$, or $\alpha$ and $\beta$ very much. As an example, 3 at. % Nb decreases $B_r$ by just 0.3 kG, does not change the Curie point, and only slightly decreases $\alpha$ and $\beta$. Analogous results were observed for Dy-free magnets. Indeed, small Nb additions are more effective than comparable amounts of Dy in Nd-Fe-Co-B based magnets because Dy decreases $B_r$ much more than Nb at levels that yield comparable ${}_MH_c$ gains. Unfortunately, only a small and critical amount of Nb can be added before $B_r$ and ${}_MH_c$ begin to rapidly deteriorate, so that Nb cannot completely replace Dy. We observed this critical amount of Nb to vary with the amount of neodymium, or (Nd + Dy) present in the magnets. This is discussed in the next section.

### E. Further observation on Nb-containing magnets

In Ref. 8 we showed a set of TMA curves for $(Nd_{0.88}Dy_{0.12})(Fe_{0.80-x}Co_{0.12}B_{0.08}Nb_x)_{5.5}$ magnets with

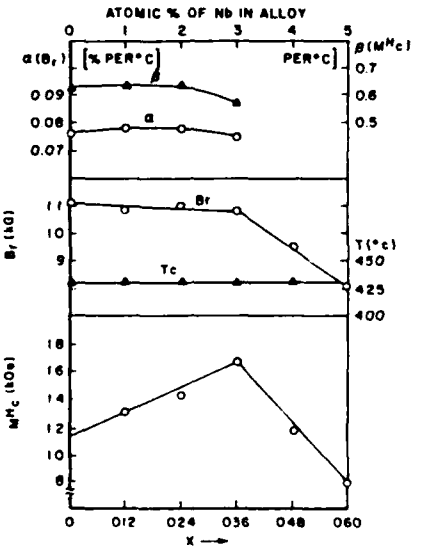


FIG. 1. The dependence of permanent magnetic properties in $(Nd_{1-x}Dy_{0.12})(Fe_{0.88-x}Co_{0.12}B_{0.08}Nb_x)_{5.5}$ magnets on the niobium content.

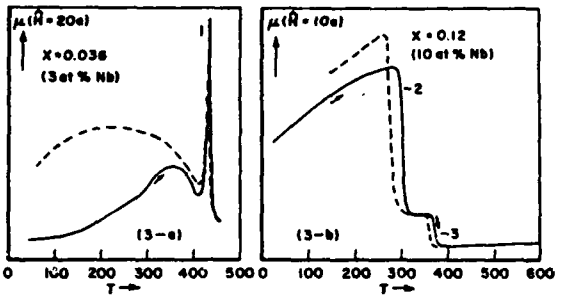


FIG. 2. TMA curves for $(Nd_{0.88}Dy_{0.12})(Fe_{0.80}Co_{12}B_{0.08}Nb_x)_{5.5}$ magnet (3-a) and cast alloy (3-b). (Low-field "permeability" at 5 kHz.) Peaks 1, 2, and 3 belong to 2-14-1, 2-17, and a new magnetic phase, respectively.

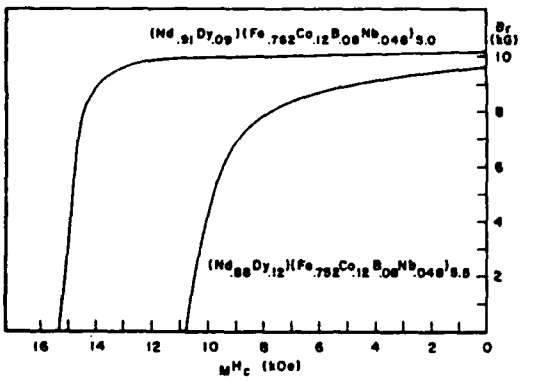


FIG. 4. Demagnetization curves of two sintered magnets with identical Nb substitution for Fe and same Dy content but with different Nd content. More Nd counteracts the adverse effects of Nb in excess of 3 at. %.

Nb contents ranging from $x = 0.012$ to 0.12 and reported that the 2:14:1 phase is the only major phase in evidence at low Nb contents ($x < 0.036$). The deterioration of $_MH_c$ and loop shape begins between 3 and 4 at. % Nb. At 5 at. % Nb content ($x = 0.060$) a second Curie point appears near 310 °C. X-ray diffraction showed that the phase with $T_c = 310$ °C is 2:17, a soft magnetic phase, which explains the loss of the permanent magnet properties. With increasing Nb content the XRD peaks of the 2:14:1 phase gradually decrease and the 2:17 peaks increase. When the Nb reaches 8 at. %, a new, third TMA peak with a Curie point near 350 °C appears and grows with increasing Nb content. At 10 at. % Nb the 2:14:1 peak has disappeared from the TMA scan and only the 2:17 peaks and the new phase peaks are observed in the XRD spectra. The TMA curves for 3 at. % and 10 at. % Nb magnets are shown in Fig. 2. They suggest that the higher Nb additions lead to decomposition of the 2:14:1 phase into 2:17 and a new magnetic phase. We have not yet been able to determine the crystal-structure or additional magnetic data of this new phase. The combined x-ray diffraction spectra for the 2:17 and the new phase are shown in Fig. 3.

Figure 1 shows both $B_r$ and $_MH_c$ begin to decrease sharply when the Nb substitution exceeds 3 at. % ($x = 0.036$) in magnets corresponding to the composition

$$(Nd_{0.88}Dy_{0.12})(Fe_{0.80-x}Co_{0.12}B_{0.08}Nb_x)_{5.5}.$$

As discussed above, at 5 at. % Nb TMA evidence of a new magnetic phase with $T_c = 310$ °C and the diffraction peaks of rhombohedral 2:17 appear. The latter results suggest that Nb in excess of $\approx 3$ at. % may preferentially deplete the 2:14:1 phase of the rare-earth components to form a 2:17 phase and a minor amount of another phase enriched in Nb, RE, and perhaps B. If the excess niobium in fact depletes the 2:14:1 phase of the rare earths, then increasing the neodymium content of the overall composition should at least partially restore good permanent magnet properties. This is indeed what occurs. Increasing the Nb substitution from 3 to 4 at. % ($x = 0.036$ to 0.048) first reduces $B_r$ from 10.8 to 9.5 kG and $_MH_c$ from 16.8 to 10.8 kOe. But increasing the neodymium content to bring the overall composition to

$$(Nd_{0.91}Dy_{0.09})(Fe_{0.762}CO_{0.11}B_{0.08}Nd_{0.048})_{5.0}$$

raises $B_r$ to 10.2 kG again, and $_MH_c$ to 15.3 kOe. The demagnetization curves for two compositions containing 4 at. % Nb are compared in Fig. 4.

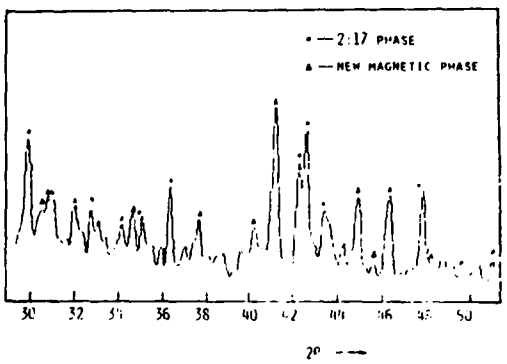


FIG. 3. X-ray diffraction pattern of a $(Nd_{0.88}Dy_{0.12})(Fe_{0.80}Co_{0.12}B_{0.08}Nb_{0.12})_{5.5}$ cast alloy.

## ACKNOWLEDGMENTS

This work was supported by U.S. Army ET&D Laboratory, Ft. Monmouth, NJ, under Contract No. DAAK20-84J-0458.

[1] S. Arai and T. Shibata, IEEE Trans. Magn. MAG-21, 1952 (1985).
[2] X. Shen, Y. Wang, Z. Diao, and X. Liu, J. Appl. Phys. 61, 3433 (1987).
[3] T. Mizoguchi, T. Sakai, H. Niu, and K. Inomata, IEEE Trans. Magn. MAG-22, 919 (1986).
[4] M. Tokunaga, M. Endoh, and H. Harada, in *Proceedings of the 9th International Workshop on Rare-Earth Magnets*, Bad Soden, FRG, 1987, edited by C. Herget and R. Poerschke (Deutsche Phys. Ges., Bad Honnef, FRG, 1987), Part I, p. 447.
[5] B. M. Ma, Mater. Res. Soc. Symp. Proc. 96, 143 (1987).
[6] Y. Xiao, H. F. Mildrum, K. J. Strnat, and A. E. Ray, Mater. Res. Soc. Symp. Proc. 96, 155 (1987).
[7] Y. Xiao, K. L. Strnat, H. F. Mildrum, and A. E. Ray, IEEE Trans. Magn. (to be published).
[8] Y. Xiao, K. L. Strnat, H. F. Mildrum, and A. E. Ray, in *Proceedings of the 9th International Workshop on Rare-Earth Magnets*, Bad Soden, FRG, 1987, edited by C. Herget and R. Poerschke (Deutsche Phys. Ges., Bad Honnef, FRG 1987), Part I, pp. 467–476.

# APPENDIX H

EVIDENCE FOR DOMAIN WALL PINNING BY A MAGNETIC
GRAIN-BOUNDARY PHASE IN SINTERED
Nd-Fe-B BASED PERMANENT MAGNETS

# Evidence for domain wall pinning by a magnetic grain-boundary phase in sintered Nd-Fe-B based permanent magnets

K. J. Strnat and H. F. Mildrum
*University of Dayton, Ohio 45469*

M. Tokunaga and H. Harada
*Hitachi Metals Corporation, Kumagaya, Japan*

Low-field thermomagnetic analysis of sintered Nd(Dy)-Fe(Co)-B magnets provides new evidence that the high coercivity near room temperature is due to the pinning of residual domain walls in a ferromagnetic grain-boundary phase. The temperature where ${}_M H_c$ drops to near zero appears to be the Curie point of that phase. It is 50–80 °C below the $T_c$ of the 2-14-1 matrix.

## INTRODUCTION

The physical origin of the high intrinsic coercivity ($H_c$) of rare-earth magnets is currently the subject of many investigations. For magnets of the "nucleation type," different magnetization reversal mechanisms have been postulated and theories developed based on a multitude of model assumptions. This type includes sintered "$SmCo_5$" as well as "Nd-Fe-B" and their variations. The rather confusing theoretical situation and experimental attempts to clarify it were recently critically reviewed by Livingston.[1]

It is now commonly agreed that a high easy-axis crystal anistropy of the main (matrix) phase is a necessary condition for high coercive force; also that $H_c$ depends very strongly on the metallurgical microstructure. In good magnets this microstructure is usually complex, it has extremely small-scale features, is not in equilibrium, and there is still much uncertainty about the nature, distribution, and properties of the phases present. It is common to speak of the processes that initiate the magnetization reversal of a matrix grain (or group of grains) generically as "nucleation." The actual mechanism can either be the spontaneous creation and subsequent expansion of a previously nonexistent reversed domain formed at a defect site or at a soft-magnetic inclusion (true nucleation); or residual small domains may still exist even after saturating the magnet in a very high field, so that the reversal actually starts with the unpinning of walls which were very strongly anchored in grain boundary regions. Experimentally and conceptually these two cases are hard to distinguish. We believe we have found a new experimental way to show that residual domain walls are indeed pinned by a ferromagnetic grain-boundary phase different from the 2-14-1 matrix but presumably crystallographically coherent with it.

The causes of high coercivity in sintered magnets of the Nd-Fe-B family are still highly controversial, as are details of the microstructure. Several different secondary phases can be seen along grain boundaries, in triple points of the matrix grains, and also as intragranular precipitates. Some investigators found a thin, probably metastable, boundary phase of bcc crystal symmetry,[2,3] which has been vaguely thought to control $H_c$. Some authors think of this phase as magnetically soft and detrimental for $H_c$,[4] others consider it an effective hard-magnetic pinning phase,[3] while still others deny its existence, saying that it is only an artifact of the sample preparation for electron microscopy. Other electron microscope studies[5,6] identified the boundary phase surrounding most 2-14-1 grains as Nd-rich and nonmagnetic. Isolated grains having a composition near $Nd_2Fe_7B_6$ were also found. They are considered by Ref. 6 as magnetically soft and are implicated as the location of nuclei for easily reversed domains, but with no magnetic data to support the claim. However, still other workers[7] speak of a $NdFe_4B_4$ phase instead that is said to be nonmagnetic at room temperature (RT). Very small amounts of $\alpha$-Fe have also been found.[8]

Any good theoretical model of the magnetization mechanisms must correctly explain the temperature dependence of the intrinsic coercivity. Several analyses of the $H_c$ vs $T$ variation for Nd(Dy)-Fe(Co)-B and similar magnets have recently been attempted,[3,7,9,10] one with emphasis on the important range between RT and the Curie point. $H_c$ drops much more rapidly with increasing $T$ than the anisotropy field, $H_A$, of the matrix phase. Sometimes, the same authors present seemingly contradictory interpretations. It must be concluded that neither the exact nature of secondary phases in sintered magnets nor the role which each phase plays in the magnetization reversal are really known at this time.

$H_c$ essentially disappears at temperatures of 50–80 °C below the $T_c$ of the 2-14-1.[7,11] Careful measurements of the coercivity at these higher temperatures on a Co + Dy-modified magnet (see Fig. 1)[3] have shown that there must clearly be two different $H_c$ mechanisms active: The main contribution to $H_c$ drops precipitously to a sharply defined "footpoint" at $T_f$, while a small $H_c < 50$ Oe persists up to the matrix Curie point of 380 °C. The latter must represent the very weak obstacles to wall motion inside the main-phase grains. $T_f$ was interpreted as the probable Curie point of the bcc boundary phase, which was thus presumed ferromagnetic below $T_f$ and capable of pinning walls on the 2-14-1/bcc phase interface.[3] The interval $T_c$-$T_f$ depends on the overall composition of the magnet alloy, but also on the final heat treating temperature which seems to determine the exact composition of the boundary phase, and therefore its Curie point.

 0021-8979/88/083321-03$02.40  

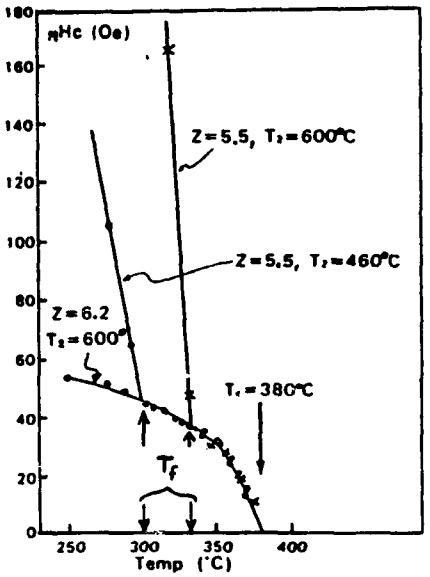


FIG. 1. Temperature variation of $_M H_c$ near $T_c$ for sintered magnets $(Nd_{0.8}Dy_{0.2})(Fe_{0.86}Co_{0.06}B_{0.08})_z$ for the compositions $z$, and final heat treatment temperatures $T_2$, indicated (Ref. 3).

## METHOD AND DESIGN OF EXPERIMENT

We have long used a low-field ac thermomagnetic analysis (TMA) for measuring Curie and other transition temperatures.[12] A $\mu_i$ vs $T$ plot of "initial" permeability shows peaks wherever the anisotropy is low, such as the Hopkinson maximum just below $T_c$. Such peaks indicate either an easing of reversible domain wall motion or of the uniform spin rotation against anisotropy forces. For mixtures or alloys containing several ferromagnetic phases of known $T_c$, such TMA "spectra" can be used to identify phases by their Curie points.[13] The metallurgical systems studied sometimes change toward a new equilibrium during such experiments, especially when very small regions of metastable phases are involved. This is no problem here: the Curie points of Nd-Fe based phases are so low that we need to heat the samples only to $<450$ °C and for short periods. Repeated thermal cycling did not change the magnetic responses discussed below.

We have extended the use of this method by analyzing alloys in two initial (RT) magnetization states: thermally demagnetized and fully saturated. The number and location of domain walls in each case is different, and if the ac field is small enough to cause a wall to reversibly oscillate while it remains pinned, its contribution to the signal should reflect the properties of the phase in which the wall is located. Assuming that a "saturated" magnet contains residual walls pinned in regions near the grain boundaries, the peaks in the TMA spectrum for the magnetized state should reveal the nature of those regions. If there is a clearly defined magnetic pinning phase present, we should see its $T_c$ and learn something about the $T$ dependence of its ability to pin. In contrast, if pinning took place in a disturbed surface region of the 2-14-1 grains, where the local anisotropy is lower or its axis misoriented, then we should only see the main-phase $T_c$, with its peak being broadened. The vehicle for this study were magnets previously prepared at Hitachi Metals Co.[3] for which Fig. 1 shows the $H_c$ vs $T$, including $T_f$ and $T_c$. The specific conditions in our experiments were $H \approx 1$ Oe, $f = 5$ kHz, heat/cool rates between 0.5 and 2 °C/min, the samples being $\sim 1$ g of mortar-ground particles of 37–177 $\mu$m.

## RESULTS AND INTERPRETATION

Figure 2 shows heating and cooling curves for a magnet with RT properties (before crushing) of $_M H_c = 21.9$ kOe, $B_r = 11.4$ kG, and 31.4 MGOe. Curve (a) was run from a thermally demagnetized initial state. It has a sharp Hopkinson peak, the upper inflection point indicating a $T_c \approx 380$ °C in agreement with the point at which all coercivity disappears (compare Fig. 1). It shows no irregularity at $T_f$ where the coercivity mechanism changes. (The cause of a very broad and low $\mu$ maximum at lower temperatures is unknown, but it could be mechanical strains from the grinding.) Curve (b), run after magnetizing the same sample in a $\sim 100$-kOe pulsed field, does not show this broad maximum on heating, but instead an entirely new smaller peak has appeared near the $T_f \approx 330$ °C previously measured on an equivalent sample (compare Fig. 1). This new maximum is gone in the cooling cycle (thermal demagnetization!) and the broad maximum around 200 °C is back. Repeated cycling of the same sample yields curves like (a), while the peak at $T_f$ returns after remagnetizing.

We interpret this to mean that there is indeed a ferromagnetic and crystallographically coherent boundary phase (BP) on the surface of the main-phase grains. (The bcc phase?) Near RT, this is capable of strongly pinning walls; in

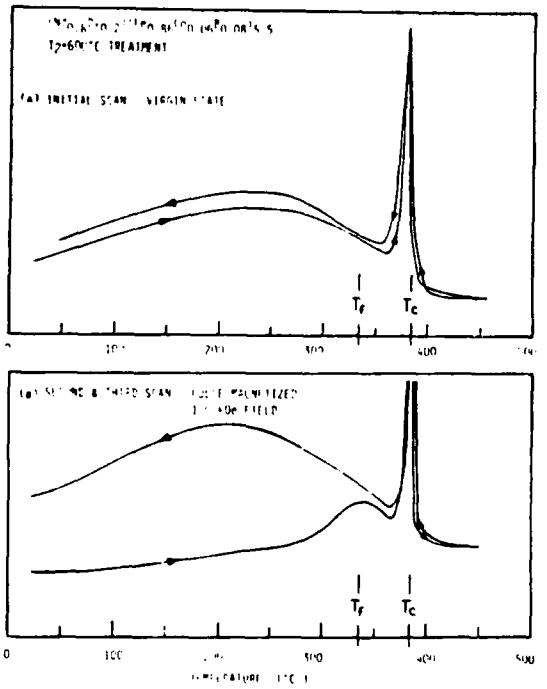


FIG. 2. Low-field ac TMA spectra for a sintered magnet with $z = 5.5$, $T_2 = 600$ °C, starting from a thermally demagnetized state (a) and from saturated condition (b).

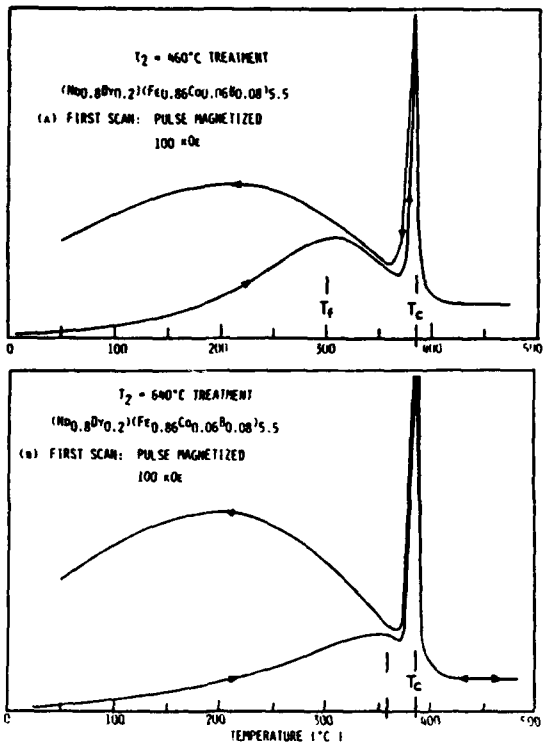


FIG. 3. TMA spectra of initially saturated magnets of the same composition ($z = 5.5$), whose final heat treatment was at different temperatures: $T_2 = 460$ °C (curve a) and 640 °C (b).

absence of an external field it releases them back into the main phase, by thermal activation, only at temperatures approaching $T_f$, which is probably the Curie temperature of this BP. The relative broadness of the $T_f$ peak indicates that the BP is of somewhat variable composition; its small height and the low values of $\mu_i$ at lower $T$ in curve (b) suggest a relatively high anisotropy field for the BP, which would restrict the amplitude of wall bulging at low $T$ and of the spin rotation near $T_f$. In the virgin state there are many highly mobile walls present in the 2-14-1 grains, but none in the very thin BP layer, where a single domain state seems to be stable. A high magnetizing field removes them, pushing some across the interface into the BP, where they are strongly pinned at local imperfections. (The absence of the broad 200 °C peak in the heating curve indicates that the "softening" mechanism underlying it occurs only in the main phase; it has no influence on a fully saturated magnet.)

The TMA curves in Fig. 3 are for magnets of the same composition and preparation, except that their final 1-h annealing step, followed by a water quench, was at $T_2 = 460$ and 640 °C, respectively.[3] Note that for the lower annealing temperature, the $T_f$ peak moves down, consistent with Fig. 1, and becomes broader, indicating greater composition inhomogeneity of the BP. A higher $T_2$ moves the peak to a higher $T_f$ and sharpens it, suggesting a more uniform composition closer to that of the main phase. The boundary layer was previously also found to become thinner, and the $H_c$ at RT is lower for samples annealed at higher $T_2$.[3]

## CONCLUSIONS

These results offer further confirmation that a thin coherent ferromagnetic layer covering the main-phase grains in Nd-Fe-B-type magnets is responsible for their high coercivity. It has an ill-defined composition, but clearly distinct from 2-14-1, and an average $T_c$ 50–80 °C lower than that of the main phase. The magnets lose their useful coercivity on heating as this boundary phase approaches its $T_c$. Thus the $H_c$ vs $T$ function of sintered magnets should be closely related to the temperature variation of the basic properties of this phase (such as its anisotropy) rather than to 2-14-1 properties. The effective mechanism envisioned is the same we suggested for "$RCo_5$" magnets,[14,15] i.e., high-field pinning of residual walls in an "epitaxial shell" of a magnetic phase with a $T_c$ below that of the main, flux-producing phase.

## ACKNOWLEDGMENT

The authors K. J. S. and H. F. M. are grateful for support of this work by the US Army ET&D Laboratory, Ft. Monmouth, NJ under Contract No. DAAK20-84J-0458.

[1] J. D. Livingston, IEEE Trans. Magn. MAG-23, 2109 (1987).
[2] K. Hiraga, M. Hirabayashi, M. Sagawa, and Y. Matsuura, Jpn. J. Appl. Phys. 24, L30 (1985).
[3] M. Tokunaga, M. Tobise, N. Meguro, and H. Harada, IEEE Trans. Magn. MAG-22, 904 (1986).
[4] M. Sagawa, S. Fujimura, H. Yamamoto, Y. Matsuura, and S. Hirosawa, IEEE Trans. Magn. Jpn. TJMJ-1, 979 (1985).
[5] M. Sagawa, S. Fijimura, H. Yamamoto, Y. Matsuura, and K. Hiraga, IEEE Trans. Magn. MAG-20, 1584 (1984).
[6] J. Fidler, IEEE Trans. Magn. MAG-21, 1955 (1985).
[7] K.-D. Durst and H. Kronmüller, in *Proceedings of the 8th International Workshop on Rare Earth Permanent Magnets* (Univ. of Dayton, Dayton, OH, 1985), p. 725.
[8] G. C. Hadjipanayis, in *Soft and Hard Magnetic Materials* (Am. Society of Metals, Metals Park, OH, 1986), p. 89.
[9] S. Hirosawa, K. Tokuhara, Y. Matsuura, H. Yamamoto, S. Fujimura, and M. Sagawa, J. Magn. Magn. Mater. 61, 363 (1986).
[10] M. Sagawa, S. Hirosawa, K. Tokuhara, H. Yamamoto, S. Fujimura, Y. Tsubokawa, and R. Shimizu, J. Appl. Phys. 61, 3559 (1987).
[11] K. J. Strnat, D. Li, and H. Mildrum, in Ref. 7, p. 575.
[12] K. J. Strnat, G. Hoffer, and A. E. Ray, IEEE Trans. Magn. MAG-2, 489 (1966).
[13] K. J. Strnat and A. E. Ray, AIP Conf. Proc. 24, 680 (1975).
[14] J. Schweizer, K. J. Strnat, and J. B. Y. Tsui, IEEE Trans. Magn. MAG-7, 429 (1971).
[15] K. J. Strnat, AIP Conf. Proc. 5, 1047 (1971).

101 Defense Technical Information Center*
ATTN: DTIC-FDAC
Cameron Station (Bldg 5)
Alexandria, VA 22304-6145

(*Note to Contractor: Two copies for DTIC will be sent from STINFO Office, Fort Monmouth, NJ.)

483 Director
US Army Material Systems Analysis Actv
ATTN: DRXSY-MP
001 Aberdeen Proving Ground, MD 21005

563 Commander, AMC
ATTN: AMCDE-SC
5001 Eisenhower Ave.
001 Alexandria, VA 22333-0001

609 Commander, LABCOM
ATTN: AMSLC-CG, CD, CS (In turn)
2800 Powder Mill Road
001 Adelphi, Md 20783-1145

612 Commander, LABCOM
ATTN: AMSLC-CT
2800 Powder Mill Road
001 Adelphi, MD 20783-1145

680 Commander
US Army Laboratory Command
Fort Monmouth, NJ 07703-5000
1 - SLCET-DD
2 - SLCET-DT (M. Howard)
1 - SLCET-DB
35 - Originating Office

681 Commander, CECOM
R&D Technical Library
Fort Monmouth, NJ 07703-5000
1 - ASQNC-ELC-I-T (Tech Library)
3 - ASQNC-ELC-I-T (STINFO)

705 Advisory Group on Electron Devices
201 Varick Street, 9th Floor
002 New York, NY 10014-4877

ELECTRONICS TECHNOLOGY AND DEVICES LABORATORY
SUPPLEMENTAL CONTRACT DISTRIBUTION LIST
(ELECTIVE)

205 Director
Naval Research Laboratory
ATTN: CODE 2627
001 Washington, DC 20375-5000

221 Cdr, PM JTFUSION
ATTN: JTF
1500 Planning Research Drive
001 McLean, VA 22102

301 Rome Air Development Center
ATTN: Documents Library (TILD)
001 Griffiss AFB, NY 13441

437 Deputy for Science & Technology
Office, Asst Sec Army (R&D)
001 Washington, DC 20310

438 HQDA (DAMA-ARZ-D/Dr. F.D. Verderame)
001 Washington, DC 20310

520 Dir, Electronic Warfare/Reconnaissance
Surveillance and Target Acquisition Ctr
ATTN: AMSEL-EW-D
001 Fort Monmouth, NJ 07703-5000

523 Dir, Reconnaissance Surveillance and
Target Acquisition Systems Directorate
ATTN: AMSEL-EW-DR
001 Fort Monmouth, NJ 07703-5000

524 Cdr, Marine Corps Liaison Office
ATTN: AMSEL-LN-MC
001 Fort Monmouth, NJ 07703-5000

564 Dir, US Army Signals Warfare Ctr
ATTN: AMSEL-SW-OS
Vint Hill Farms Station
001 Warrenton, VA 22186-5100

602 Dir, Night Vision & Electro-Optics Ctr
CECOM
ATTN: AMSEL-NV-D
001 Fort Belvoir, VA 22060-5677

603 Cdr, Atmospheric Sciences Lab
LABCOM
ATTN: SLCAS-SY-S
001 White Sands Missile Range, NM 88002

607 Cdr, Harry Diamond Laboratories
ATTN: SLCHD-CO, TD (In turn)
2800 Powder Mill Road
001 Adelphi, MD 20783-1145